UNIVERSITÀ DEGLI STUDI DI NAPOLI FEDERICO II

Department of Biology

PhD in Biology- XXXII cycle

Transcriptional control orchestrated by p63 in skin disease

Marco Ferniani

A.A. 2019/2020

Tutor: Prof. Caterina Missero

Index

Part II: p63 in Heterozygous Genetic disease

Abstract

The p63 gene encodes a master regulator of epidermal development. Mutations or alteration of its expression can lead to different pathological phenotypes. In particular, p63 is often overexpressed or its gene is amplified in squamous cell carcinomas, behaving as a pro-oncogenic factor and facilitating tumor formation. In a first part of this thesis, we focused the attention on gene regulation downstream of p63 in cutaneous squamous cell carcinoma (cSCC). We find that p63 regulates a large number of genes crucial for cell proliferation, and that its ablation impairs cell proliferation, clonogenicity and tumor-sphere formation. To identify p63 protein partners in search for therapeutic targets for skin disease, we identified novel interactors by LC-MS/MS. Among them, we focused on PARP1. PARP1 is an enzyme that add Poly-ADP-Ribose (PAR) moieties onto target proteins and regulates different cellular processes including DNA repair and transcriptional regulation. To investigate whether PARP1 and p63 coordinately regulate global patterns of gene expression, either PARP1 or p63 were depleted in SCC cells followed by RNA-seq. Correlation analyses of the transcriptomic profile under basal condition, demonstrate a strong genetic interaction between p63 and PARP1 regulating a largely overlapping set of genes involved in mitosis and cell cycle progression.

In the second part of my thesis, we investigated heterozygous mutations in p63 gene that can cause different rare genetic disorders with partially overlapping phenotypes, such as Ankyloblepharon-Ectodermal defects-Cleft lip/palate (AEC) syndrome, Ectodermal Ectrodactyly Cleft-lip palate syndrome (EEC), and Acro–dermato–ungual–lacrimal–tooth syndrome (ADULT) syndrome. Using the fibroblast conversion to Keratinocytes like cells (iKC) assay, we investigate the different molecular mechanisms affecting p63 involved in skin genetic diseases. In particular, we identified that AEC-associated p63 mutations lead to thermodynamic protein destabilization, misfolding, and aggregation abolishing the DNA binding and the disruption of the aggregation leads to rescue of the p63 transcriptional activity. In contrast, we also characterize some EEC and ADULT

mutations that can partially affect transcriptional activity with different mechanisms involving binding to the DNA.

Introduction

1. The skin and epidermis development

Skin plays a key role in protecting the body from external agents such as mechanical and chemical insults, heat, infections, water, and electromagnetic radiation. The skin is divided into two main structural compartments: the epidermis and the dermis (Baroni et al.). The epidermis is the outermost component of the skin and it is mainly composed by keratinocytes but also by resident dendritic cells: Langerhans cells, epidermal T lymphocytes, melanocytes and the neuro-epithelial Merkel cells, with sensory function. The epidermis receives its nutrients from blood vessels in the underlying dermis, which contains several types of mesenchymal cells among which are fibroblasts that produce proteoglycans, collagen and elastic fibers. The epidermis consists of four distinct cell layers, from bottom to top: the basal, the spinous, the granular and the stratum corneum or cornfield layer (Fig 1).

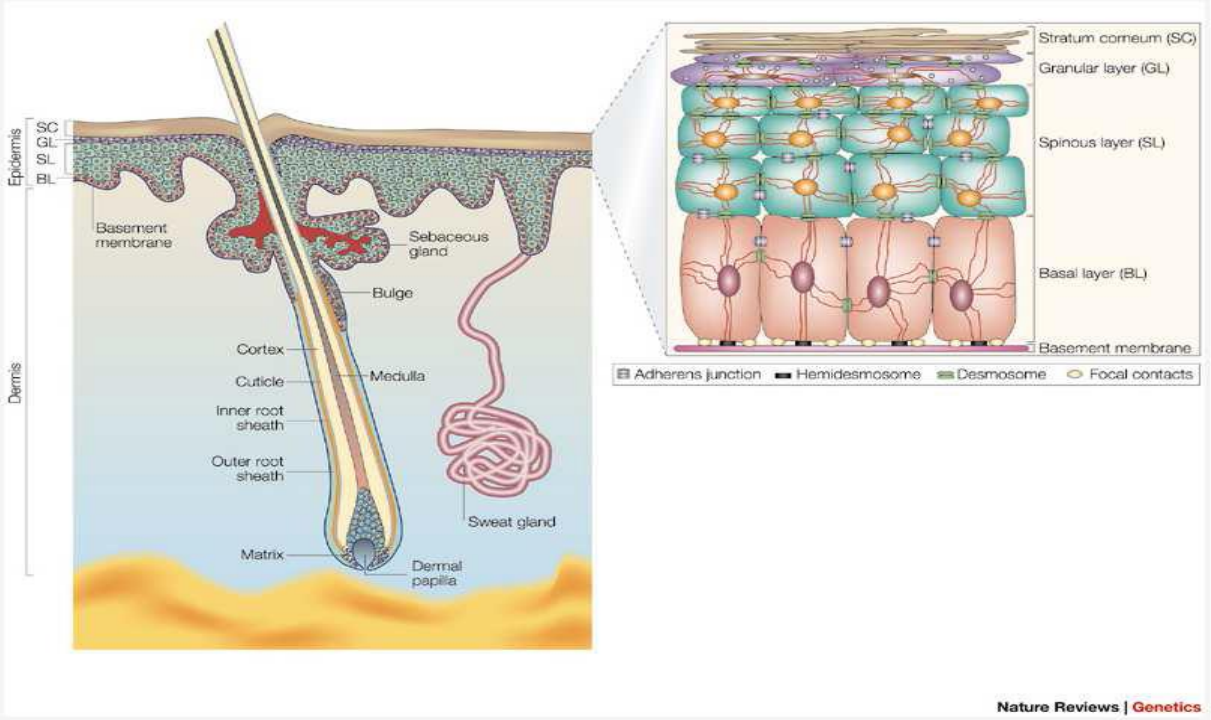

Figure 1. The skin and its appendages. Mammalian skin consists of the epidermis and dermis, separated by a basement membrane. The epidermis is a stratified squamous epithelium composed by: the basal layer (BL), on top of the basement membrane consisting of proliferating, transit- amplifying cells (TA) interspersed to epidermal stem cells, spinous layer (SL), granular layer (GL) and the stratum corneum (SC). The transcription factor p63 is mainly expressed in the basal layer. *Adapted from Fuchs, Getting under the skin of epidermal morphogenesis, Nat Rev Genet, 2002*)

1.1 Skin structure

The basal layer is the deepest layer of the epidermis and it consists of a single layer of cubical or cylindrical cells, the keratinocytes, anchored to the basement membrane through junctions called hemi-desmosomes. Cells are strongly bound to each other through desmosomes, which are organized on the lateral surface. These cells are able to divide and replace the superficial cells of the skin that are lost every day. Keratin-14 (KRT14) and Kreratin-5 (KRT5) and the transcription factor p63 (TP63) are characteristic markers of the basal layer (Fig.2).

The spinous layer is a thick layer, consisting of several rows of progressively differentiating cells that express marker such as Keratin-1 (KRT1) and Keratin-10 (KRT10) (Fig.2). The spinous layer also contains Langerhans cells, which are derived from a precursor in bone marrow and are involved in immune response. Above the spinous layer, keratinocytes contain numerous granules of keratohyalin in their cytoplasm, hence the name "*stratum granulosum*". Filaggrin (FLG) and loricrin (LOR) are examples of markers of granular layer.

The stratum corneum is the outermost layer of the epidermis. It is constituted by many layers of flatten cells that lose their nucleus and continuously shed from the surface (desquamation). In normal skin, the rate of divisions equals the rate of lost cells, taking about two weeks for a cell to migrate from the basal cell layer to the top of the granular cell layer, and an additional two weeks to cross the stratum corneum. Therefore the epidermis, like other stratified epithelia, has a self-renewing capacity throughout life, and this continuous turnover is mediated by stem cells in the basal layer of the interfollicular epidermis (Watt, 2002) and in the bulge region of the hair follicle (Cotsarelis et al., 1990). After a few rounds of cell division, epidermal stem cells become transit-amplifying cells (TA) that divide few times and then permanently exit from the cell cycle and initiate a terminal differentiation program. Further epidermal maturation occurs when spinous cells differentiate into granular cells and finally, cornified cell envelopes are assembled by cross-linking of structural proteins and lipids (Rice and Green, 1977).

Stem cells in the epidermis have a crucial role in maintaining tissue homeostasis by providing new cells to replace those that are constantly lost during tissue turnover or following injury (Blanpain and Fuchs, 2009).

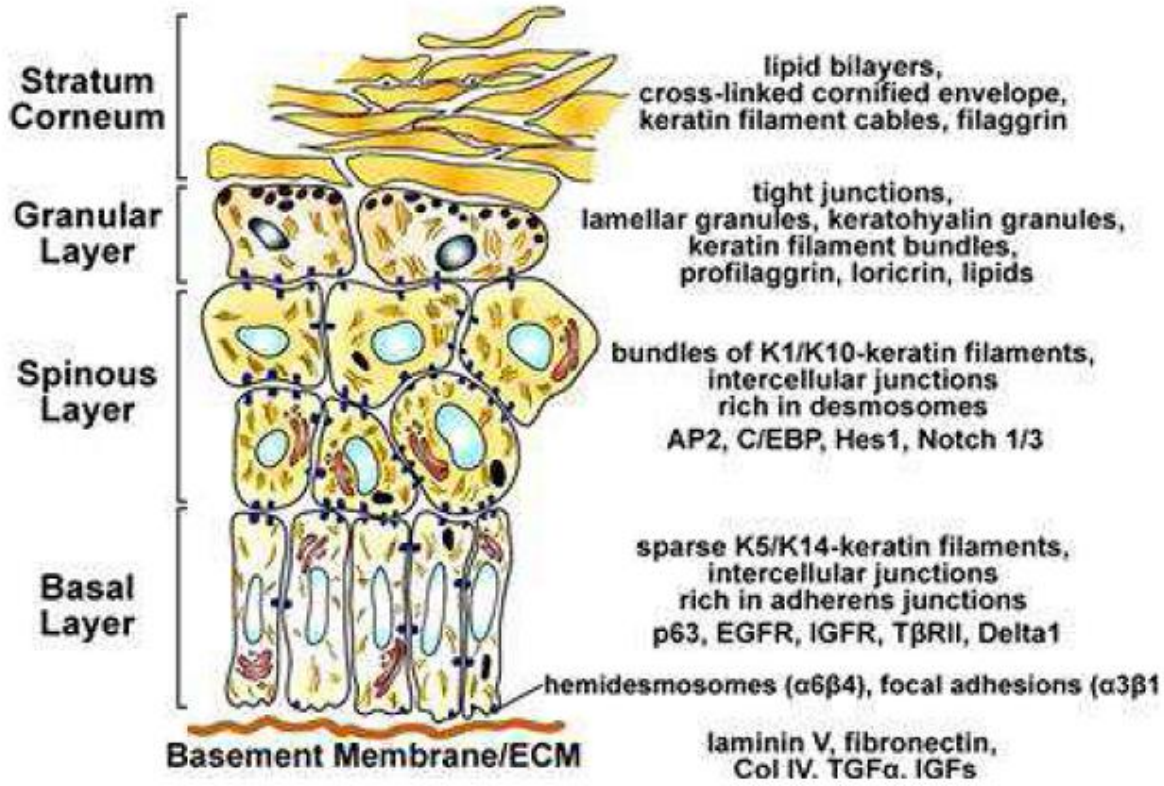

Figure 2: Epidermal differentiation. The program of epidermal differentiation is shown in this scheme, illustrating the basement membrane at the base, the proliferative basal layer, and the three differentiation stages: spinous layer, granular layer, and outermost stratum corneum. Key molecular markers are shown on the right. (From Fuchs, *Skin stem cells:* rising to the surface, J Cell Biology, 2008)

1.2 Skin development

The skin epidermis originates from the ectoderm, which expresses keratin-18 (KRT18), during embryonic development. A single layer of epidermal cells forms and persists from embryonic stage E9.5 to E12.5. Mesenchymal cells populate the skin and transmit signals that instruct the stratification of the epidermis. Epidermal cells adhere to this basement membrane, which serves not only as a growth-promoting platform but also as a physical boundary between the epithelium and the dermis (Blanpain and Fuchs, 2009). During the initial stages of stratification (E12.5- E15.5), cell divisions occur in the basal and suprabasal compartment. Suprabasal cells soon differentiate and complete the stratification around E17.5. During their transition toward the skin surface, suprabasal cells undergo several discrete transcriptional stages as they form the spinous layers, the granular layers and finally the dead, flattened stratum corneum cells (Blanpain and Fuchs, 2009). Upon the formation of the periderm, KRT5 and KRT14 are expressed. Subsequently, at E15.5, the epidermis forms the spinous and granular layers with the concomitant switch off KRT14 and KRT5 and the expression of the differentiation markers, KRT1 and KRT10. At E17.5, epidermal stratification and maturation are complete. In the adult, the epidermis continuously regenerates with a finely regulated differentiation program. Then, the epidermis is continuously renewed due to a regulated balance between proliferation and differentiation. The renewal capacity is due to the presence of epidermal stem cells and transient amplifying cells in the basal layer.

An essential regulator of skin development is the transcription factor p63 (Mills et al., 1999; Yang et al., 1999a). It is required for the early steps of the skin stratification and for maintaining the self-renewal of the basal layer of epidermis. The Notch signaling pathway is also crucial for the epidermal stratification, inducing the switch from the basal to spinous layer (Blanpain et al., 2006) causing the exit from the cell cycle and commitment to cell differentiation (Rangarajan et al., 2001). Notch signaling pathway and p63 act as a negative feedback loop controlling the balance between keratinocyte self-renewal and differentiation. In particular, p63 expression is suppressed by Notch1

activation and p63 acts as a modulator of Notch1-dependent transcription (Nguyen et al., 2006). Like p63, IRF6 plays a crucial role in the epidermal differentiation. Its gene transcription is induced in differentiated keratinocytes both by p63 and by a Notch dependent pathway (Restivo et al.). Furthermore, Notch signaling act also influencing the expression of the CCAAT/ enhancer-binding protein (C/EBP), which work with AP2 family members regulating the commitment for terminal differentiation (Wang et al., 2008).

2. The Transcription Factor p63

The TP63 gene encodes a master regulator of epidermal commitment, development, and differentiation (Koster et al., 2004; Mills et al., 1999; Senoo et al., 2007; Vanbokhoven et al.; Yang et al., 1999a). It is located on chromosome 3q28 and comprises 16 exons. TP63 belongs to the p53 gene family consisting of three genes, TP53, TP63, and TP73, that show significant sequence homology (Yang et al., 2002). The p53 gene family is derived from a common ancestor that appeared very early during evolution in the metazoan sea anemone more than a billion years ago. This ancestor gene duplicated in early vertebrates resulting in the appearance of the gene that is closely related to p53, whereas its second duplication in bony fish led to the appearance of the p63 and p73 genes (Belyi et al.).

The p63 DNA binding domain (DBD) is highly homologous to the DBD of its family members, p53 and p73. Therefore, p63 and binds to canonical p53 DNA-binding sites and shares some biological functions with the other members of the family (Vanbokhoven et al.; Yang et al., 1998). TP63 gene present two different promoters, P1 and P2, which generate two classes of proteins (Fig. 3) (Vanbokhoven et al.). The TAp63 transcript contains an N-terminal trans-activation domain, whereas the N-terminal truncated (ΔNp63) isoforms lacks this domain, but both TAp63 and ΔNp63 can be alternatively spliced at the 3' terminus to produce α-, β-, γ- and δ- isoforms. In contrast to the other isoforms, the α-isoforms contain a sterile alpha motif (SAM, a protein-

protein interaction domain) and a trans inhibitory domain, which blocks trans-activation by masking a few residues on the N-terminal TA isoform(Vanbokhoven et al.). SAM domains are the most abundant protein-protein interaction motifs (~70 amino acids), are usually found in the context of larger multi-domain proteins, and may be found in all cellular compartments, implying roles in complex and wide-ranging cellular processes. These domains are found in a wide variety of proteins involved in cell signaling, in developmental regulation, signal transduction and transcriptional activation, and repression (Schultz et al., 1997).

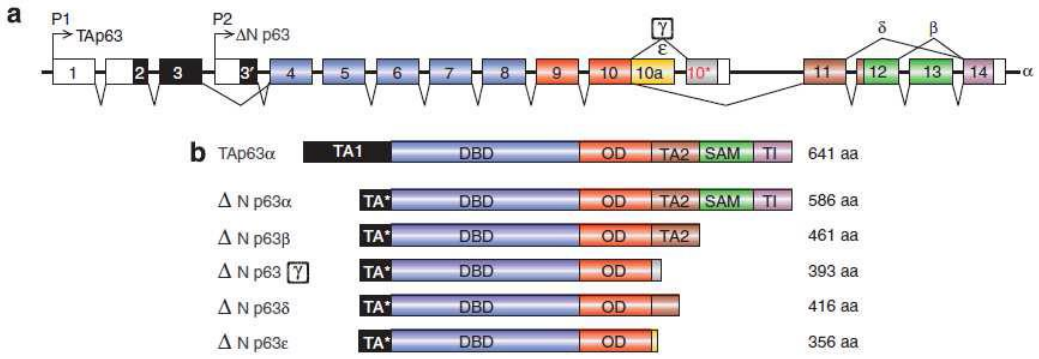

Figure 3: The human p63 splicing isoforms. (a) Representation of the organization of the human p63 gene and the alternative splicing events. Alternative promoter use (P1 and P2) give rise to TA (trans-activation) and N-terminally (ΔN) isoforms. (b) Representation of the human p63 protein splicing variants. For TA isoforms, only TAp63a is shown. However, TA1-containing isoforms also occur as TAp63b, g, d, and e splice variants. aa, amino acid; DBD, DNA-binding domain; OD, oligomerization domain; SAM, sterile alpha motif; TA*, transactivation domain of the DN isoforms; TI, transactivation inhibitory domain (*H. van Bokhoven, p63, a story of mice and men, 2011*).

The TAp63 isoform is mainly involved in oocyte quality control in the female germline due to its activation by DNA damage that causes a molecular switch from dimeric to tetrameric form leading to a cell cycle arrest (Deutsch et al., 2011). Instead, the N-truncated isoform, ΔNp63α, is one of the first genes to be specifically expressed in the surface ectoderm around E8.5 and it continues to be expressed during skin development

and in the basal proliferative layer in postnatal life (Koster et al., 2004). In the basal layer, ΔNp63α is mainly involved in maintaining cell proliferation and cell adhesion. It has been proposed that p63 plays a dual role in keratinocyte differentiation, as it is required for initiating epithelial stratification (Chikh et al.; Koster and Roop, 2004; Sen et al.), whereas concurrently it inhibits the expression of some differentiation markers (King et al., 2003; Masse et al.). In 1999, two research groups demonstrated that the p63 knock out mice leads to developmental and morphological defects in squamous epithelia including the epidermis, causing abnormal craniofacial development, truncated limbs, and loss of salivary glands, hair follicles, and teeth (Mills et al., 1999; Romano et al.; Yang et al., 1999a). Since then the critical role of p63 in promoting expression of epidermal specific genes and inhibiting non-epidermal genes has been demonstrated by several studies. p63 plays a role in epigenetic regulation in epidermal keratinocytes via several mechanism (Kouwenhoven et al.; Sethi et al.). It can recruit HDAC1/2 complex to control the repression of cell cycle genes such as CDKN1A and 14-3-3σ (LeBoeuf et al.). Furthermore, p63 plays an essential role in regulating enhancer landscape bounding specific keratinocytes enhancer sequences that are nucleosome-enriched in cells where p63 is not expressed (Qu et al.). The co-operation of p63 with BAF is required for opening chromatin near the regulatory sequences of genes important for epidermal commitment (Bao et al.). Furthermore, p63 can co-operates with others chromatin associated protein such as AP-2 and KMTD2 to regulate the epithelial homeostasis and differentiation (Lin-Shiao et al.; McDade et al.) This suggest that p63 plays a role of pioneer factor in the epidermal development. Studies on the molecular pathway during the epidermal development reveal an interaction of p63 with the Bone Morphogenetic protein (BMP) signaling binding directly the promoter of SMAD7 and repressing its expression (De Rosa et al., 2009). Latest studies have shown the importance of BMP4 and Retinoic Acid (RA) in helping p63-mediated transcriptional regulation during the surface ectoderm commitment. p63 cannot function without morphogens, indicating the importance of these downstream factors in helping p63-mediated transcriptional mechanism contributing to regulate the dynamic of chromatin interactions during

epidermal commitment (Pattison et al.). Furthermore, p63 expression is controlled by a positive auto-regulatory loop through a long-range enhancer (p63LRE) (Antonini et al., 2006). This enhancer is high conserved in human and mouse and it is also bound by several TF including Cebpa, Cebpb, Pouf3f1 and AP2 members repressing the expression of p63. Chen et al. also clarify the role of p63 as master regulator for proper epidermal commitment and maintenance. The authors showed that p63, in combination with KLF4, one of the Yamanaka's factor (Takahashi and Yamanaka, 2006) and also an epidermal differentiation factor, is able to convert human dermal fibroblast (HDF) into Keratinocytes like cells (iKC) with the consequential gene expression of the typical keratinocytes markers (KRT14, KRT5, DSP, DSC3 etc.) (Chen et al., 2014). Most recently, Lingjie Li et al have identified TFAP2C and p63 as key factors for ectoderm surface initiation and keratinocytes differentiation; furthermore, they reveal a TFAP2C-p63 feedback regulation during epidermal commitment. In particular, TFAP2C prepares the underlying chromatin landscape for p63-dependent keratinocyte maturation. Subsequently, p63 drives maturation both by positive autoregulation of its own locus and by inhibition of the immature surface epithelial landscape. Therefore p63 levels are boosted by it self-activation from the p63 C40 enhancer (Antonini et al.), facilitating the activation of keratinocyte-specific targets. By contrast, p63 reduces the level and binding site accessibility of TFAP2C repressing the transcription of TFAP2C itself through the binding to distal sites to the TSS of TFAP2C looping with this TSS (Li et al.).

Part I: p63 in skin cancer

3. Skin cancers

Skin cancers develop from the skin, when abnormal cells, with the ability to proliferate in an unchecked manner, invade or spread other parts of the body, arise from the different layers of epidermis. Two main tumors arise from the epithelial components of the skin: the basal-cell carcinoma (BCC) and the squamous-cell carcinoma (SCC) and are known as non-melanoma skin cancer (NMSC), the most frequent tumor in humans. While, BCC is less aggressive, and rarely metastatizes, the SCC can be highly invasive.

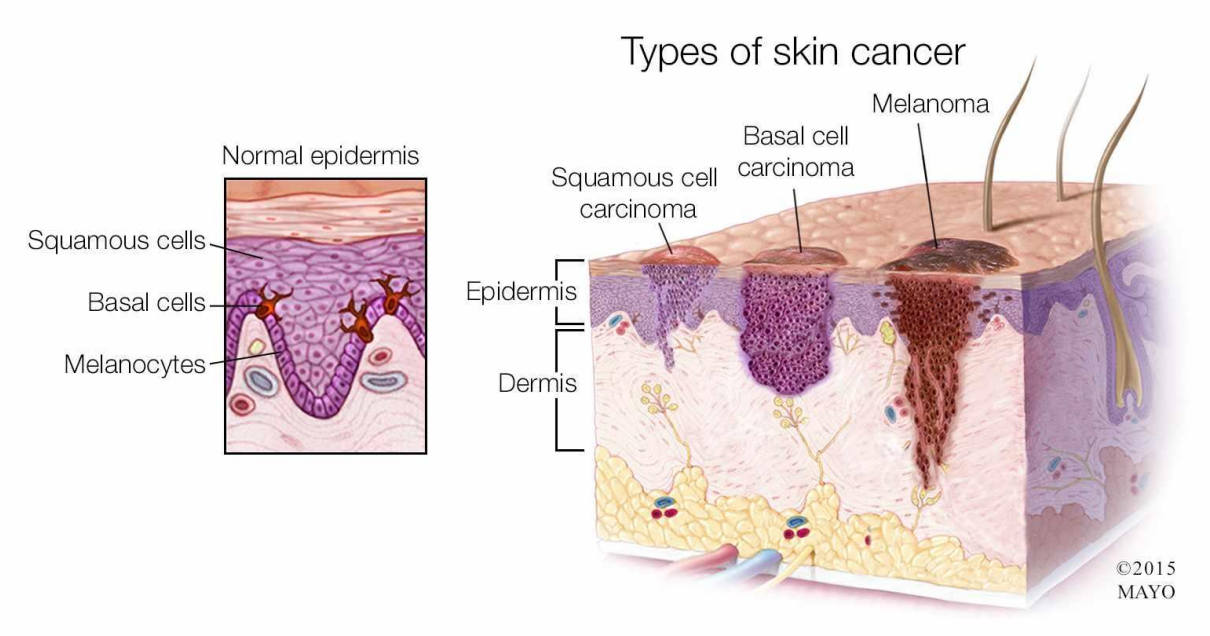

Figure 5: Type of skin cancer*. From the left to the right squamous cell carcinoma, basal cell carcinoma and melanoma.*

3.1 Cutaneous Squamous cell carcinoma

Cutaneous Squamous cell carcinoma (cSCC) is the second most common human malignancy, often arising from the progression of benign lesions called actinic keratosis (AK). The progression from AK to cSCC is likely a multistep process involving sequential DNA mutation in tumor suppression genes and to a less extent in proto-oncogenes, leading to increase of genomic instability and/or loss of cell cycle control (Missero). The most common causes of this type of cancer is ultraviolet (UV) irradiation, and to much lesser extent, ionizing irradiation, human papillomavirus, chemical agents immunosuppression drugs and chronically injured or inflamed skin. UV are directly genotoxic, forming dimers of pyrimidines in DNA and leave a distinctive signature. Mutations are predominantly C to T translation, including CC to TT base changed. A very frequent and early target is the tumor suppressor gene p53. In cells with dysfunctional p53, cell cycle arrest or apoptosis is prevented upon a second dose of UV, leading to clonal expansion of defective cells (Zhang et al., 2001). Similarly to p53, NOTCH1 and NOTCH2 are often inactivated, consistent with their crucial role in keratinocyte differentiation (Martincorena et al.). Similarly, the cell cycle inhibitor gene CDKN2A, the protocadherin FAT1, the chromatin remodeling genes KMT2D and KMT2C (MLL3) are likely to act as tumor suppressor (South et al.). Oncogenic activating mutations in HRAS and in KRAS have been identified in 3–10% of cSCC. However, other genes involved in the RTK/RAS/PI3K pathway are also mutated in a relatively low percentage of cases and therefore overall this signaling pathway is affected (Li et al.). Novel candidate tumor suppressors with putative links to cancer or differentiation, PARD3 and RASA1, were also identified as possible drivers in cSCC (Pickering et al.). Additional mutations have been included by Imman et al. HRAS, MAP3K9, PTEN, SF3B1, VPS41 and WHSC1 all of which are known genetic alterations in human malignancies (Inman et al.).

On the other hand, UV-A radiation causes cell and DNA injury via the formation of reactive oxygen species, such as hydrogen peroxides and hydroxyl radicals and 8-oxo-guanine formation, leading to chromosomal aberrations and widespread alterations in cellular proteins and lipids. These molecules are formed after UV-A radiations that are directly absorbed by endogenous intracellular photo-detectors such as porphyrins and NADH. UVA can indirectly induce DNA mutations through production of reactive oxygen species (ROS) as well ultraviolet radiation also down-regulates host immune function by the up-regulation of the action of suppressor T cells.

Furthermore, Human Papilloma Virus (HPV) is an etiological factor, which leads to squamous cell carcinoma onset. HPV is an encapsulated, double strand-DNA virus that infect epithelial cells. It produces specific viral proteins encoded by the E6 and E7 genes, which bind directly the tumor suppressor gene products p53 and pRB thereby affecting their function. Recent studies have shown that the viral infection alone does not lead to tumor formation, but it is necessary the recruitment of other carcinogenic factors, such as UV irradiation or ionizing irradiation, to have the spontaneous formation of tumor mass. Therefore, p53 mutant clones expand in chronically UV exposed skin to the expenses of normal surrounding cells, resulting in a substantial number of keratinocytes predisposed to cancer. Some mutations are involved in development of Squamous Cell Carcinoma (Fig. 6).

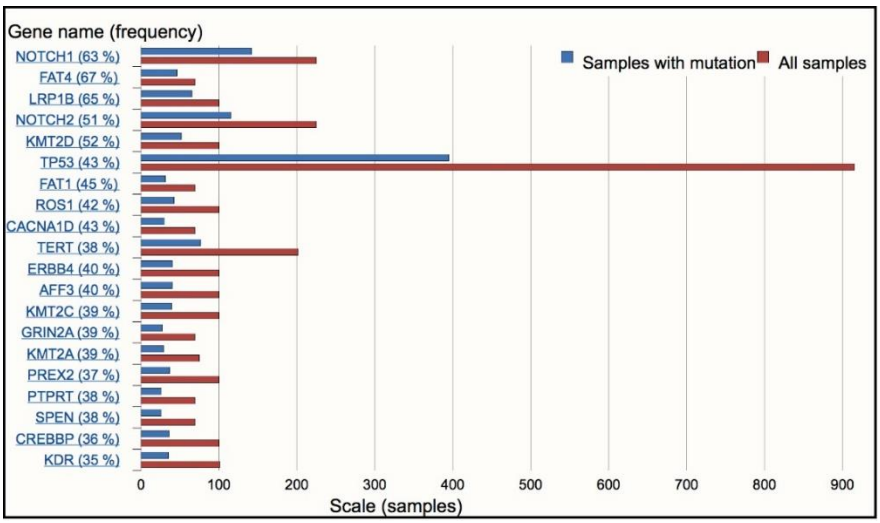

Figure 6: Top 20 genes frequently mutated in skin squamous cell carcinoma. *From COSMIC v84 13-feb-2018: http://cancer.sanger.ac.uk/cosmic*

3.2 p63 in cancer

ΔNp63a is the main p63 isoform expressed in the basal layer of the epidermis and in SCC and controls several biological functions such as cell proliferation and stem-ness, differentiation, survival, senescence and adhesion (Missero and Antonini). ΔNp63 has been proposed to act as an oncogene and cells that express high levels of it acquire a growth advantage in early stages of squamous cell carcinoma (Keyes et al.; Ramsey et al.; Ramsey et al.; Rocco et al., 2006). p63 overexpression is observed in up to 80% of Head & Neck SCC (HNSCC) and lung SCC, where p63 genomic locus is often amplified (Hibi et al., 2000; Massion et al., 2003; Tonon et al., 2005).

In HNSCC, ΔNp63α expression promotes survival by inhibiting TAp73 pro-apoptotic functions (DeYoung et al., 2006; Rocco et al., 2006).Furthermore, in HNSCC, p63 preferentially interacts with SOX2 and jointly regulating gene expression and exhibits genomic overlapping occupancy in a large number of loci (Watanabe et al.). Moreover, Saladi et al. demonstrate that ACTL6, a chromatin remodeling factor, which belong to SWI/SNF complex, is co-amplified in HNSCC as TP63 gene. ACTL6A and p63 physically interact and cooperatively control the transcriptional program promoting cell proliferation suppressing differentiation in head and neck squamous cell carcinoma, in

part through activation of the Hippo-YAP pathway via their regulators including WWC1. Indeed, ectopic ACTL6A/p63 expression promotes tumorigenesis (Saladi et al.).

The above-mentioned studies indicate that p63 plays a complex role in SCC derived from various epithelial tissues; but little is known about p63-specific functions in SCC of the skin. In human and mouse skin p63 has a basal-layer-like distribution in premalignant lesions and in low-grade cSCCs, whereas its expression is broadly distributed in high-grade cSCCs (Missero and Antonini). It has become progressively clear that ΔNp63 isoforms favor early stages of skin tumorigenesis by inhibiting senescence and/or apoptosis (Keyes et al.; Ramsey et al.). Ablation of p63 in mouse cSCC induces apoptosis and tumor regression at least in part by impairment of FGFR2 signaling (Ramsey et al.). Nevertheless, a recent study leaded by Devos et al. (2017) shows that mice overexpressing ΔNp63α are characterized by a hair coat defect and mild epidermal hyperplasia with expansion of each epidermal layer and no signs of inflammation (Devos et al.). The hair coat phenotype was in line with previous observations in a ΔNp63a tetracycline-inducible mouse model system (Romano et al.). However, in the latter mouse model, p63 overexpression was more pronounced, causing epidermal hyperplasia, dry and scaly skin, and severe morbidity, leading to early death. To test whether induced ΔNp63a expression confers an advantage in the tumorigenesis process, Devos et al. demonstrated by chemical carcinogenesis, that the onset of benign lesions, that is, papillomas, was accelerated by ΔNp63α overexpression in a dose-dependent manner, and increased number of papillomas was observed in time with a persistently higher number at late time points (Devos et al.). These studies provide evidence that ΔNp63α overexpression observed in human SCCs results in a proliferative advantage for tumorigenic cells at early stages of carcinogenesis, and they are complementary to previous studies showing that p63 is required for skin SCC formation and maintenance (Ramsey et al.). Indeed, genetic ablation of p63 in mouse SCC caused

tumor regression associated with inhibition of cell proliferation and induction of apoptosis, without any adverse consequence on normal epithelia.

4. Biology of Poly (ADP-Ribose) Polymerases (PARPs)

The protein family of poly (ADP-Ribose) Polymerases (PARPs), also named diphtheria toxin-type ADP-ribose transferases, is composed of multi-domains proteins identified originally as DNA repair factors. There are 17 PARPs enzymes in human and 16 in mice (Bai). The majority of the PARP-mediated function are related to cellular stress response, nevertheless, latest studies, have enlarged the functions of PARP enzymes, ranging from tumor biology to oxidative stress, from inflammatory to metabolic diseases. The most well studied family member, PARP1, contains three zinc-finger DNA binding domains; an auto-modification domain in which is present a BRCT domain, involved in protein-protein interaction; a WGR domain for nucleic acid binding and a catalytic domain. The catalytic domain is responsible for the enzymatic activity of the protein (Fig.6).

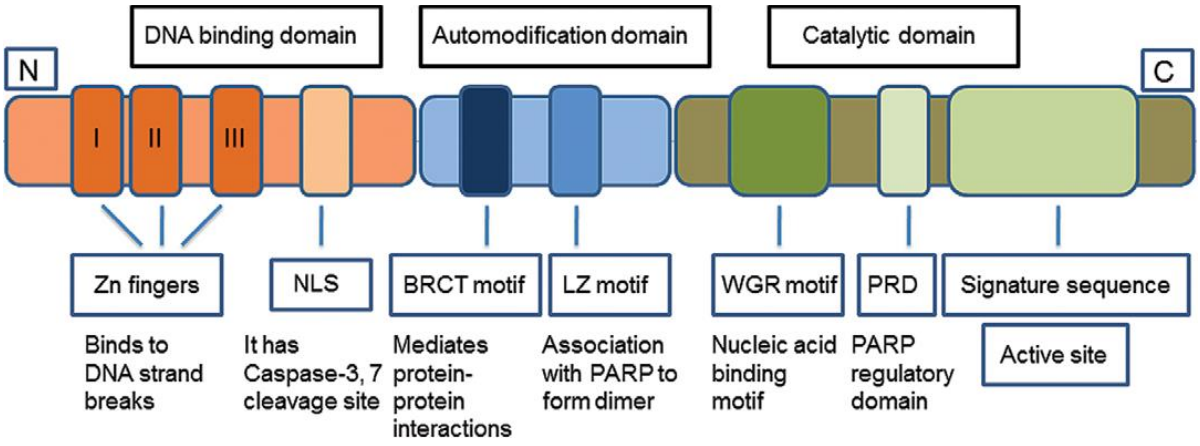

Figure 7: Structure of PARP-1 enzyme*. It contains a (1) DNA binding domain with three zinc fingers and an cleavage site. (2) an auto-modification domain that include a BRCT motif to mediate the protein-protein interaction and a LZ motif to form dimers with itself. (3) a catalytic domain composed of WGR motif for the binding of nucleic acid, and an active site that catalyze the reaction (From Rajawat, therapeutic Targeting of Poly(ADP-Ribose) Polymerase-1 (PARP1) in Cancer: Current Developments, Therapeutic Strategies, and Future Opportunities Medicinal Research Reviews 2017.*

4.1. Enzymology of PARPs

The ADP-ribosylation is a post-translational modification where single units (mono-ADP-ribosylation) or polymeric chains (poly-ADP-ribosylation) of ADP-ribose are loaded on the protein targets by ADP-ribosyl-transferases. This post-translational modification can be added onto different amino acids such as aspartate, glutamate, lysine, arginine and cysteine and is involved in several process including DNA repair, transcription, translation, cell signaling and cell death. Furthermore, dysregulation of ADP-ribosylation has been linked to diseases including cancer, diabetes, neurodegenerative disorders, inflammation and heart failure. Interestingly, ADP-ribosylation has been shown to be a therapeutically important modification in cancer and other diseases (Daniels et al.).

PARP enzymes bind and cleave NAD^+ to nicotinamide (NAM) and ADP-ribose (ADPr) and couple one or more ADPR units to acceptor proteins that are called mono, oligo, or poly-(ADP-Ribosy)-ation as a function of the number of ADPr units. In particular, PARP-1, PARP-2, TNK1 and TNK2 (Tankyrase 1 and Tankyrase 2) synthesize branched Poly (ADP-ribose) polymers, whereas the others PARPs are either mono or oligo ADPr-transferases, with the exception of PARP-13 that is inactive. The catalytic domain is responsible for the enzymatic activity of the protein. This domain catalyzes the addition of ADP-ribose chains to target proteins, including PARPs enzymes.

Poly-ADP-Ribose (PAR) has a rapid turnover and a short half-life. A series of enzymes that are involved in the degradation of ADPr groups such as poly (ADP-ribose) glycohydrolase (PARG), ADP-ribosyl-acceptor hydrolase-3 (ARH3), ADP-ribosyl lyase.

The majority of cellular PARP activity is localized to the nucleus, although the cytoplasm is known to have PARP enzymatic activity too. PAR and PARylated proteins are present in the cytoplasm and in other cellular compartments such as mitochondria, moreover the PAR-degrading activity is present in all compartments but the PARG activity is absent in mitochondria, suggesting that the degradation of PAR chains changes between compartments.

Historically, DNA damage was described as the strongest signals that led to increase PARylation in cells; nonetheless, the activity of the PARPs is also regulated by different signals such as post-translational modifications and other signal transduction pathways.

4.2. PARP1 and poly-(ADP)-ribosylation in DNA repair

PARP1 has a DNA-binding domain containing three zinc finger motifs, the first two of which are primarily responsible for the recognition of various features in DNA secondary structure, such as single- and double strand breaks, cruciform structures and nucleosome linker DNA(Langelier et al.).

The roles of PARP1 in the DNA Damage Repair (DDR) have been studied extensively. Induction of various kinds of DNA damage results in rapid recruitment of PARP1 to sites of damage through its DNA-binding domain (Huambachano et al.). This stimulates the catalytic activity of PARP1, which results in the synthesis of PAR chains on itself and on histones and non-histone proteins (Gagne et al., 2008; Jungmichel et al.). Upon DNA damage induction, chromatin orchestrates rapid changes in their architecture. DNA damage triggers the localized expansion of chromatin in an ATP-dependent manner, in particular PARP1 recruits to the site of the DNA damage the proteins involved in the DDR and in DNA metabolism, which can bind to PAR on PARP proteins through non-covalent interactions. Single strand breaks (SSBs) are very rapidly detected and bound by PARP1. This is followed by the addition of PAR onto PARP1 itself, resulting in its activation, and the addition of PAR on other target proteins. The mechanism by which PARP1 activates SSB repair could be by promoting the accumulation of SSB repair components and/or their stabilization at SSBs. A core factor in SSB repair is X-ray repair cross-complementing protein 1 (XRCC1), which acts as a scaffold for SSBR proteins, thereby stimulating the repair process (El-Khamisy et al., 2003). The rapid recruitment of XRCC1 to SSBs is dependent on PARP1 or PARP2. PARP1 is also involved in the Nucleotide Excision Repair (NER) pathway that is responsible for the repair of bulky DNA lesions that arise from multiple sources of mutagenic agents, including ultraviolet

(UV) irradiation. Recent studies have shown that PARP1 functions in the initial steps of damage recognition in global genome nucleotide excision repair (GG-NER), which is a dominant sub-pathway of NER. The NER pathway uses multiple proteins for damage recognition, removal of stretches of ssDNA that contain damage, gap filling of the excised region and ligation. UV damage is recognized by xeroderma pigmentosum group C-complementing protein (XPC) and RAD23B, which associate with the DNA damage-binding protein 1 (DDB1)–DDB2 complex (Marteijn et al.). XPC binds to PAR through its PAR-binding sites, and this is important for XPC recruitment to UV lesions. PARP1 also interacts with DDB2, and its binding to DDB2 at chromatin damaged by UV radiation stimulates its catalytic activity (Pines et al.; Robu et al.). PARP1 has been also implicated in the control and recruitment of important Homologous Recombination (HR) proteins. Most important among them is breast cancer type 1 susceptibility protein (BRCA1), which controls not only the initial steps of DSB resection but has also been implicated in the loading of RAD51 onto DNA, which is essential for strand exchange during HR(Li and Yu). Recent studies have also shown a role of PARP1 in the Non Homologous End Joining pathway (NHEJ). This DNA repair pathway is active throughout the cell cycle but is the preferred mechanism for DSB repair in G1, when a DNA template that could be used for HR is absent. In vitro studies have shown that PARP1 can PARylate DNA-dependent protein kinase catalytic subunit (DNA-PKcs), which is an important NHEJ factor. PARylation stimulates the kinase activity of DNA-PKcs, without the requirement of the KU70–KU80 complex (Rybanska et al.; Spagnolo et al.). Furthermore, PARP1 can also recruit the chromatin remodeler chromo-domain helicase DNA-binding protein 2 (CHD2) to sites of DSBs through the recruitment of XRCC4 (Luijsterburg et al.).

4.3. PARP1 involvement in chromatin structure and gene transcription control

The role of PARP1 is historically associated with DNA damage repair, but in the last two decades, a growing literature has revealed an important role for PARP1 in the regulation of chromatin architecture, gene expression and transcription. PARP1, enzymatically silent, inhibits transcription by contributing to the condensation of chromatin, which create a barrier against gene transcription. However, once it is activated by environmental stimuli and developmental signals, PARP1 can modify itself and chromatin–associated proteins, and allows the loosing of chromatin to facilitate gene transcription. Recent studies have demonstrated functional association of PARP1 with a variety of regulatory complexes, including a TLE (Transducin-like enhancer of split), co-repressor complex, a Mediator co-regulator complex, a condensing I/XRCC1 repair complex, a macroH2A1.1 nucleosome complex and a CTCF insulator complex (Kraus, 2008). Therefore, PARP1 regulates gene expression through a variety of mechanisms, including: (1) modulating chromatin or the activity of enzymes that modulates chromatin such as KDM5b, a histone demethylase, ISWI and ALC1 or DNMT1 a DNA-methylase; (2) functioning as a transcriptional co-regulator, which may promote factor exchange; (3) modulating the DNA methylation (Kraus and Hottiger) (Figure 8).

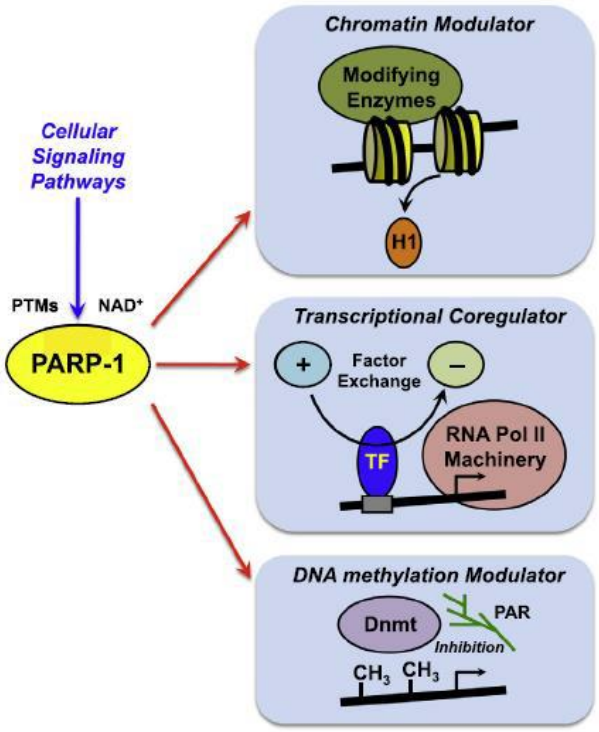

Figure 8: PARP-1 regulates gene expression through a variety of mechanisms*: (1) as a chromatin modulator; (2) as a co-regulator: (3) as a modulator of DNA methylation. From Kraus, Hottiger PARP-1 and gene regulation: Progress and puzzles Molecular aspect of Medicine 2004*

Many early studies on the nuclear functions of PARP1 and PAR showed that they can modulate chromatin structure, promoting the de-compaction of chromatin by reducing interactions between nucleosomes and reducing nucleosome-dependent higher-order structures (Kraus and Lis, 2003). For example, in Drosophila, activation of dPARP (the PARP1 homologue) promotes de-condensation of chromatin in response to heat shock or other cellular signaling pathways (Petesch and Lis; Tulin and Spradling, 2003). Furthermore, PARP1-dependent PARylation promotes de-condensation mediating the PARylation of histone H1 or competing with it for binding to nucleosomes (Kim et al., 2004; Krishnakumar et al., 2008). Its effects on core histones or core histone variants mediate other effects of PARP-1 on chromatin. PARP1 has been shown to PARylate histones, as well as non-histone, chromatin-associated proteins. Histone ADP ribosylation (either mono- or poly-) affects the biochemical properties of the histones, thus altering nucleosome structure, or promotes interactions with chromatin-modulating proteins that contain ADPR-binding modules (Messner and Hottiger). Emerging evidence supports the conclusion that damaged DNA is not required to stimulate the

enzymatic activity of chromatin-associated PARP1. In addition to its direct effects on components of chromatin, PARP1 may also modulate the localization and activity of a broad array of histone modifying and nucleosome remodeling enzymes. For example, PARylation of KDM5B, a histone lysine demethylase that acts on histone H3 lysine 4 trimethyl (H3K4me3), inhibits KDM5B binding and demethylase activity at specific sites in the genome(Krishnakumar and Kraus). This leads to an increase in the levels of H3K4me3 at the promoters of PARP1-regulated genes, supporting continued gene expression. Likewise, physical and functional interactions with PARP1 can alter the activity of ATP-dependent nucleosome remodeling enzymes.

In addition to its role as a modulator of chromatin structure to control gene expression, PARP1 has also been shown to act as classical transcription factor-dependent coregulatory protein. As a co-regulator, PARP1 functions with the basal transcription machinery, other co-regulators with enzymatic activities (e.g., histone-modifying enzymes and nucleosome remodelers), and sequence-specific DNA-binding transcription factors, such as NF-κB, HES1, ELK1, SOX2, and nuclear hormone receptors (Kraus and Lis, 2003). In this regard, two types of coregulatory functions have been ascribed to PARP1: (1) scaffold and (2) exchange factor. PARP1 may act as scaffold by interacting with and promoting the recruitment of other co-regulators independent of its DNA binding and catalytic activities. In this regard, PARP1 has been shown to interact with the protein arginine methyltransferase PRMT1 and the protein acetyltransferase p300/CBP to support NF-κB dependent gene expression (Hassa et al., 2003; Hassa et al., 2005). Furthermore, PARP1 facilitates the binding of the pioneer transcription factor SOX2 to poised genomic loci in embryonic stem cells independently of its poly-(ADP-ribosyl) transferase activity. PARP1 is required in this context to maintain the expression of pluripotency genes and the stem cell phenotype (Liu and Kraus). In response to appropriate cellular signals, PARP1 PARylates SOX2 at the FGF4 enhancer, promoting the dissociation and degradation of SOX2 and leads to enhanced expression of FGF4 (Gao et al., 2009).

Finally, PARP1 seems to have a function also in the regulation of DNA methylation. PARP1 can alter the methylation of genomic DNA by regulating the expression or activity of the DNA methyltransferase DNMT1 (Caiafa et al., 2009; Caiafa and Zampieri, 2005). In this regard, PARP1 may directly interact with DNMT1 through newly synthesized PAR polymers to inhibit DNMT1 DNA methyltransferase activity (Reale et al., 2005). Furthermore, PARP1 has been shown to interact functionally with the methyl-cytosine dioxygenase TET2, an enzyme that catalyzes the conversion of 5-methylcytosine (5mC) to 5-hydroxymethylcytosine (hmC). These interactions may play a key role during somatic cell reprogramming (Doege et al.).

Aim I

The first aim of my PhD project focus the attention on the regulation of transcription leaded by p63 in cutaneous squamous cell carcinoma. The transcriptional dysregulation is one of the fundamental features in tumors and the dysregulation of key transcription factors lead to alteration in the normal cell state provoking pathological changes.

p63, being a key transcription factor in the homeostasis of epidermal tissue, if it is altered, can cause different skin pathology.

In this first part of my thesis, I focus the attention on the p63 transcriptional program in cSCC, characterizing the molecular and functional role of the interaction between p63 and PARP1 in cSCC.

Results

1. p63 is overexpressed in cutaneous squamous cell carcinoma (cSCC)

In contrast to p53 that is usually mutated in cancer, p63 is rarely mutated but often overexpressed in squamous cell carcinoma and has a role as a pro-oncogene (Hibi et al., 2000; Li et al.; Massion et al., 2003; Tonon et al., 2005). Importantly, cSCC maintenance has been shown to depend on p63 in a mouse model of skin carcinogenesis (Ramsey et al.). In spite of these findings, the role of p63 in cutaneous skin cancer remains poorly investigated. Preliminary data of our laboratory indicate that p63 is overexpressed of p63 in cSCC. p63 was analyzed by quantitative immunofluorescence analysis in a large cohort of actinic keratosis (AK), cutaneous SCC (cSCC) and normal skin (NS) (Fig. 9 A-B). Interestingly, analysis of global gene expression of microarray performed in cSCC, AK and NS show high levels of p63 mRNA in tumor skin compared to healthy skin (Fig. 9 C). Accordingly, higher p63 protein and mRNA levels were detected also in several human cSCC cell lines as compared to primary keratinocytes (Fig. 9 D-E). These data suggest that the elevated p63 expression in AK and cSCC may favor tumor formation and/or progression in human skin.

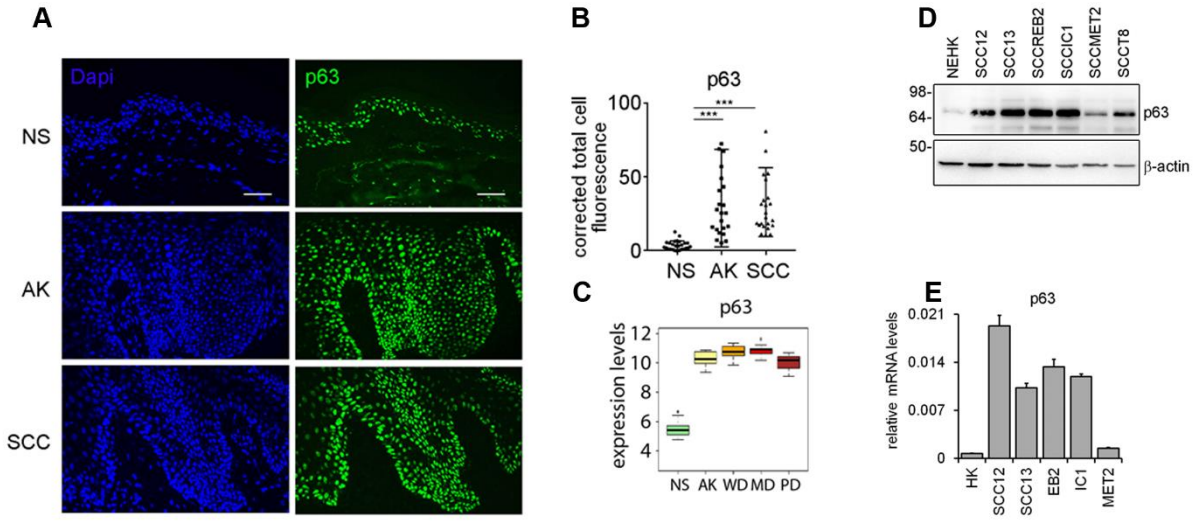

Figure 9: p63 is over-expressed in AK and cSCC*: A-B) IF analysis with p63 (green) specific antibodies was performed on tissue microarrays in AK, SCC and NS. Histograms represent quantitative comparison of IF normal skin (n=32), AK (n=10) and SCC (n=30) . *** p-value <0.05. (C) p63 mRNA expression was compared in published microarray data sets derived from NS, AK, and SCCs. (D-E) p63 protein expression levels in the indicated skin SCC derived cell lines, and normal newborn keratinocytes.*

2. p63 gene regulation in cSCC

Subsequently, to identify the genes mainly regulated by p63 we performed ChIP-seq experiments and RNA-seq experiment performed in a cSCC cell line depleting the endogenous p63 by specific siRNA (Fig. 10A). We focused the attention on the differentially expressed genes (DEGs) directly regulated by p63. Next, to understand the biological process and pathway mainly altered by p63 depletion, we first divided genes in downregulated and upregulated upon p63 knockdown and then we performed a Gene ontology (GO) analysis through DAVID database of the two classes of genes. Interestingly, the downregulated genes are mainly enriched in cell cycle, mitosis, DNA repair and DNA replication biological process. These data suggest a crucial role of p63 in the regulation of genes involved in cell proliferation.

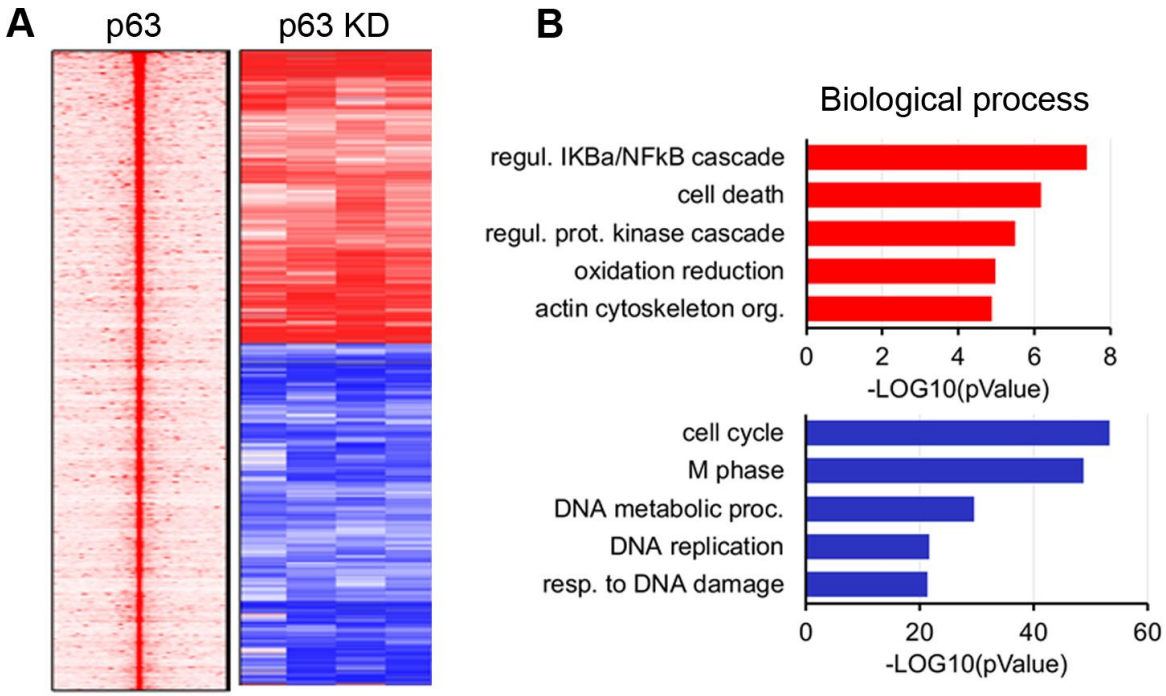

Figure 10: Identification of genes directly regulated by p63 in cSCC. *A) ChIP seq using p63 antibodies in cSCC coupled to gene expression profile obtained from p63- depleted SCC13 RNA-seq data. B) The most significant enriched GO categories (BP) of upregulated (top) and downregulated (bottom) genes directly regulated by p63 are indicated (DAVID gene expression analysis).*

3. p63 sustain cSCC cell proliferation

To assess the biological significance of the above findings, we evaluated the consequences of modulating p63. p63 depletion strongly inhibited DNA synthesis and cell proliferation as measured by 5-bromo-2'-deoxyuridine (BrdU) incorporation (Fig. 11 A-B). Consistent with these findings, depletion of p63 significantly reduced the clonogenic capability of SCC cells, which in the absence of p63 failed to proliferate into large colonies and produced only small colonies (Fig. 11C). To further test its regenerative potential, we performed an oncosphere assay, in which cells are grown in defined serum-free medium under ultra-low attachment conditions and form colonies in suspension. Knockdown of p63 inhibited oncosphere formation in cSCC cells, indicating a central role for p63 in the maintenance of an undifferentiated, proliferative population in squamous epidermal tumors (Fig. 11D).

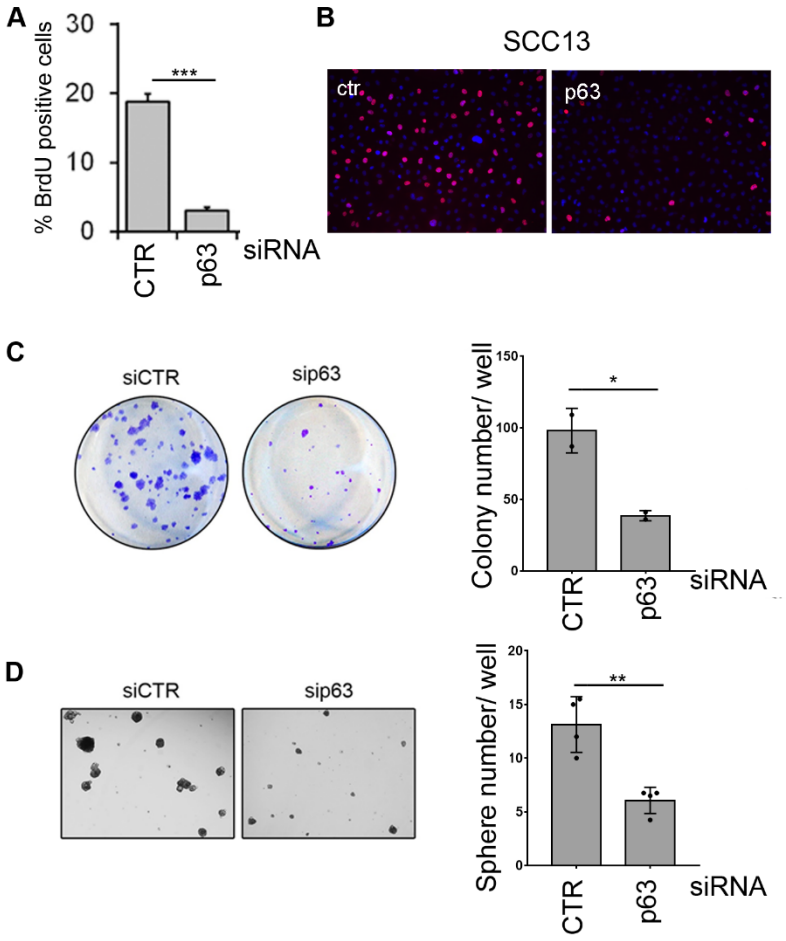

Figure 11: Cell proliferation is strongly reduced in p63 depleted SCC. *A-B) BrdU in cSCC depleted for p63.C) p63 depleted SCC13 have a reduced ability to form colonies when plated as single cells. D) Similarly, p63 depleted SCC13 have a reduced ability to form spheroids in low attachment condition.*

4. PARP1 is a novel interactor of p63.

   Transcription factors are not easily targeted by small molecules. To identify novel p63 partners that may be amenable for therapeutic targeting, we set up to identify the p63 interactome to search for protein partners with an enzymatic activity. To this end we performed an immunoprecipitation (IP) followed by a LC-MS/MS from nuclei of HEK293T cells transfected with FLAG-ΔNp63α (Fig.12 A-B).

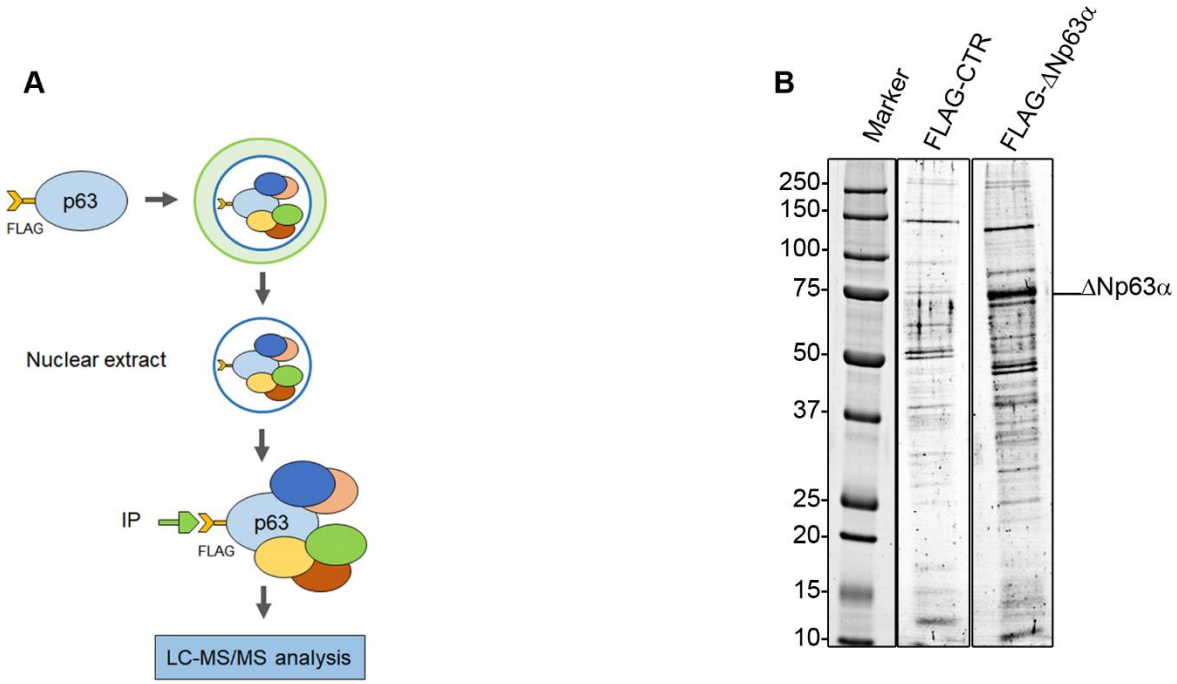

Figure 12: Identification of p63 protein partners*: A) Schematic representation of IP-MSMS strategy B) SDS-PAGE of Immunoprecipitated samples (CTR and FLAG-ΔNp63α).*

Protein partners were classified in two major categories of interests: chromatin associated proteins, and protein associated to the proteasome or co-chaperones

Chromatin associated proteins

swiss prot	gene name	description	n° peptides
P22670	RFX1	MHC class II regulatory factor RFX1	3 (1)
P09874	PARP1	Poly [ADP-ribose] polymerase 1	5 (0)
P42166	TMPO, LAP2A	Lamina-ass Polypeptide 2, alpha	4 (2)
Q9Y265	RUVBL1	RuvB-like 1	11 (9)
P35998	ILF2, NF45	Interleukin enhancer-binding factor 2	3 (1)
Q53X93	CREB1	CREB1 protein	2 (1)
P61978	HNRPK	Heterogeneous nuclear ribonucleoprotein K	4 (1)
P61964	WDR5	WD repeat-containing protein 5	5 (3)
Q96P16	RPRD1A	Regulation of nuclear pre-mRNA dom.cont. prot. 1A	4(1)
P19387	POLR2C	DNA-directed RNA polymerase II subunit RPB3	2 (1)
Q9BQA1	WDR77	Methylosome protein 50	7(4)
O95983	MBD3	Methyl-CpG-binding domain protein 3	4(2)
P50402	EMD	Emerin	4(1)
Q9Y657	SPIN1	Spindlin-1	5(2)
P10412	HIST1H1E	Histone H1.4	7(3)
P16401	HIST1H1B	Histone H1.5	4(3)

proteasome proteins and co-chaperones

swiss prot	gene name	description	n° peptides
Q99460	PSMD1	26S proteasome non-ATPase regulatory Sub 1	2 (1)
P55072	VCP	Transitional endoplasmic reticulum ATPase	3 (2)
Q99615	DNAJC7	DnaJ homolog subfamily C member 7	2 (1)
P62191	PSMC1	26S protease regulatory sub 4	4 (1)
P35998	PSMC2	26S protease regulatory subunit 7	4 (1)
O00231	PSMD11	26S proteasome non-ATPase regulatory sub. 11	4 (2)
P31689	DNAJA1	DnaJ homolog subfamily A member 1	2 (1)
P62195	PSMC5	26S protease regulatory subunit 8	6 (3)
Q15008	PSMD6	26S proteasome non-ATPase regulatory sub. 6	5 (1)
Q9BT78	COPS4	COP9 signalosome complex subunit 4	9 (4)
P62333	PSMC6	26S protease regulatory subunit 10B	5 (4)
Q9UNM6	PSMD13	26S proteasome non-ATPase regulatory sub. 13	3 (2)
P82933	MRPS9	28S ribosomal protein S9, mitochondrial	3 (0)
Q92905	COPS5	COP9 signalosome complex subunit 5	4(2)
Q7L5N1	COPS6	COP9 signalosome complex subunit 6	2(1)
P23396	RPS3	40S ribosomal protein S3	7(1)
Q9NXV2	KCTD5	BTB/POZ domain-containing protein KCTD5	3(2)

Table 1: List of the protein partners divided in 1) Chromatin associated protein 2) proteasome proteins and co-chaperones

We focused on PARP1. To validate the interaction between PARP1 and p63, we performed an IP-Western Blot in HEK293T cells co-transfected with a FLAG-PARP1 (bait) and a MYC-p63. The immunoprecipitation demonstrated that the two protein can interact (FIG 14A) in exogenous condition. We tested also an interaction with PARP2, the other nuclear family members of the PARPs, but we did not identify any interaction

(Fig 14B). The HDAC1, identified in our screening and previously reported as p63 protein partner (LeBoeuf et al.; Ramsey et al.), was used as positive control of interaction with p63 in our immunoprecipitation assay.

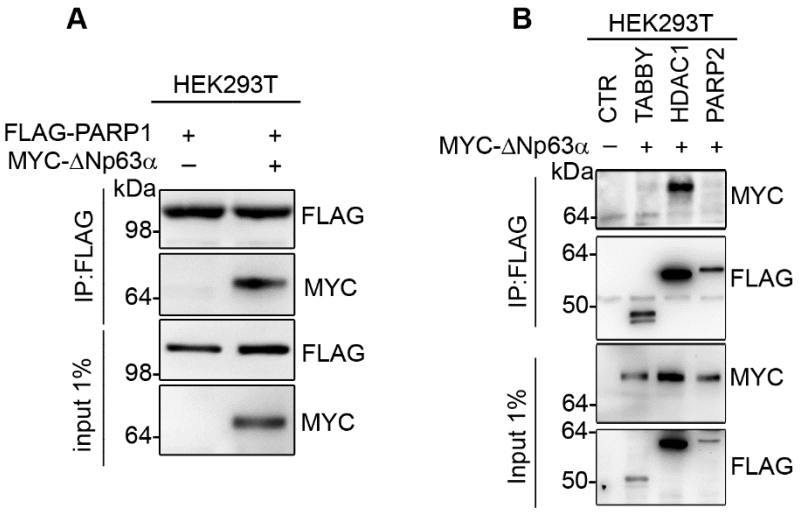

Figure 14: Validation of p63-PARP1 interaction. *A) IP-WB in HEK293T co-transfected with FLAG-PARP1 (bait) and MYC-p63. B) IP-WB in HEK293T co-transfected with FLAG-PARP2 and MYC-p63. HDAC1 is used as positive control of interaction.*

To further characterize the interaction between p63 and PARP1, we performed IP-Western blot using different p63 mutants. Two mutation are clustered in the C-terminal domain of p63 (L514F and R598L) and two clustered in the DNA binding domain of p63 (R204W and R304W) abolishing the ability to bind the DNA. These last two mutants completely abolished the interaction with PARP1, possibly suggesting that p63 and PARP1 interacts on chromatin (Fig. 15A). To confirm this hypothesis, we also performed an IP-western blot experiment using FLAG-PARP1 as bait, and TAp63α and its mutant TAp63αFWL (F16A, W20A, L23A) ectopically expressed in HEK293T. The TA isoform is unable to bind the DNA due as it forms closed dimer because its TI domain interacts with the TA domain that hides the DNA binding domain. In contrast, the FWL mutant presents three mutation in TA domain that disrupt the interaction with TI domain, thus creating a permanently open structure that binds DNA. PARP1 interacts with the mutant TAp63α FWL, but not with WT TAp63α. This reinforce the idea that the interaction between PARP1 and p63 depends on the open conformation that exposes the DNA binding domain, allowing its binding to DNA (Fig. 15B). To assess whether DNA

is required for PARP1 to interact with p63, we performed IPs in the presence of the endonuclease benzonase. In these conditions, PARP1 and p63 did not interact to each other, whereas p63 was still able to bind to other interactors such as the histone deacetyl transferase HDAC1, the SWI/SNF subunit BAF60b and to lesser extent also the transcription factor RFX1(Fig. 15C). These results suggest that p63 and PARP1 interact on the DNA possibly through some shared protein partners.

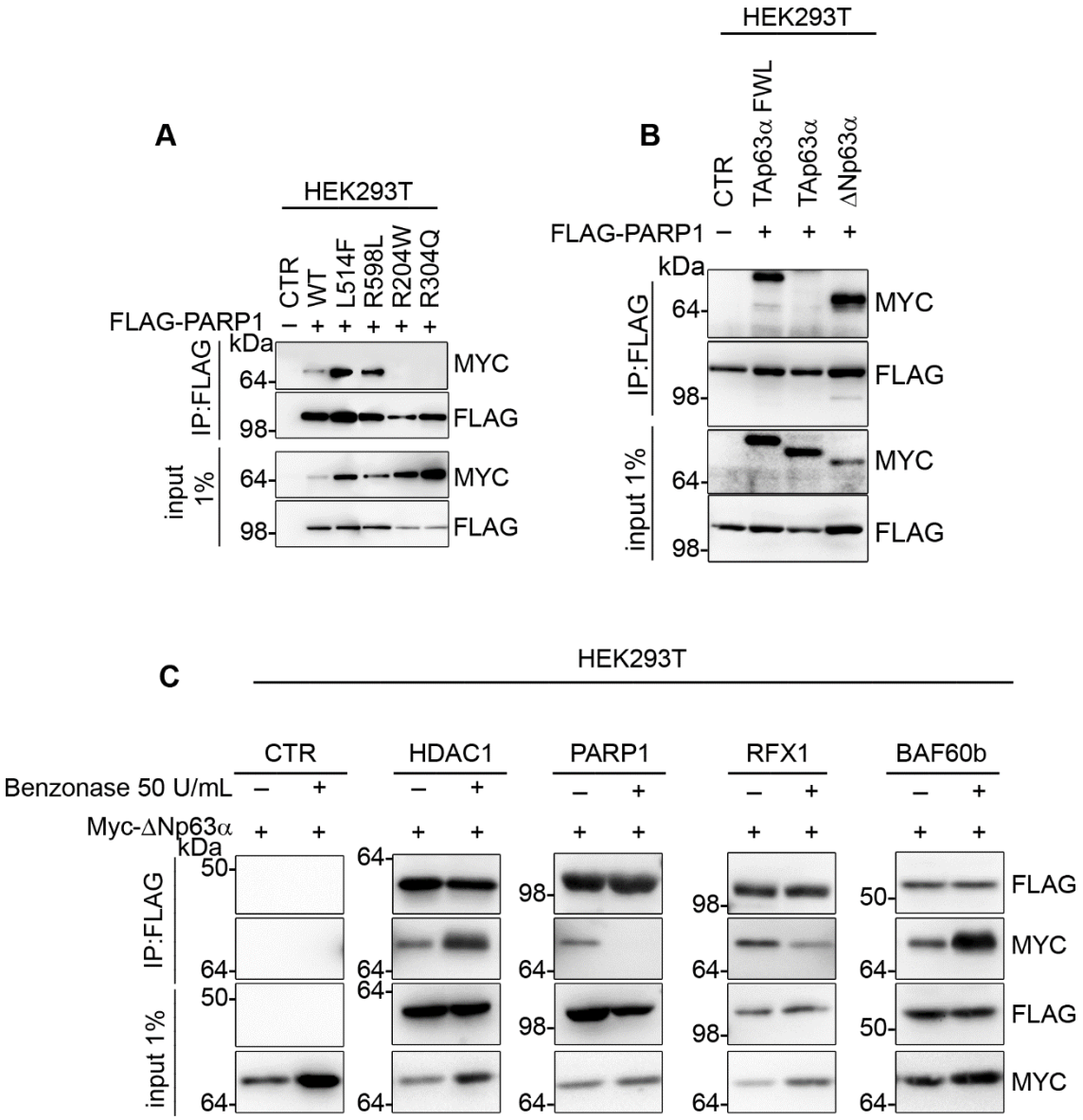

Figure 15: p63 and PARP1 interact on the chromatin*. A) IP-WB in HEK293T co-transfected with FLAG-PARP1 (bait) and p63 wild type or mutants. B) IP-WB in HEK293T co-transfected with FLAG-PARP1 (bait) and the TAp63 isoform and the TAp63FWL. ΔNp63α is used as positive control. C) IP-WB in HEK293T co-transfected with different FLAG-protein partners of p63 and MYC-p63 followed by treatment with endonuclease benzonase.*

5. PARP1 is overexpressed in cSCC

To understand the physiological role of PARP1-p63 interaction, we first assessed PARP1 expression in skin since we found that p63 is overexpressed in cSCC compared to normal skin, but little is known about the expression and the role of PARP1 in skin tumor. Immunofluorescence analysis performed on cSCC and normal skin biopsies using specific antibody for PARP1 showed that it is mainly localized in the undifferentiated and proliferative layers of the epidermis, similar to p63 (Fig. 15A). Furthermore, quantification of the fluorescence intensity signal showed an overexpression of PARP1 in tumor skin compared to healthy skin (Fig. 15B). In addition, we analyzed global gene expression of 32 biopsies of normal skin and 30 biopsies of cSCC confirming an overexpression of PARP1 mRNA levels in cSCC compared to normal skin (NS) (Fig. 15D). Accordingly, higher PARP1 protein levels were identified in different cutaneous squamous cell carcinoma as compared to normal adult or newborn keratinocytes (Fig. C, E)

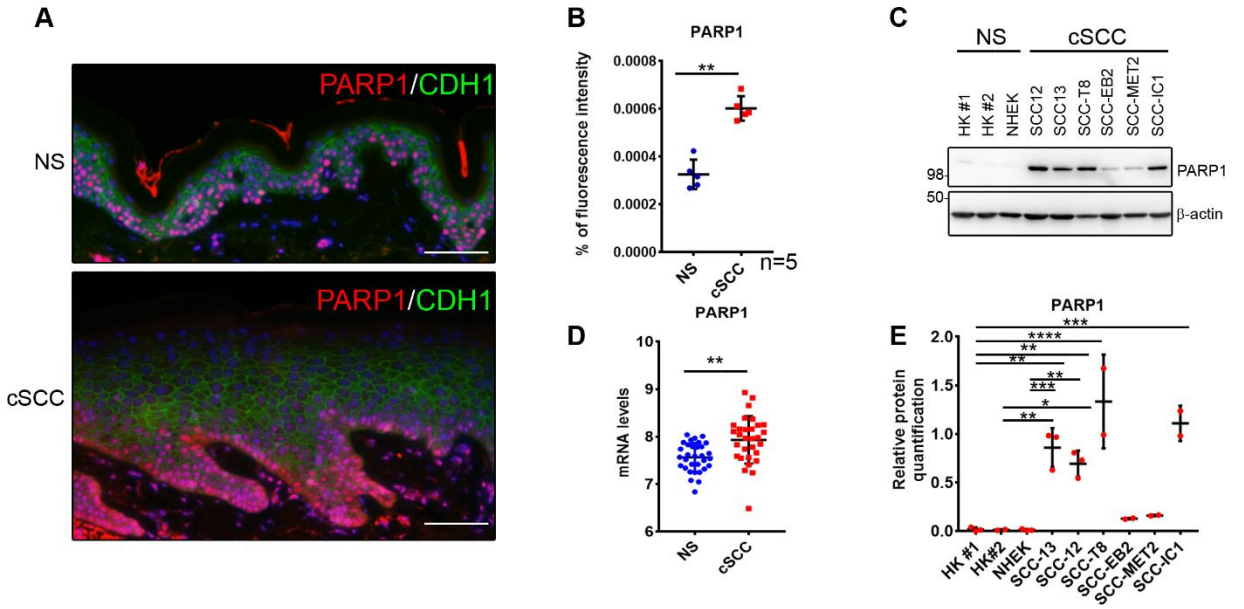

Figure 33: PARP1 is overexpressed in cSCC*. A-B) IF performed on tumor skin and healty skin with specific antibody for PARP1. CDH1 is used as marker of epithelial cells. C) WB performed on different cSCC cell lines and normal skin cell line using the indicated antibodies. In E) the relative protein quantification. D) microarray data leaded on normal skin (32) and cSCC(30) biopsies to identify the expression of PARP1 mRNA.*

Since p63 and PARP1 co-localize in cSCC skin biopsies, in the undifferentiated and proliferative layers (Fig 16B), we tested the interaction between p63 and PARP1 in a cSCC cell line by IP. Using p63 specific antibody we were able to precipitate PARP1, indicating that the two endogenous proteins interact in the relevant cells (Fig. 16A). To test whether p63 is poly-ADP-ribosylated by PARP1, we performed an IP with the macrodomain Af-1521 in cSCC cell line. This macrodomain is able to isolate all the PARylated proteins in cells. To confirm that a possible modification would be carried out by PARP1, we performed the IP with the same macro-domain in PARP1 knockdown cells. A mutant macrodomain was used as negative control. Although PARP1 PARylated itself we observed no PARylation of p63, indicating that at least under basal condition, p63 is not PARylated (Fig. 16C).

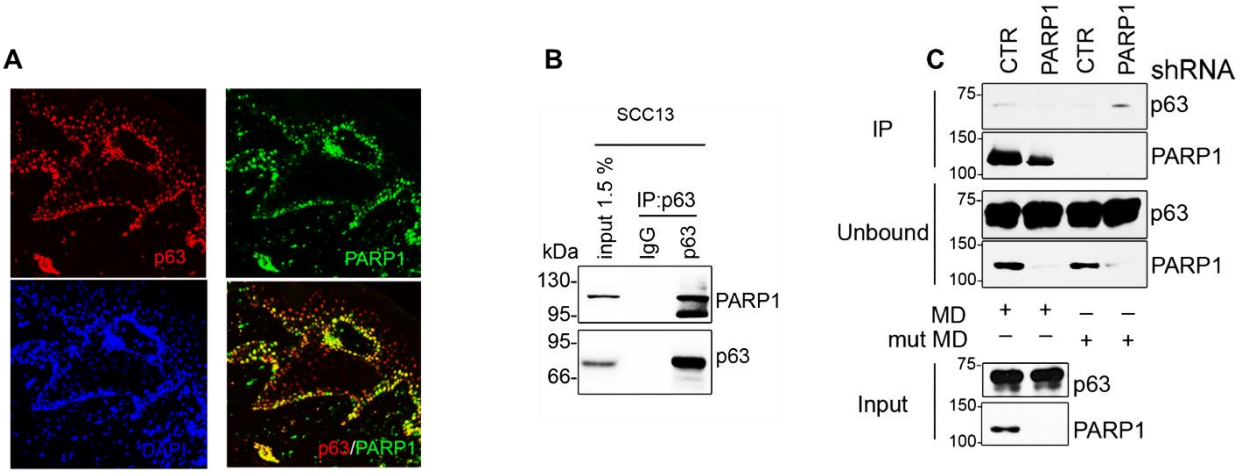

Figure 16: p63 and PARP1 interacts in cSCC*. A) IF performed on cSCC biopsies with antibody for PARP1 and p63. B) IP-WB performed in SCC13 with specific antibody for p63. C) IP in SCC13 and SCC13 depleted for PARP1 using the macrodomain Af_1521 and a mutated macrodomain unable to identify the PARylated proteins.*

6. p63 and PARP1 regulates genes involved in cell proliferation and DNA repair

To confirm the possible role of PARP1 in the p63 dependent transcription, we performed a RNA-seq analysis on cSCC depleted for PARP1 and p63 with a specific short interfering RNA. A principal component analysis (PCA) showed a movement from the right to the left for both the conditions, with a stronger perturbation for p63 compared to PARP1 (Fig 17A). All Genes regulated by PARP1 and p63 are represented with a Volcano plot, positioning the log FC on the x-axis and the –log10 of FDR on the y-axis (Fig 17B). To define the differentially expressed set of genes (DEGs) more robustly regulated by PARP1 and p63 knockdown we applied an FDR ≤ 0.05 and represent them by heat-map (Fig. 17C). Furthermore, the Pearson correlation model defined a strong genetic relationship between p63 and PARP1 perturbation, with an R square equal to 0.83 (Fig. 17D).

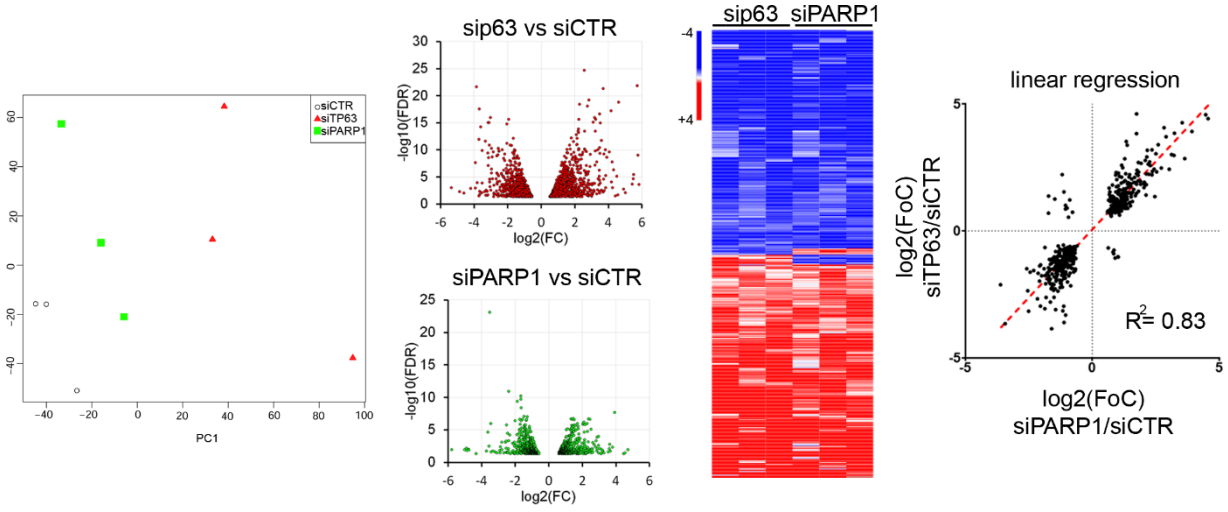

Figure 17 Genetic relationship between PARP1 and p63. *A) Principal Component Analysis (PCA) of the cSCC cell population depleted for p63 or PARP1. The white dots are associated with the control. B) Volcano plots positioning the log2FoC on the x axis and the –log10 of FDR on the y axis of the different mutants and the Wild-type. C) Heat map representation of the differentially expressed genes (DEGs). D) Linear regression and Pearson correlation for PARP1 and p63.*

Next, we separated the downregulated gene from the up-regulated genes and calculated the Hypergeometric distribution (HD) for both groups of genes (fig 18 A-B). Analysis of our expression RNA-seq data defined 1360 genes downregulated by silencing of p63 and 799 downregulated by silencing of PARP1, with 373 genes shared (Hypergeometric distribution (HD) = 3.1*e-141). Conversely, 1299 genes were upregulated upon silencing of p63 and 726 upon silencing of PARP1 with 352 genes shared (HD = 1.9*e-145). To explore the function of genes most robustly regulated by PARP1 and p63 knockdown, we performed a GO analysis using the DAVID database. Genes that are downregulated by knockdown of either proteins are predominantly enriched in cell cycle process and DNA repair. Furthermore, The KEGG pathway analysis showed an enrichment in cell cycle and DNA replication, Homologous recombination and mismatch repair.

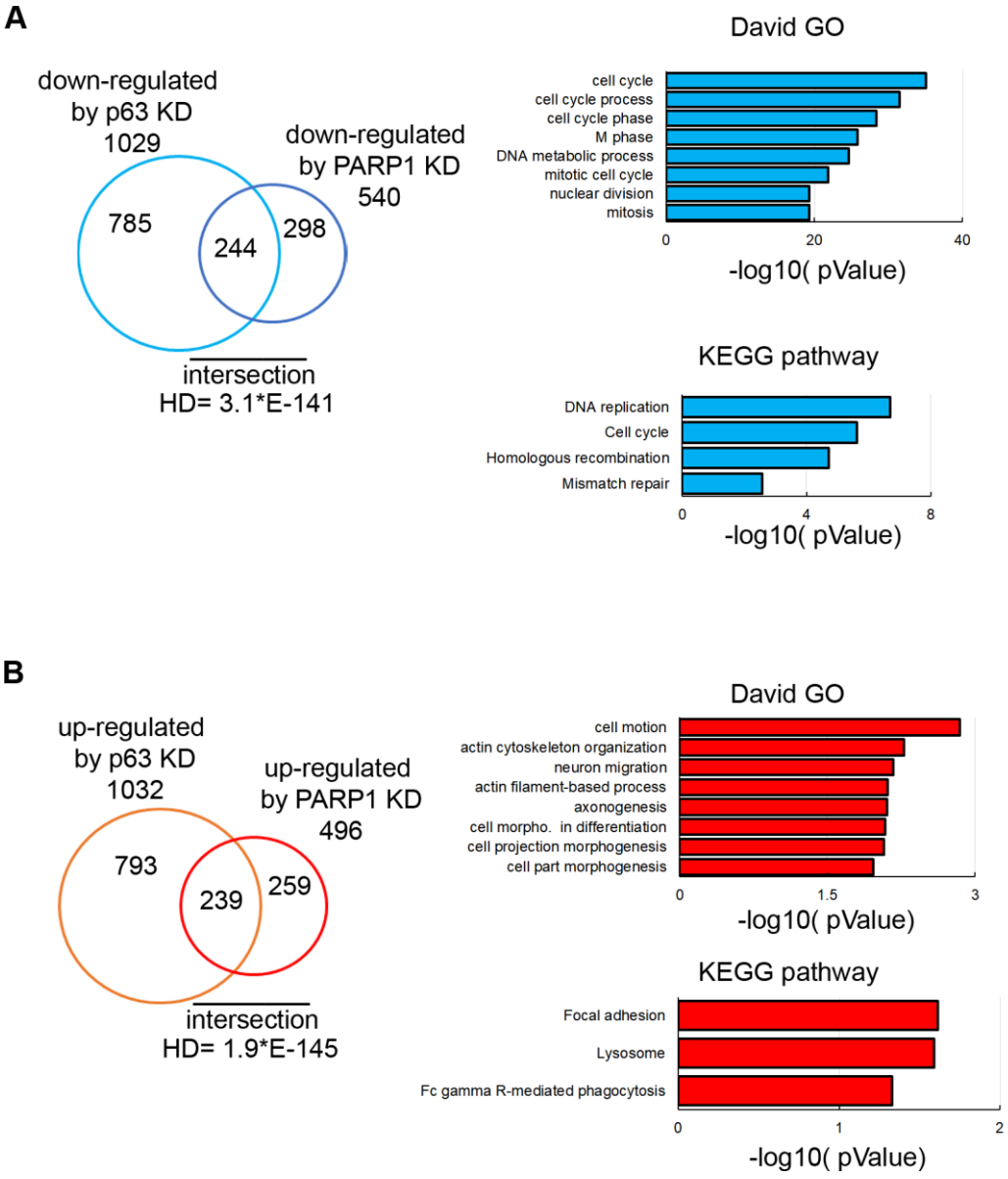

Figure 18: Biological process regulated by p63-PARP1 interaction. *A) Positively regulated genes by both proteins with relative Biological process (top) and KEGG pathway (bottom) B) negatively regulated genes by both proteins with relative biological process (top) and KEGG pathway (bottom)*

To restrict the number of genes and identify those directly regulated by p63 and PARP1 we compared the data of a ChIP-seq performed in SCC13 targeting p63 and the data of the gene expression profiling performed in SCC13 depleted of p63 and PARP1 independently (Fig. 19A). Next, we performed the gene ontology analysis to identify the biological process mainly regulated by both proteins. The David GO analysis confirmed the involvement of p63 and PARP1 in the regulation of cell cycle and the DNA repair. The KEGG pathway also confirmed an enrichment of these biological process (Fig. 19B). For each given gene list, protein-protein interaction enrichment analysis was carried out. The resultant networks containing the subset of proteins that form physical interactions with another list members, were processed using Molecular Complex Detection (MCODE), in order to identify densely connected network components. The MCODE networks identified for the individual gene lists revealed that the most enriched molecular complex was associated to homologous recombination and mitotic prometaphase (Fig. 19C).

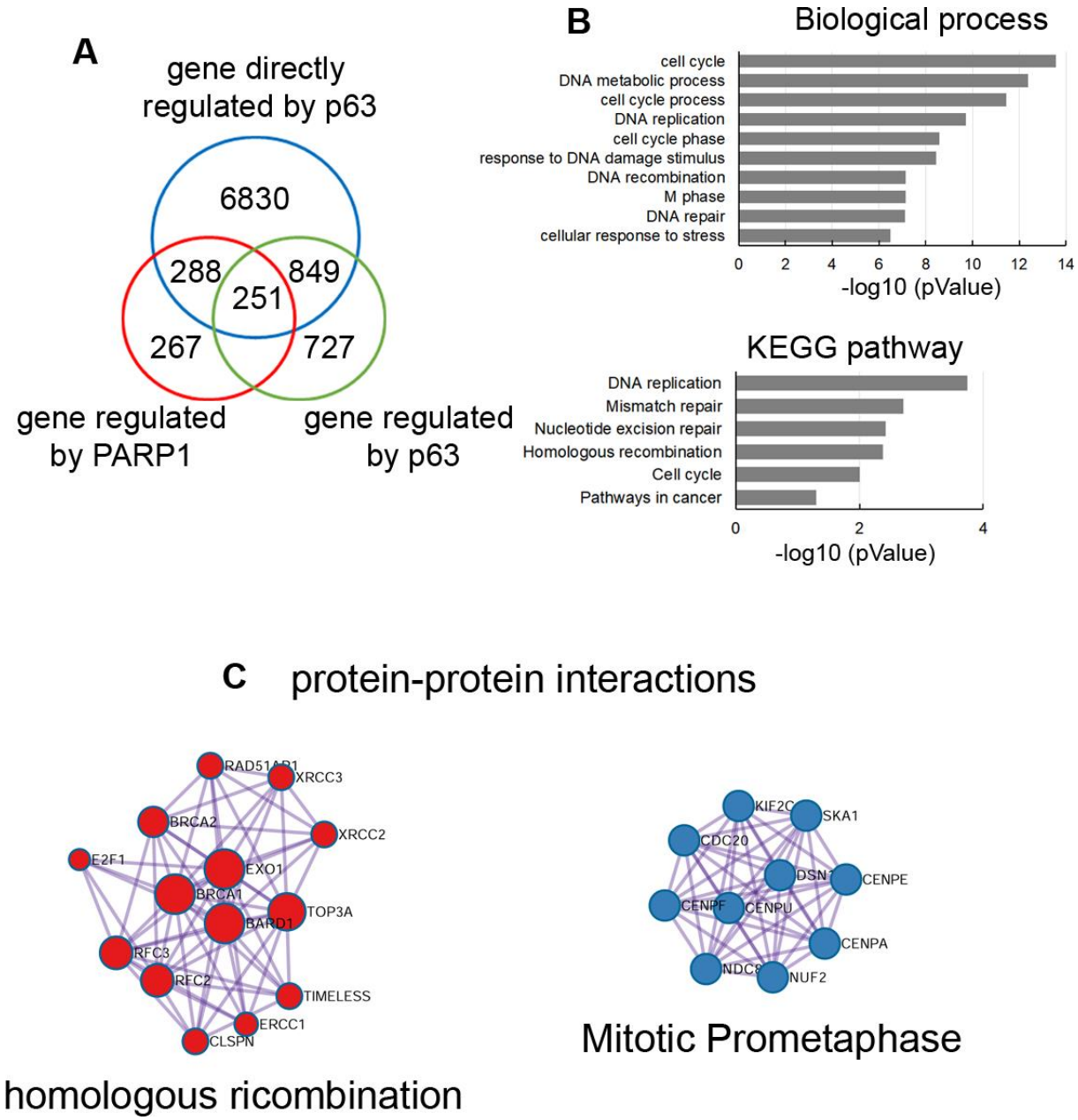

Figure 19: Integration of p63 ChIP-seq*: A) Venn Diagrams with the p63 ChIPseq data and RNA-seq data in SCC13 depleted for p63 or PARP1. B) Biological process (top) and KEGG pathway (bottom) of genes directly regulated by p63 influenced by PARP1. C) Protein-protein complex regulated by p63 and PARP1 in cSCC.*

7. PARP1 is involved in the regulation of cancer cell growth

To address how PARP1 affects the tumor environment, we evaluated the phenotypic consequence of the PARP1 depletion and in cSCC cells. PARP1 depleted cells showed an increase in CDKN1A mRNA and protein levels (Fig 20 A-B). This mechanism is likely to be independent of p53, because of PARP1 depletion leads to decrease of p53 protein levels (Fig 20C), suggesting a possible direct role of PARP1 on the regulation of CDKN1A gene.

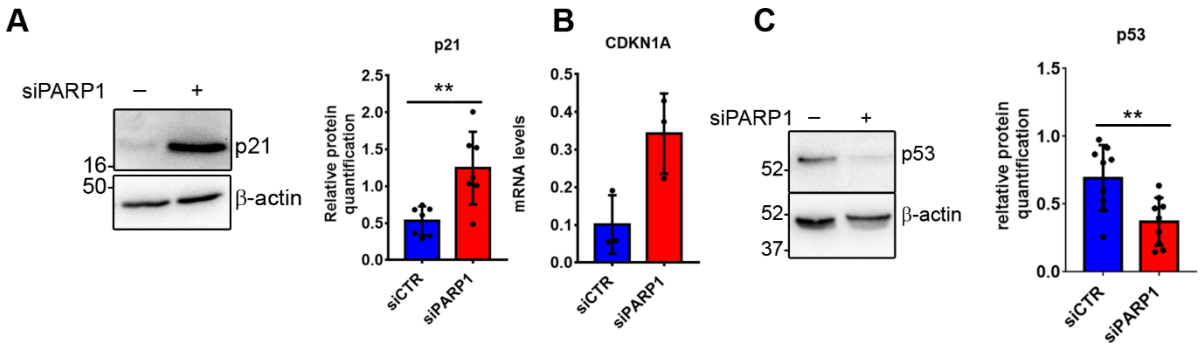

Figure 20: PARP1 depletion induce p21 in a p53 indipendent-manner*. A) WB on cSCC transiently depleted for PARP1 with specific siRNA to see the expression of p21 protein (left) and relative quantification (right). B) RT-qPCR on CDKN1A gene upon depletion of PARP1. C) WB on cSCC depleted for PARP1 to see the expression of p53 protein levels (left) and relative protein quantification (right)*

Depletion of PARP1 expression reduced the clonogenic capability of SCC cells (Fig. 21A) and, to further test its regenerative potential, we performed an oncosphere assay. PARP1 knockdown lead to a formation of smaller sphere in cSCC cells (Fig. 21B), indicating that it is involved in the maintenance of an undifferentiated, proliferative population in squamous epidermal tumors.

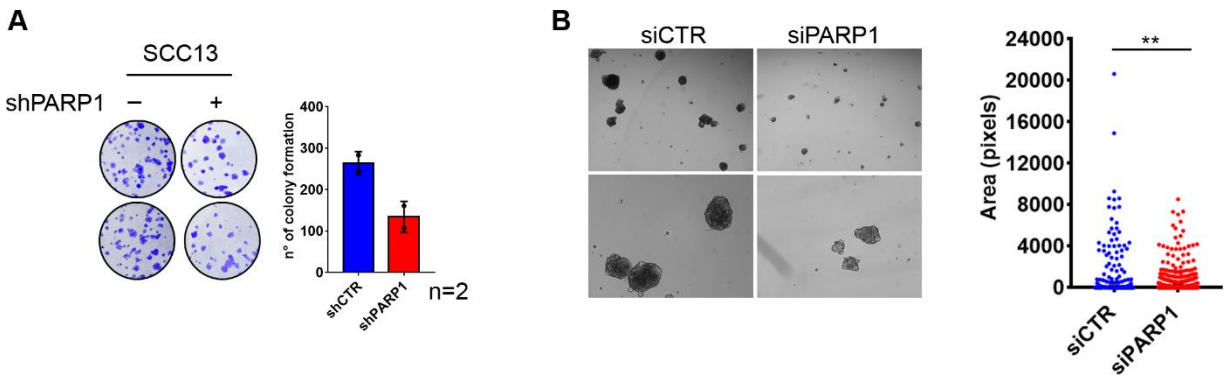

Figure 21. PARP1 depletion reduces the proliferative population of cSCC*. A) Clonogenic assay using SCC13 and SCC13 stably depleted for PARP1. B) Sphere assay in low attachment condition using SCC13 and SCC13 transiently depleted for PARP1 with specific siRNA.*

Furthermore, the depletion of PARP1 lead to an increase of micronucleated cells (Fig 22A) and a decrease of mitotic index (Fig 22B), suggesting increased of genomic instability. Finally, through three-dimensional (3D) organotypic cultures using the cSCC cancer cells depleted for PARP1, we have been able to show a decreased invasiveness of tumorigenic cells (Fig. 22C), with more organized and differentiated structure of the skin, suggesting that lacking of PARP1 can promote the keratinocytes differentiation, blocking the cell proliferation of cSCC tumor cell.

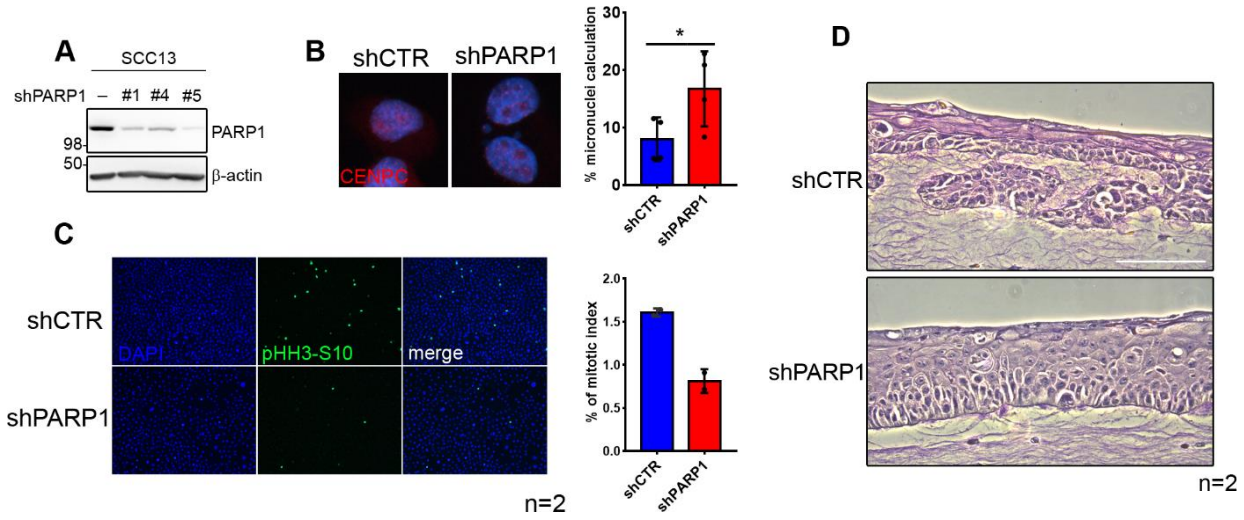

Figure 22: PARP1 depletion leads to a genomic instability, decrease of mitotic index and skin differentiation. *A) SCC13 stably depleted for PARP1 with specific short hairpin RNA. B) representative image of micronucleated cells upon PARP1 depletion (left) and relative calculation (right). C) IF for pHH3-S10 to identify the mitotic cells (left) and calculation of mitotic index (right) upon PARP1 depletion. D) 3D- organotypic culture of cSCC depleted or not for PARP1.*

Part II: p63 in Heterozygous Genetic Disease

p63 associated genetic disorders

.Heterozygous mutations in the transcription factor gene *p63* are causative for genetic developmental disorders characterized by ectodermal dysplasia, orofacial clefting and limb malformations (Rinne et al., 2007), namely: ectrodactyly, ectodermal dysplasia and cleft lip/palate syndrome (EEC, OMIM 604292), ankyloblepharon-ectodermal defects-cleft lip/palate syndrome (AEC, OMIM 106260), limb mammary syndrome (LMS, OMIM 603543), acro-dermato-ungual-lacrimal-tooth syndrome (ADULT, OMIM 103285) and Rapp- Hodgkin syndrome (RHS, OMIM 129400). Furthermore, two non-syndromic human disorders are caused by *p63* mutations: isolated split hand/foot malformation (SHFM4, OMIM 605289) and recently non-syndromic cleft lip (Celli et al., 1999; Ianakiev et al., 2000; Leoyklang et al., 2006; McGrath et al., 2001; van Bokhoven et al., 2001; van Bokhoven et al., 1999).

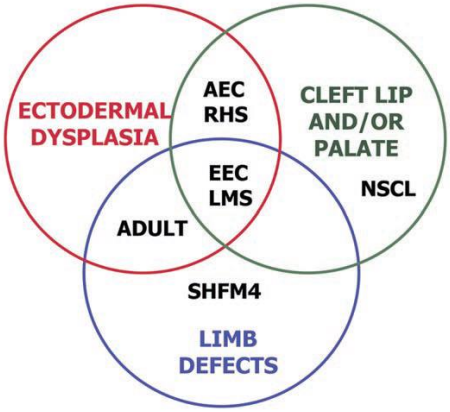

Figure 23: Various combinations of ectodermal dysplasia, orofacial clefting and limb malformations are the hallmark of p63-associated syndromes. EEC syndrome is the prototype of these syndromes and together with LMS showsall three hallmarks. ADULT syndrome patients never show orofacial clefting,whereas AEC and RHS never show limb defects. Non-syndromic limb defectcondition (SHFM4) and non-syndromic cleft lip/palate (NSCL) are alsocaused by mutations in the p63 gene. *(p63-Associated Disorders, Tuula Rinne, Hans G. Brunner, Hans van Bokhoven*. Cell Cycle 2007)*

EEC syndrome. EEC syndrome patients are invariably characterized by one or more features of ectodermal dysplasia, which can present defects of hair, skin, nails, teeth and glands. The severity and type of the ectodermal features is highly variable. EEC patients occasionally also have mammary gland/nipple hypoplasia (14%) and hypohidrosis (11%). About two-thirds of these patients have ectrodactyly, and syndactyly is also frequent (43%). Cleft lip/palate is present in about 40% of the EEC patients, mostly as CL with or without CP (Rinne et al., 2006a). EEC syndrome is mainly caused by point mutations in the DNA binding domain (DBD) of the *p63* gene. Only few mutations are outside the DNA binding domain: one insertion (e.g. 1572InsA, 1572DelTT, 1743DelAA) (Celli et al., 1999; Rinne et al., 2006a). In earlier studies, five frequently mutated amino acids: R204, R227, R279, R280 and R304 were found in the EEC population. These five mutations explain almost 90% of the EEC syndrome patients (Rinne et al., 2006a; van Bokhoven and Brunner, 2002). The five p63 arginine hotspot mutations and probably also other DNA binding domain mutations that are found in EEC syndrome are likely to impair the p63 protein binding to DNA (Celli et al., 1999). The autosomal dominant inheritance of EEC syndrome suggests that the EEC mutations have a dominant negative effect. However, recent genotype-phenotype analyses for the five hotspots mutations revealed significant differences between the corresponding phenotypes. For instance, cleft lip/palate, syndactyly and ectrodactyly are present in the R304Q/W mutation population (80%), whereas patients with R227Q mutation have cleft lip/palate, genitourinary defects (40%), while syndactyly is completely absent in R227 population.

(Rinne et al., 2006a). It thus seems that these hotspot mutations exert specific effects. Recent studies published by Qu et al. demonstrate how p63 mutants associated to EEC syndrome alter the enhancer landscape in skin keratinocytes. More specifically p63 lose the ability to bind active enhancer in patient keratinocytes carrying EEC mutation (R204W, R304W, and R279H) (Qu et al.). Interestingly, a large number of gained active enhancers in all three p63 mutant keratinocytes were present. These mutant-specific enhancers were enriched for motifs of TFs that normally cooperate with p63 in keratinocytes. Many of these TFs were deregulated in p63 mutant keratinocytes and are direct p63 target genes, such as RUNX1. This indicates that rewiring of the transcriptional program is caused not only by loss of p63-bound active enhancers but also by an indirect effect of altered expression of p63 co-regulating TFs (Qu et al.). Intriguingly, single-cell transcriptomic analysis on iPSC derived from EEC fibroblast patients showed that the majority of differentiated EEC iPSCs deviated from the normal route of epidermal commitment to a more mesodermal cell identity (Soares et al.).

ADULT syndrome. ADULT syndrome phenotype is characterized by the presence of hair and skin defects and absence of orofacial clefting. Teeth, skin and nail defects are constantly present in ADULT syndrome (Teeth 100%, skin 93% and nail 100%), hair (53%) and lacrimal duct defects are present (67%) (Amiel et al., 2001; Propping et al., 2000; Propping and Zerres, 1993; Rinne et al., 2006b). All the families and one of the sporadic cases have a point mutation in exon 8, changing R298 in the DNA binding domain into either a glutamine or a glycine (Amiel et al., 2001; Chan et al., 2004). Interestingly, while EEC syndrome mutations in the DNA binding domain impair the binding of p63 protein to DNA (Celli et al., 1999), arginine 298 is not located close to the DNA-binding interface, and mutation of this arginine does not affect DNA binding (Duijf et al., 2002). Two other mutations are located in the N-terminus: N6H mutation affects only the DN-isoforms and in another isolated patient a missense mutation G134D* is located just front of the DBD in exon 4 (Amiel et al., 2001; Slavotinek et al., 2005).

AEC syndrome. The AEC syndrome phenotype differs from the other conditions mainly by the severity of the skin phenotype, the occurrence of an eyelid fusion at birth and the absence of limb malformations (Fig. 23). Approximately 80% of the patients have severe skin erosion at birth or just after birth, which usually will recover in the first years of the life. The eyelid fusion, also called ankyloblepharon, is present in about 45% of AEC patients, but only rarely in other p63-associated conditions. The other Ectodermal dysplasia symptoms, such as nail and teeth defects are present in more than 80% of patients, and hair defects and/or alopecia are almost constant features (94%). Lacrimal duct obstruction is seen in 50% of patients, whereas mammary gland hypoplasia and hypohydrosis occur occasionally (both 13%). Interestingly, almost 40% of patients have hearing impairment and genito-urinary defects. Cleft lip is present in 44% and cleft palate in about 80%. Limb malformations are almost absent. Ectrodactyly has never been reported, but 25% of patients have mild syndactyly (Rinne et al., 2006a). A mouse model for AEC syndromes demonstrated that the AEC mutation L514F affects primarily ectodermal cell proliferation during development through a highly selective mechanism, leading to epidermal and palatal hypoplasia and reduced expansion of epithelial progenitor cells. In addition, this work demonstrated a novel functional link between p63 and FGF signaling in controlling progenitor cell expansion providing significant mechanistic insights into the pathogenesis of AEC syndrome (Ferone et al., 2012). Furthermore, p63 positively regulates desmosome adhesion by directly controlling the expression of several desmosome genes, including Desmoplakin (Dsp), Desmocollin-3 (Dsc3) and Desmoglein-1 (Dsg1), and this pathway is altered in both human and mouse AEC keratinocytes, leading to a less cell-cell junction and cell-adhesion. This altered gene regulation contributes to reduce mechanical resistance in AEC skin (Ferone et al., 2013).

Aim II

The second aim of my PhD project is the molecular characterization of p63 mutations, causative of heterozygous genetic disease changing the transcriptional activity of p63. In collaboration with V. Dötsch from Goethe University of Frankfurt, I characterized the transcriptional activity of mutations located at the C-terminal domain, causative of the rare genetic disease AEC, and at the DNA binding domain, causative of the EEC and ADULT syndrome.

Results of research group

1. Transcriptional activity of AEC-associated p63 mutants is impaired by a propensity to protein aggregation.

Previous studies, leaded by my colleagues, show the effect of C- terminal associated mutations on ΔNp63α to trans-activate the regulatory regions of KRT14, a typical p63 target genes. Wild-type ΔNp63α efficiently activated the KRT14 promoter, whereas an EEC causative mutation that directly impairs DNA binding (R304Q), abolished p63 activity. All tested AEC-associated mutations, including missense mutations in the SAM and TI domains and frameshift mutations, invariably abolished or severely reduced p63 transcriptional activity, whereas two missense mutations in the PS domain causative of SHFM syndrome (Q630X and E635X) retained transactivation activity in this context (Fig. 24).

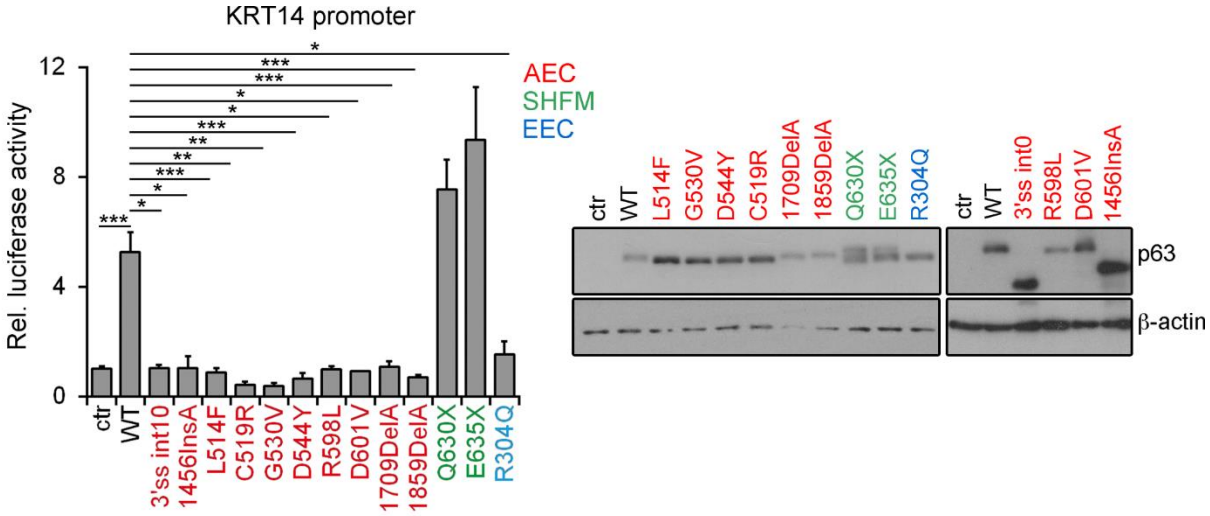

Figure 24: AEC associated mutations *abolish or reduce the p63 transcriptional activity. Luciferase assay (left) using a construct with the KRT14 promoter positioned before the luciferase, shows that the AEC-associated mutations impair the p63 transcriptional activity. On the right, the Western blot show the protein expression of the different p63 mutants. Published in Russo et al. 2018 PNAS.*

Next, To test whether impaired transcriptional activity of AEC associated p63 mutants affected its biological function in a more physiological context, they performed a protocol to convert human dermal fibroblasts (HDFs) into induced keratinocyte-like cells (iKCs) by coexpression of ΔNp63α and Krüppel-like factor 4 (KLF4) (Chen et al., 2014) (Fig. 25 A-B). Fifteen days after p63/KLF4 transduction, HDFs had converted into iKCs and expressed keratinocyte-specific p63 transcriptional targets, including KRT14, the transcription factor IRF6 involved in keratinocytes differentiation, and desmocollin 3 encoding a desmosome component expressed in basal keratinocytes. Similarly, to the EEC mutant R304Q, AEC mutants were unable to induce expression of keratinocyte-specific target genes, indicating that they are functionally incapable to convert HDFs into iKCs (Fig. 25 C-D).

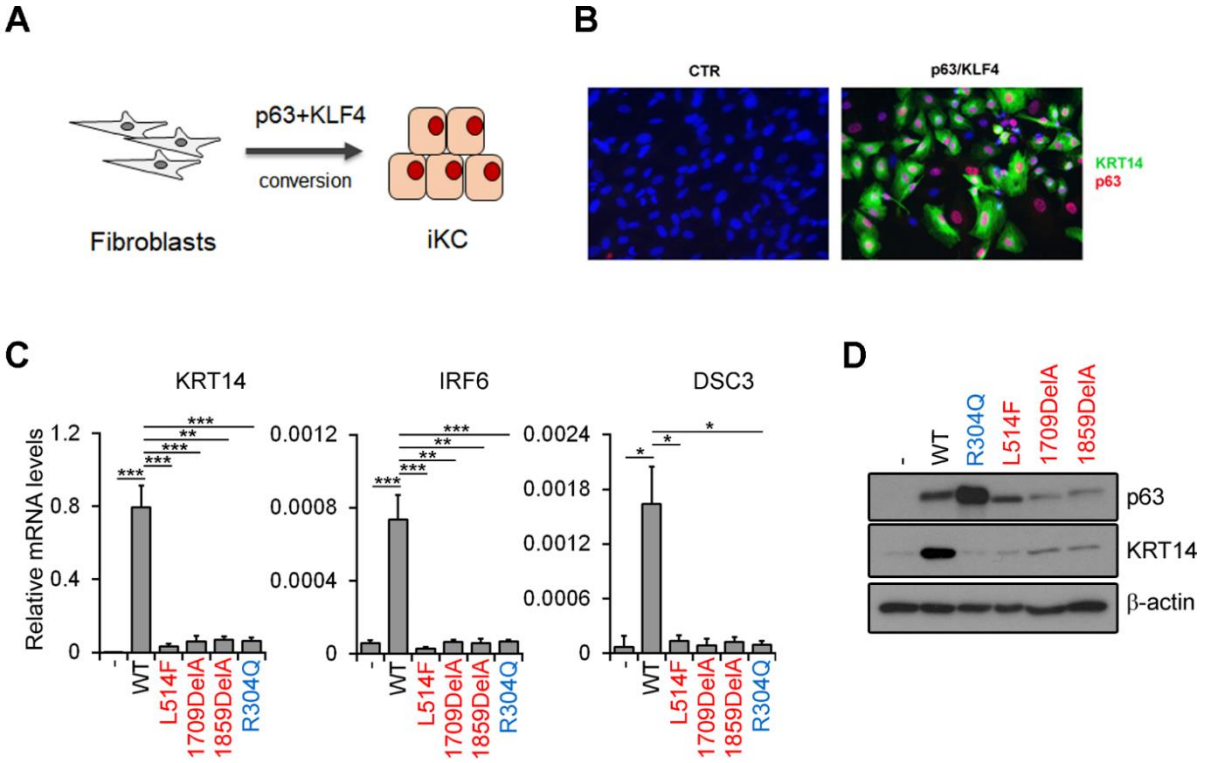

Figure 25: AEC associated mutations impair the ability of p63 to convert fibroblast into iKC*. A) Schematic representation of the conversion of fibroblast into iKC. B) Immunofluorescence on converted fibroblast to identify the KRT14 and p63. C) RT-qPCR on fibroblast co-infected with KLF4 and the different AEC mutants. The mutants are unable to induce the expression of different iKC markers (KRT14, IRF6, DSC3) compared to the WT. D) Western blot on fibroblast co-infected with KLF4 and AEC-associated mutants. Published in Russo et al. 2018 PNAS.*

Subsequently, they analyze the p63 amino acid sequence to investigate whether AEC mutants might be prone to destabilization and precipitation due to an increased aggregation propensity. To this aim, they use the TANGO algorithm that predicts aggregation prone regions (APRs) in proteins (Fernandez-Escamilla et al., 2004). This analysis indicated that two peptides (peptides 1 and 2), located in the first and third helix of the SAM domain, displayed some aggregation propensity, which was enhanced by the L514F and G530V mutations, respectively (Fig.26A). To assess whether AEC-associated mutant p63 proteins have the propensity to form aggregates in mammalian cells, wild-type and mutant p63 were overexpressed in H1299 cells that are devoid of p53 and its family members, and run on Blue-Native polyacrylamide gel electrophoresis (BN-PAGE) followed by Western blotting. Transiently overexpressed wild-type p63 and EEC mutations (R304Q, 1576DelTT, 1743DelAA, 1572InsA) run primarily as monomers (Fig. 26B). In contrast, overexpression of p63L514F and all other tested AEC mutants caused a shift in molecular mass, consistent with the formation of large multimeric assemblies (Fig. 26B). Similar results were obtained by size exclusion chromatography (SEC), in which most of the L514F mutant protein eluted at high molecular weight (Fig. 26C), whereas wild-type p63 eluted at low molecular weight.

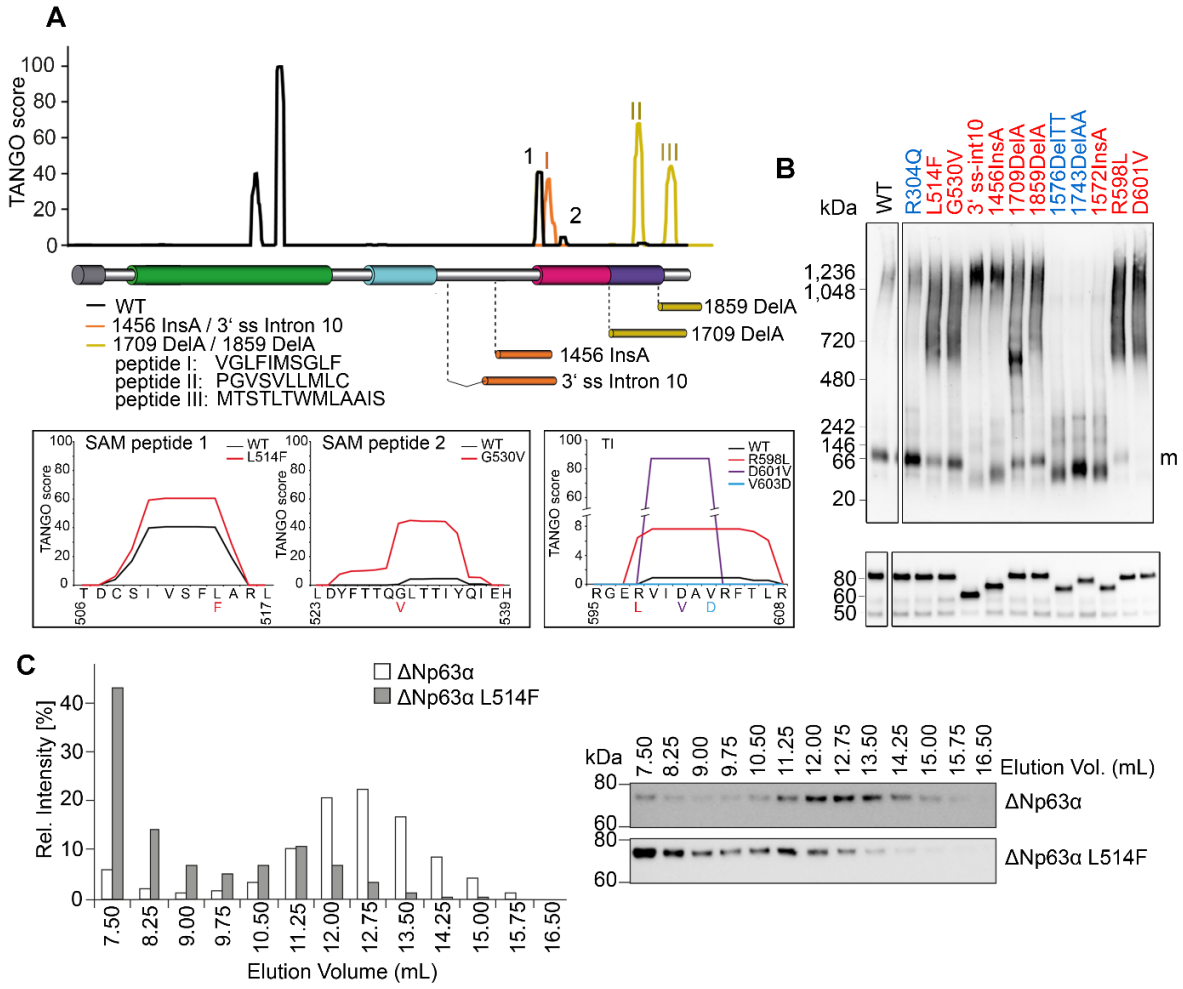

Figure 26: p63 AEC-mutants have a propensity to protein aggregation*: A) TANGO analysis for the wild-type ΔNp63α (in black) and for the indicated AEC mutations caused by protein elongation (Upper: aggregating peptide I-III) or missense mutations in the SAM and TI domains (Lower). The V603D variant is predicted to abolish mutant aggregation. F) BN-PAGE (Upper) and SDS/PAGE (Lower) followed by Western blot for p63 in H1299 extracts expressing wild-type (WT) and the EEC (blue) or the AEC (red) mutations. Soluble ΔNp63α protein runs mainly as a monomer (m). G) SEC followed by Western blot of H1299 cell lysates overexpressing wild-type ΔNp63α and p63L514F mutant. Published in Russo et al. 2018 PNAS.*

Results

1. Transcriptional Activity is restored by reducing the aggregation propensity of AEC-associated mutant p63.

To investigate whether reversing aggregation would be sufficient to restore transcriptional activity of AEC mutants, we use a genetic approach introducing new point mutations predicted by TANGO to alleviate aggregation, or deleting APRs. Introduction of the point mutation V603D completely inhibited the aggregation propensity of the R598L or D601V. Instead, for L514F mutant, the aggregation was alleviated by the introduction of three point mutations (V603D, V511D, and T533D). For APRs, deletion of peptide I for the splice mutant 3′ ss-int10, peptide II and III for the 1709DelA, and peptide III for the 1859DelA. Using the native Blue-PAGE we identified the reduced aggregation propensity of the rescue mutants (Fig 27 A-C).

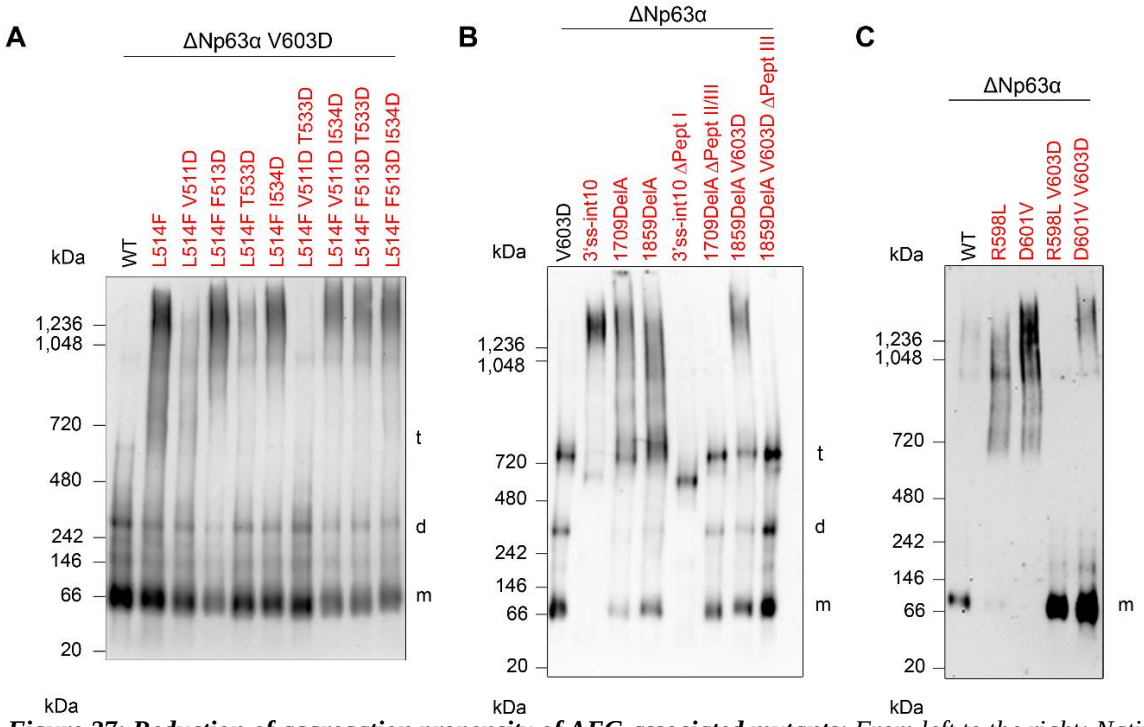

Figure 27: Reduction of aggregation propensity of AEC-associated mutants*: From left to the right: Native-PAGE show a rescue of the aggregation propensity upon the introduction of point mutations or upon the deletion of the aggregation prone regions (APRs). Published in Russo et al. 2018 PNAS.*

We next used transactivation assays to test whether abolishing aggregation rescued the transcriptional activity of p63 mutants. Consistent with the aggregation data, L514F and L514F/V603D mutants were inactive in luciferase assays, whereas L514F/V603D bearing the V511D/T533D double mutation exhibited restored transcriptional activity (Fig. 28A). Similarly, p63 transcriptional activity was fully restored upon deletion of the aggregating peptides in the elongated C-terminal domain caused by the frameshift mutations 1709DelA and 1859DelA (Fig. 28B). Finally, the V603D variant completely rescued the activity of the two point mutants R598L and D601V in the TI domain (Fig. 28C)

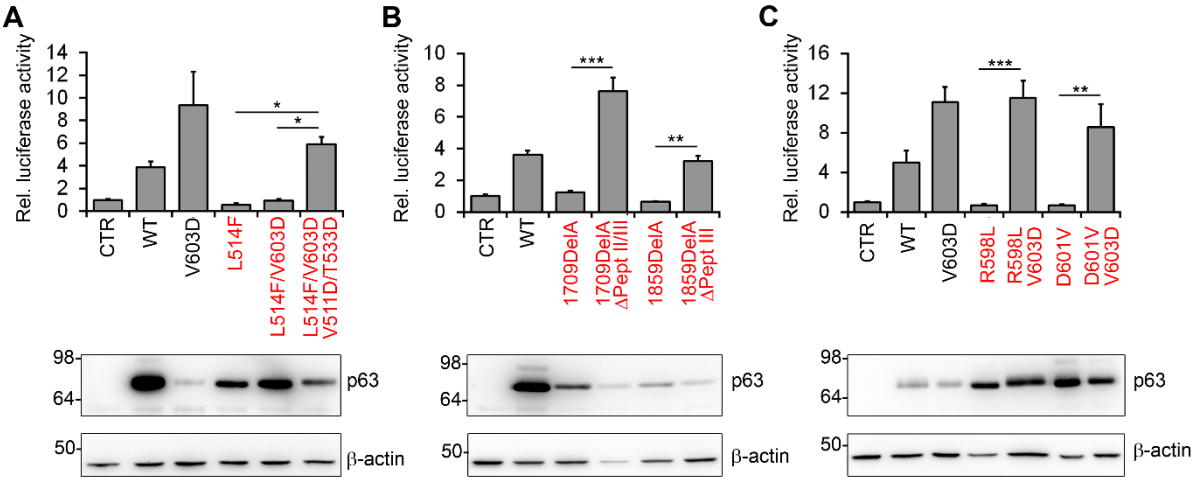

Figure 28: Rescue of the aggregation propensity restore the transcriptional activity of mutants p63*. A-C) Luciferase reporter assays of wild-type and mutant p63 on the KRT14 promoter in HEK293 cells (n = 3) (Upper). Luciferase data were normalized for Renilla luciferase activity. SDS/PAGE (Lower) followed by Western blot of wild-type and mutant p63 are shown as control. Published in Russo et al. 2018 PNAS.*

To directly test the functional consequence of the increased aggregation for keratinocyte homeostasis, we resorted to the HDF to iKC conversation assay that is impaired by AEC mutations. Deleting the aggregation peptides of the 1709DelA mutant or introducing V603D into the R598L mutant fully rescued their ability to induce expression of KRT14 and IRF6 in HDF (Fig. 29 A-B). Similarly, alleviating aggregation of the p63L514F mutant rescued its ability to convert HDF to iKC (Fig. 29B), demonstrating that aggregation is associated with an impairment of p63 activity.

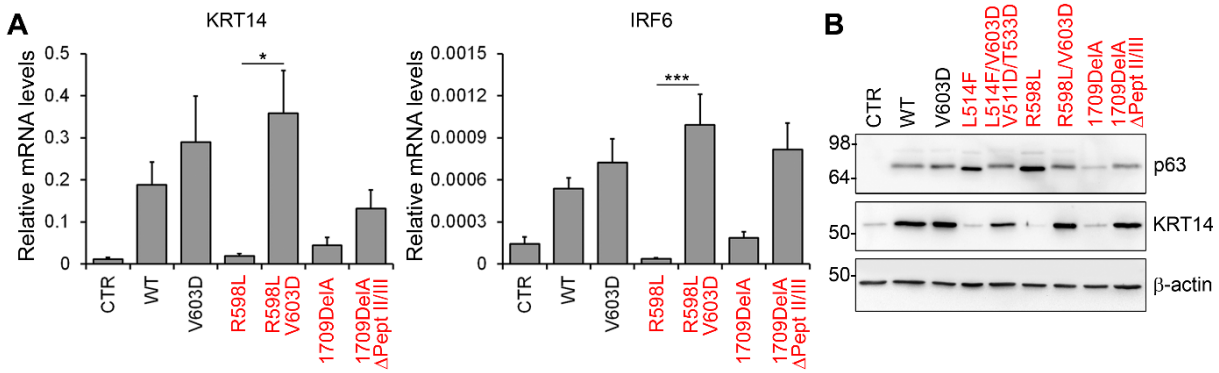

Figure 29: Rescue of the aggregation propensity restore the ability to convert fibroblast into iKC*. A) Real-time RT-PCR of the indicated keratinocyte-specific p63 target genes in HDFs converted to iKCs by coinfection with KLF4 and the indicated p63 viruses. B) Western blot of KRT14 and p63 in iKCs. β-actin was used as loading control. Published in Russo et al. 2018 PNAS.*

2. EEC and ADULT p63 mutants display different transcriptional activity.

The mutations causative of EEC and ADULT syndromes usually cluster in the DNA binding domain (DBD) of p63. These pathologies are characterized by wide range of phenotypic differences, despite the fact that the mutations fall in the same domain. To investigate the molecular behavior of these DBD mutants, we tested the ability of a variety of DBD mutants to convert human fibroblasts into iKC by co-expression of KLF4 and different p63 DBD mutants.

After 15 days, the HDF converted into iKC express the molecular target of keratinocytes. Immunofluorescence and Western blot analysis showed that some p63 mutants (R204W, R304W, R279H, R280S and R313G), are unable to induce the expression of KRT14 (KRT14 negative cells). Surprisingly, some DBD mutants (R227Q, R298Q, R280H, K193E and K194E) are still able to induce keratinocytes commitment (Fig. 30A). These data were confirmed by RT-qPCR and Western blot analysis of the expression of specific molecular target (DSP, KRT14 and IRF6) (Fig.30 B-C).

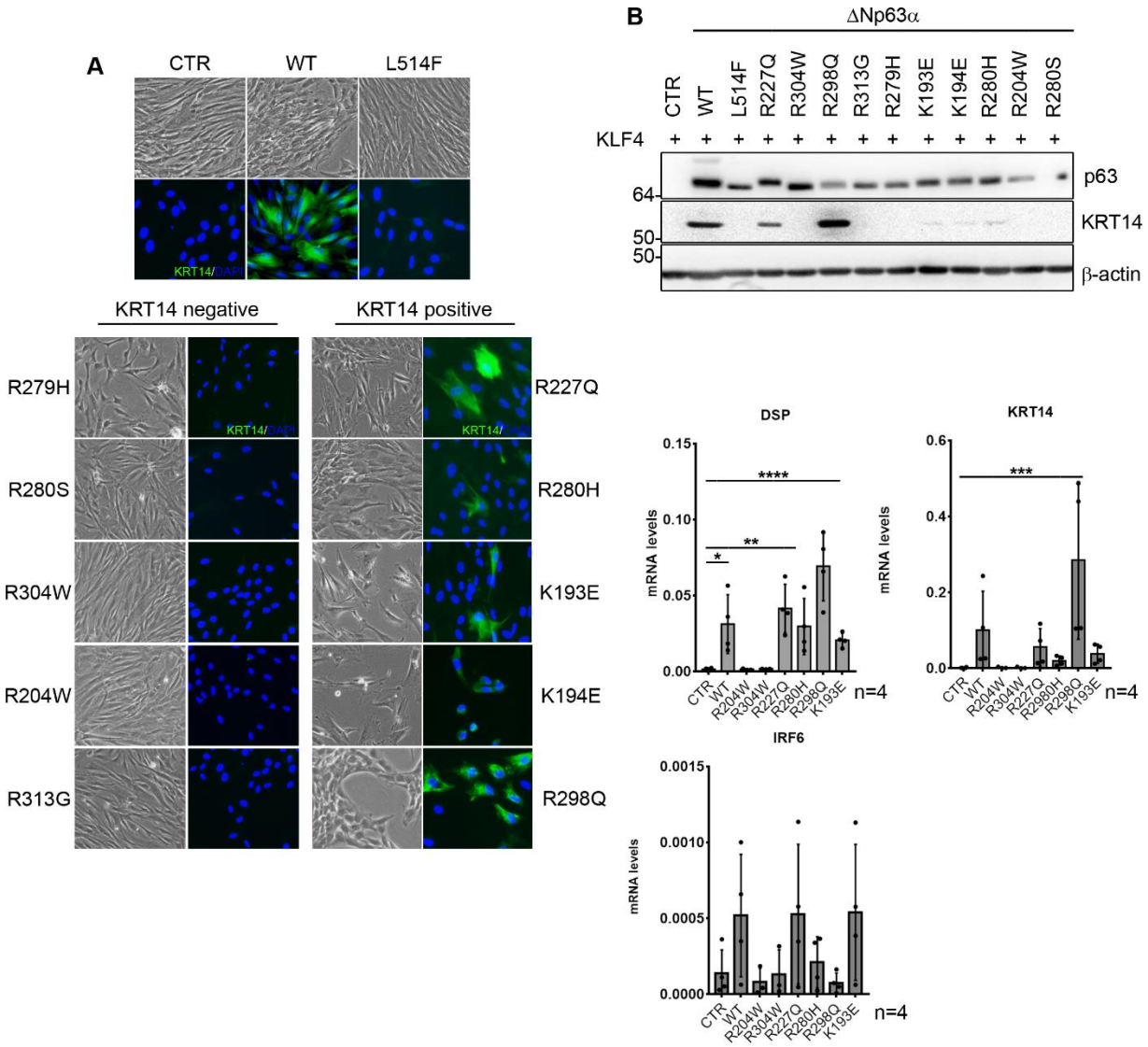

Figure 30: Some EEC and ADULT mutants are able to induce an epidermal commitment*. A) Fibroblast conversion to iKC show that some mutation in the DNA binding domain of p63 allow to induce a trans-differentiation of fibroblast in iKC (KRT14 positive cells). B) Western blot analysis s of KRT14 and p63 in iKCs. β-actin is used as control. C) Real-time RT-PCR of the indicated keratinocyte-specific p63 target genes in HDFs converted to iKCs by coinfection with KLF4 and the indicated p63 viruses.*

Interestingly, the R298Q mutant (ADULT syndrome) had a selective effect on different targets, while it was at least as effective as the WT to induce DSP and KRT14; it was unable to induce IRF6 expression. In contrast, the R227Q mutants (EEC syndrome) was able to convert the fibroblast into iKC although to a lesser extent than WT (Fig. 30C). These observations suggest that these two mutant are still able to bind some regulatory

sequence on the DNA and induce the transcriptional regulation of p63 target genes in a mutation-specific manner.

3. Wide Transcriptomic analysis of mutant iKC show that the R298Q mutant and the R227Q mutant have a partial transcriptional activity.

To better characterize the effect of p63 DBD mutants on the iKC transcriptional landscape, we performed a transcriptomic analysis using the RNA-seq technology on iKC cells co-infected with KLF4 and EEC or ADULT associated mutants. To this purpose, we used the HDF co-infected with KLF4 and an empty vector as an internal control of the transcriptional landscape of dermal fibroblast.

Total RNA was isolated from three sets experiments. The use of three independently generated populations of cells represents a stringent approach to control for experimental variability.

In principal component analysis (PCA) the R227Q mutant and the R298Q mutants moved from the left of PC1 to the right of PC1 overlapping with the WT, instead the two "dead mutants" (R304W and R204W) remained in the PC1 left side overlapping with the internal control (Fig. 31A). Next, we analyzed the differentially expressed gene (DEG) (FDR $\leq$ 0.05) comparing all the conditions with the internal control (empty). The gene perturbation was represented by Volcano plot, positioning the log2FoC on the x-axis and the –log10 of FDR on the y-axis. Subsequently, we overlapped the gene perturbation of the different mutant transcriptomic profiles with that of the wild type. This analysis showed that the p63R298Q and p63R227Q mutants have a strong correlation with the WT, unlike the other two mutants (R204W and R304W) that do not present any overlap with the WT (Fig 31 B-C). This trend is also explained by the calculation of the Pearson correlation coefficient and linear regression for each mutant compared to the WT. The two "partial" mutants present a Pearson coefficient equal to 0.80 for the p63R227Q and 0.72 for the p63R298Q, while the two "dead mutant" have a Pearson coefficient close to 0.2. Taken together, these

analyses demonstrate that the transcriptional landscape of p63R227Q and p63R298Q strongly correlates with the wild-type p63 (Fig. 31D).

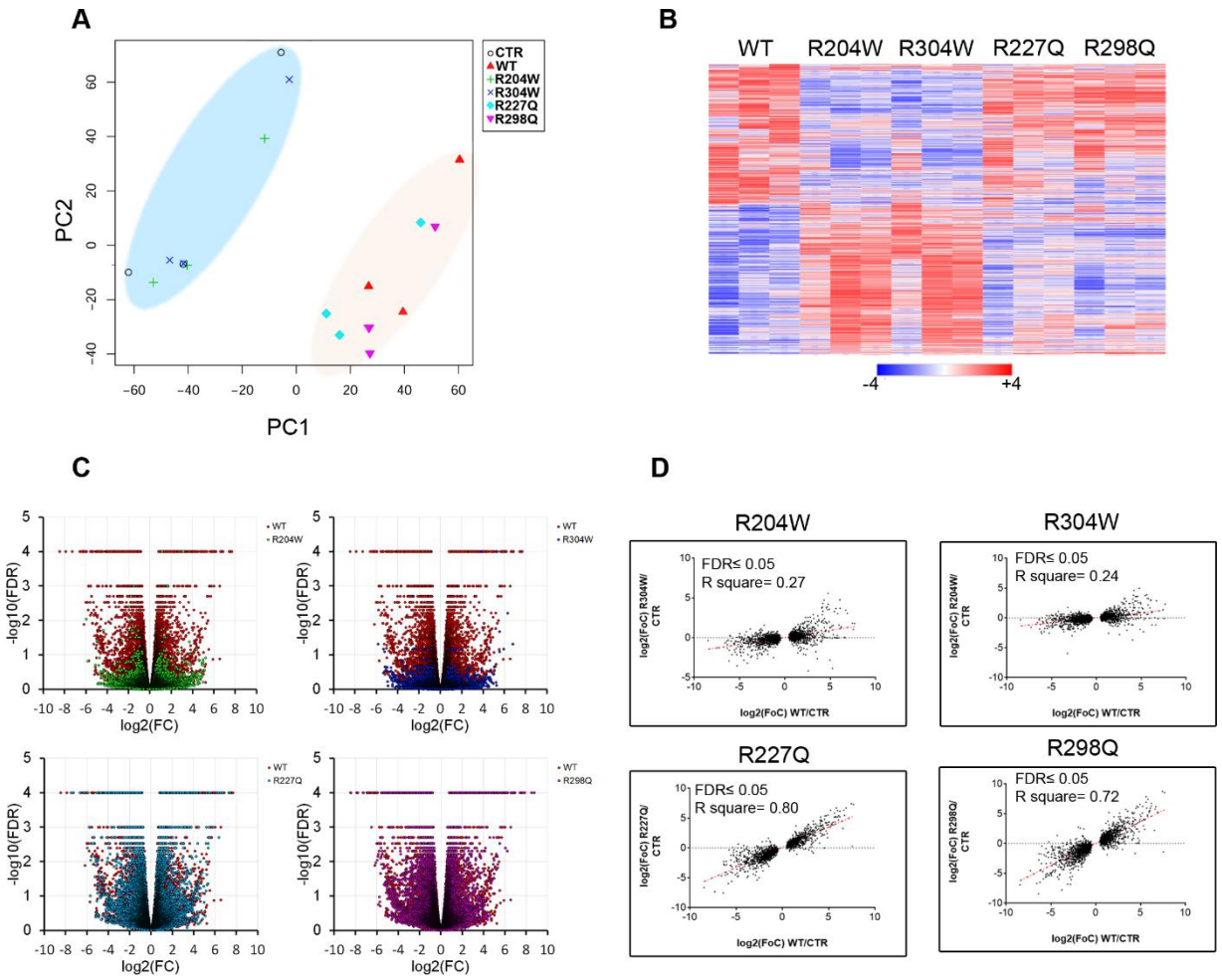

Figure 31: p63 R227Q and p63 R298Q induce the transcription similar to the p63 wild type*. A) Principal Component Analysis (PCA) of the p63 wild type and mutants different cell population. The white dots are associated with the fibroblast co-infected with KLF4 and an empty vector. B) Heat map representation of the differentially expressed genes (DEGs). C) Volcano plots positioning the log2FoC on the x-axis and the –log10 of FDR on the y-axis of the different mutants and the Wild type. D) Linear regression and Pearson correlation of the four p63 mutants compared to the wild-type p63.*

Next, we identified 1106 genes in common between the p63R227Q and the p63WT; whereas, R227Q mutants differentially regulated 493 genes compared to WT. In addition, 1178 genes were in common between p63R298Q and p63WT, while 917 genes were differentially regulated. The David GO analysis of the DEGs clustered in the PC1 right side showed that the commonly regulated genes are involved in organ development, cytoskeleton organization, and developmental processes (Fig.32).

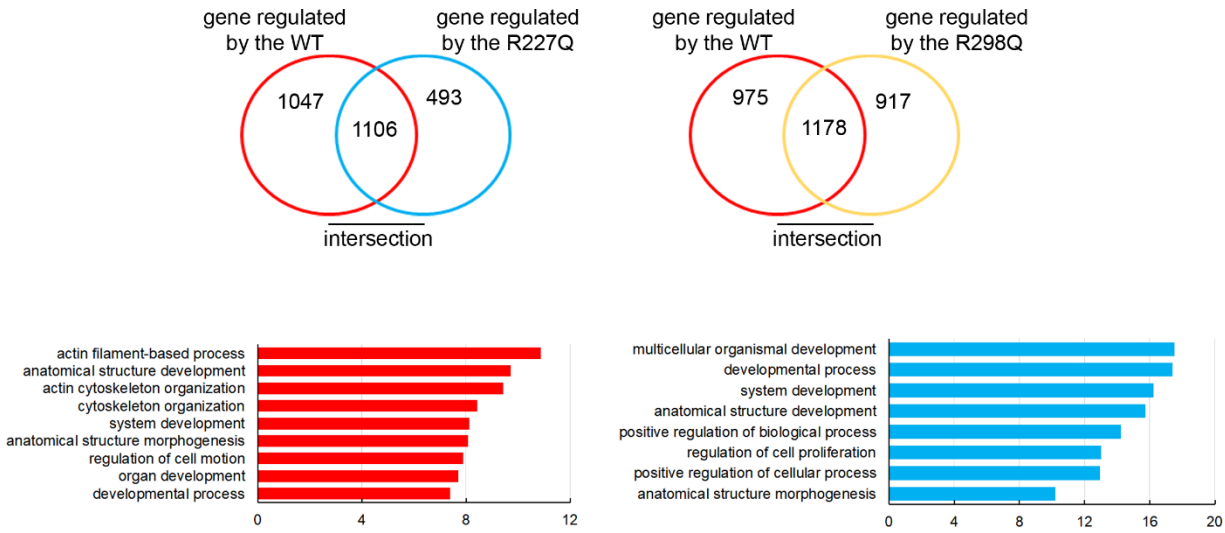

Figure 32: Genes similarly regulated by the p63WT and by p63R227Q and p63R298Q are involved in cell development. *Genes commonly regulated by p63WT and p63R227Q (left) with the relative biological process (bottom, left). Genes commonly regulated by p63WT and p63 R298Q (right) with the relative biological process (bottom, right)*

To identify the genes differentially regulated by the p63 WT and the p63R227Q and R298Q, we performed a transcriptome comparative analysis between the two mutants and the p63WT. We filtered the gene mainly altered by the p63R298Q and p63R227Q mutants compared to the WT using an FDR ≤0.05. We identify 248 and 691 genes not regulated by p63 R227Q and p63 R298Q respectively. Intriguingly, the genes dysregulated by the two mutants, were mainly involved in the regulation of cell proliferation, cell adhesion and cell differentiation (Fig. 33).

Furthermore, we performed a phenotype analysis using the HPO (Human Phenotype Analysis) software. The HPO provides a standardized vocabulary of phenotypic abnormalities encountered in human disease. Each term in the HPO describes a phenotypic

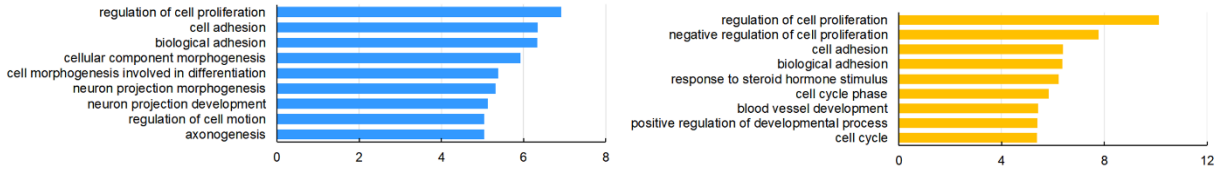

Figure 33: Genes specifically regulated by p63WT and not by p63R227Q or p63R298Q. *Gene Ontology of 258 genes regulated by WT and not by p63R227Q (left) Gene Ontology of 691 genes regulated by WT and not by p63R298Q (right).*

abnormality. The HPO is currently being developed using the medical literature, Orphanet, DECIPHER, and OMIM (Kohler et al.). This analysis show that these two mutants do not present the same phenotypes of the canonical EEC- associated mutants. In particular, the R298Q present the typical phenotypic alteration of the ADULT syndrome, instead, the R227Q mutation, causative of the EEC syndrome, has some phenotypic feature that differ from the p63R204W and p63R304W. In particular, the cutaneous syndactyly, typical feature of the EEC syndrome, is absent in the p63R227Q phenotype (Fig. 34). These differences between mutants clustered in the same pathology (R227Q, R304W, R204W) can explain the strong variability in the phenotype of the pathology itself, suggesting that this specific mutations can only partially alter the p63 transcriptional activity.

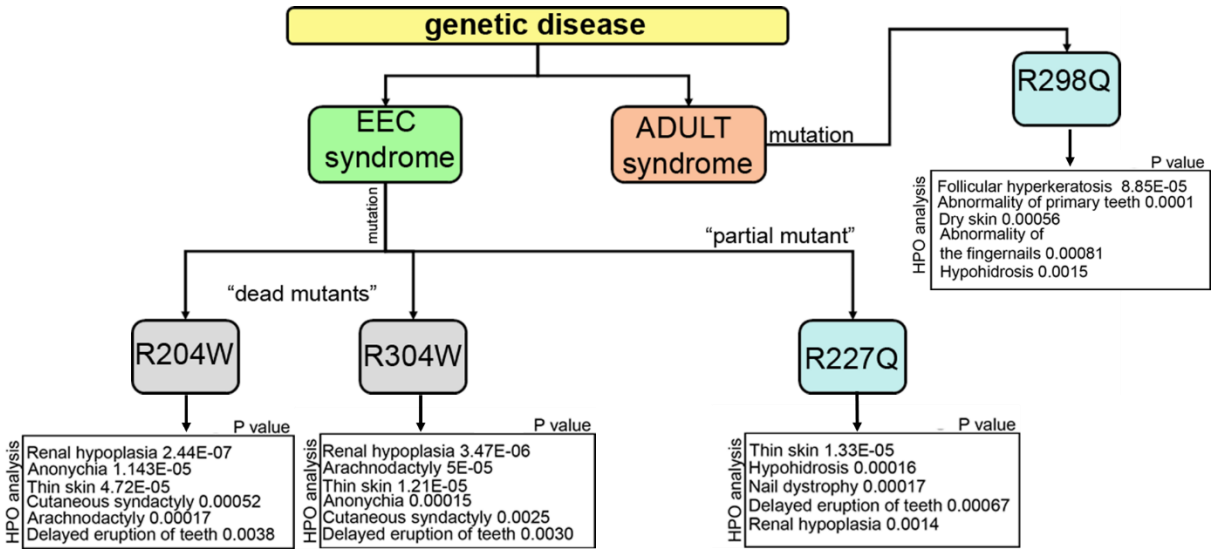

Figure 33: Human Phenotype Ontology (HPO) analysis show the characteristic features of the different mutants.

To establish the direct transcriptional mechanism of the R227Q and R298Q mutants, we compared ChIP-seq data obtained from Kouwenhoven et al 2015(Kouwenhoven et al.) and the data obtained from the RNA-seq performed on the fibroblast infected with p63 WT and mutants. We clustered the peaks in three classes (Fig 35 A, C):

1) Peaks related to genes induced in HDF infected with WT p63

2) Peaks related to genes lost in HDF infected with mutants p63 (R227Q and R298Q)

3) Peaks related to genes kept (still induced) in HDF infected with mutants p63 (R227Q and R298Q)

Next, we performed a DNA Motif Analysis using MEME Discovery Motif (Bailey et al., 2006). The Motif analysis showed a strong enrichment, as expected, of the p53 family DNA binding motif, for the all mutants (Fig. 35B). Interestingly, the *de novo* motif discovered from peaks associated to gene that are lost or kept by the R227Q mutant do not present a particular enrichment, suggesting that the transcriptional activity of this mutant is not closely related to the DNA sequence recognized by it (Fig. 35D). While,

the *de novo* motif discovered from peaks associated to genes that are still regulated by p63R298Q is a hemi site, suggesting that the distance between the two-hemi sites is predominantly more than zero (Fig. 35E). This analysis suggest that the R298Q mutant do not recognized the typical full-response element (two hemi sites with 0 spacing).

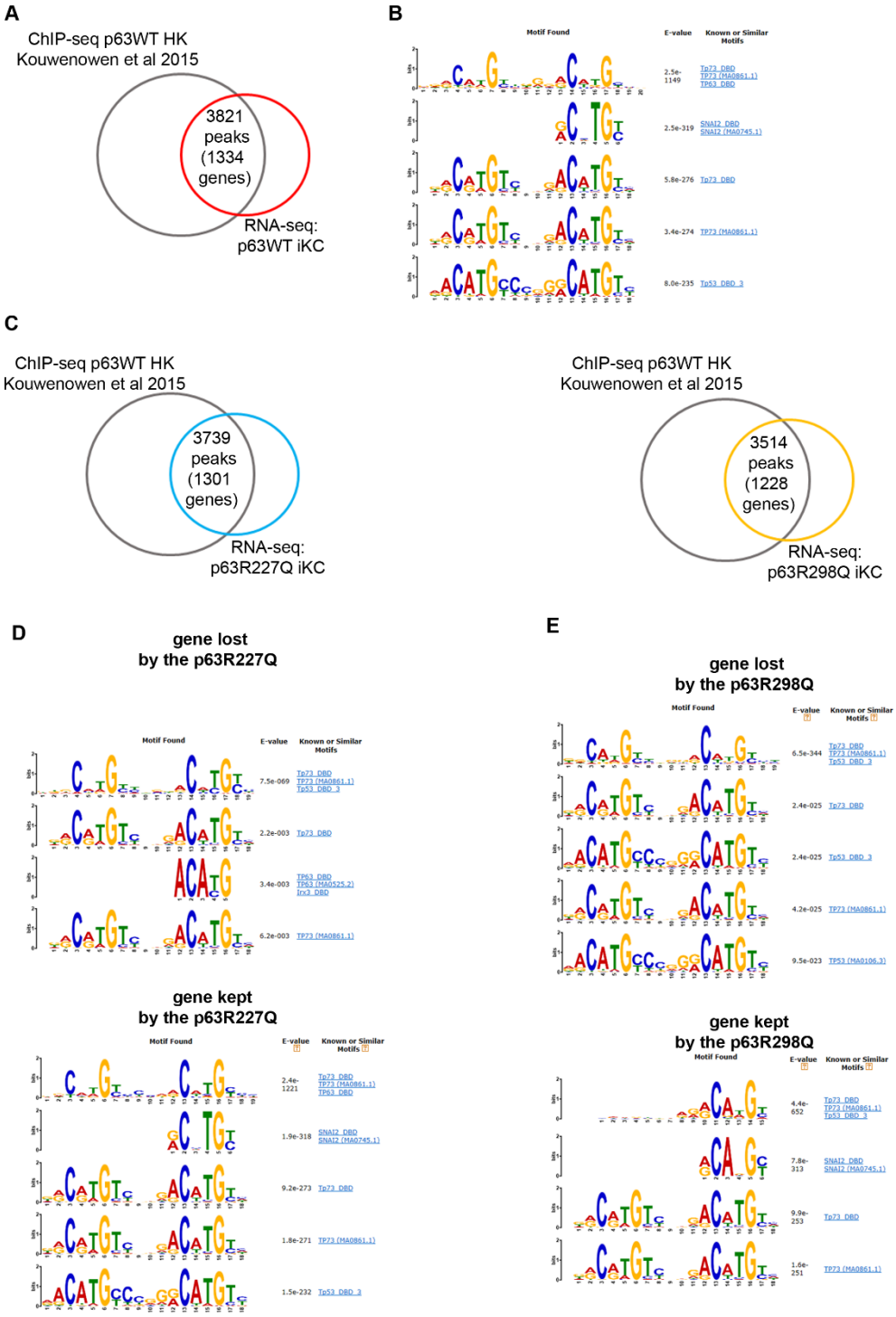

Figure 35: Identification of the sequences recognized by p63R227Q and p63R298Q. *A) Comparative analysis of the ChIP-seq data from Kowenowen et al. 2015 and Quant-seq performed in converted fibroblast infected with p63WT. B) The p63 canonical motif identify by MEME-ChIP. C) Comparative analysis of the ChIP-seq data from Kowenowen et al. 2015 and Quant-seq performed in converted fibroblast infected with p63R227Q or p63R298Q D) The DNA motif lost or kept by p63R227Q. E) The DNA motif lost or kept by p63R298Q.*

4. The EEC-frameshift associated mutants show a transcriptional hyper-activation and induce the epidermal commitment.

EEC syndrome is mainly caused by point mutations in the DNA binding domain (DBD) of the *p63* gene. Nevertheless, there are some frameshift mutations in the C-terminal domain that are not associated with the AEC syndrome, but to the EEC syndrome. These mutations lacks of some portions of the C-terminal domain creating truncated proteins that loose completely the TI and partially the SAM domain (1576delTT and 1572InsA) or that retain the SAM domain but loose the TI domain (1743delAA) (Fig. 35A-B).

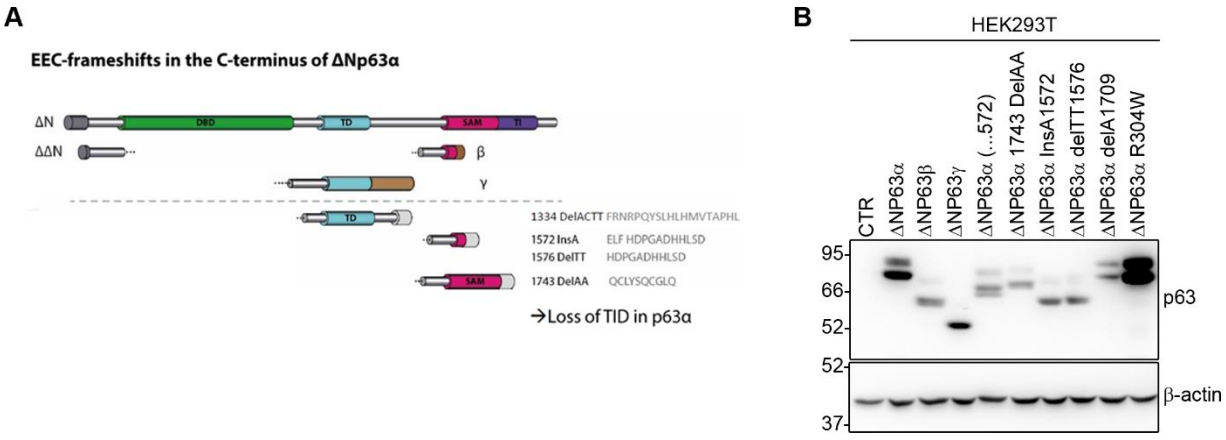

Figure 36: Structure of the frameshift mutants associated to EEC syndrome*. A) Schematic representation of the others isoform of p63 and of the EEC-Frameshifts mutants. B) Western-blot of HEK293T overexpressing the p63 isoforms and EEC-frameshifts mutants.*

Loss of part of the C-terminal domain make them similar to the ΔNp63 beta isoform. Furthermore, although they are mutations that clusters into the C-terminal domain, they do not have a propensity for the aggregation as AEC syndrome mutants, as they run mostly as monomeric protein in BN-PAGE (Fig. 26B). Patients with these specific frameshift mutations of the p63 gene, do not present a strong skin phenotype, as the canonical EEC mutant, but rather have mainly present limb phenotype. Preliminary studies leaded by Volker Dötsch and colleagues, showed that these mutants and the beta isoform have a transcriptional hyper-activity on some canonical promoters (K14, SHFM,

PUMA, p21). To better understand the role of these mutants in a more physiological context, we performed a fibroblast to iKC conversion assay overexpressing three frameshift EEC mutants (1576delTT, 1572InsA and 1743delAA), an artificial frameshift mutant (p63 (…572)) or the ΔNp63β in combination with KLF4. Immunofluorescence and Western blot (WB) analysis showed that all these mutants and the beta isoform are able to induce the expression of KRT14, while the ΔNp63γ do not induce the KRT14 expression, behaving as the 1709DelA frameshift mutant (AEC syndrome) and the R304W missense mutant (EEC) (Fig. 36 A-B). Furthermore, the analysis of the molecular target by RT-qPCR, show that the ΔNp63β and the different frameshift mutants induce the expression of target genes to a larger extent than the ΔNp63α, especially noticeable with the IRF6 target gene (Fig. 36C). This molecular behavior is probably due to the lack of the TI domain of p63 that can inhibit the transactivation domain of p63 causing a strong hyper-transactivation of gene targets. These data suggest that, ΔNp63β and the EEC-frameshift mutants falling in the C-terminal domain induce the epidermal commitment at the same level or even more efficiently than ΔNp63α by hyper-activating genes important for skin development and differentiation.

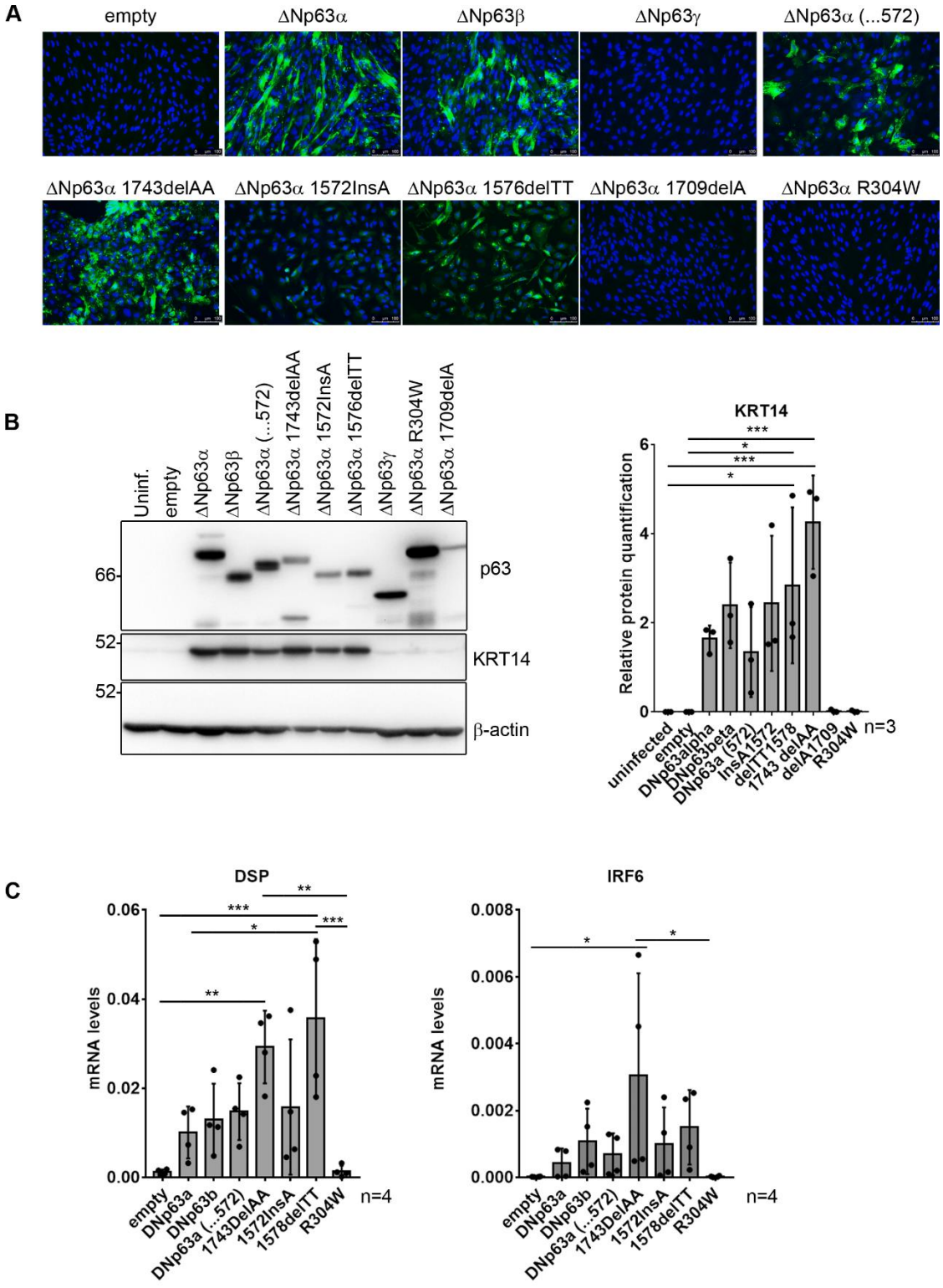

Figure 36: The ΔNp63β and EEC-FS mutants are able to induce the fibroblast conversion. *A) Immunofluorescence on converted fibroblast overexpressing the different p63 EEC-frameshifts mutants using KRT14 antibody. B) Western blot (left) with the relative quantification (right) on fibroblast converted into iKC to identify the protein expression of KRT14 upon the transfection of the different p63 isoforms and EEC-frameshifts mutants. C) RT-qPCR to identify the expression of DSP and IRF6 gene upon the transfection of all p63 constructs.*

Discussion

Since 1999 with the generation of the p63 KO mouse model (Mills et al., 1999; Yang et al., 1999a; Yang et al., 1999b), it became clear that p63 is a crucial transcription factor for limb development and epidermal specification. It is not only involved in the epidermal commitment during development, but also in skin homeostasis, regulating genes important for keratinocyte differentiation and sustaining the self-renewal of the adult stem cell in the basal layer of the epidermis. Despite the large body of the literature on the p63 functions, still little is known about the molecular mechanisms at the basis of skin pathology in which p63 is involved. When the gene structure or its gene expression is altered, p63 escapes from its normal function as regulator of the skin homeostasis, leading to different pathological phenotypes. In particular, when p63 gene is aberrantly expressed it behaves as a pro-oncogenic factor leading to a cell proliferation and survival and sustaining the tumor growth. In particular, it is quite clear that p63 drives the oncogenic programs of different epithelial tumors, co-operating also with other oncogenic transcription factors, such as SOX2 or YAP1 (Saladi et al.; Watanabe et al.)sustaining the growth of tumor cells. Nevertheless, little is known about the role of p63 in cSCC, the second most frequent world- wide cancer in the population. This tumor belongs to NMSC and it is due to the exposition of the UV radiation, which leads to an accumulation of mutation in tumor suppressor and proto-oncogenes.

Here we focused our studies mainly on gene transcription regulation leaded by p63 in this type of tumor. p63 is overexpressed in pre-neoplastic and neoplastic lesions, compared to normal skin. Through ChIP seq and RNA-seq studies in a cSCC line depleted for p63, we identified its direct target genes. Gene Ontology analysis identified an enrichment for genes directly regulated by p63 that are mainly involved in cell proliferation. In fact, the depletion of p63 leads to a strong decrease of tumor cell proliferation, suggesting that this transcription factor is crucial for the sustainment and growth of cutaneous tumor. Since transcription factors are difficult to target for therapy, through a LC-MS/MS analysis we identified different p63 protein partners to find some

hypothetical therapeutic target that can alter the abnormal p63 transcriptional activity. From this analysis, we identified PARP1 as a novel interactor of p63. PARP1 is a ubiquitous enzyme that leads a PTM modification called Poly-ADP-Ribosylation and inhibitors of its enzymatic activity was approved by FDA as treatment for different tumors (Feng et al.). It is mainly well known for its role in DNA repair, but in the last decades, more studies have been focused on its role in transcription regulation and chromatin modification. Our data indicate that p63 and PARP1 interacts in a DNA-dependent manner. PARP1 is overexpressed in cSCC and localized, as p63, in the basal layer of the epidermis. We performed an RNA-seq in cSCC cells depleted for p63 and PARP1 to identify the genes co-regulated by both proteins. The transcriptomic analysis demonstrated a strong relationship between the transcriptomic profiles of the cells depleted by either factor. Genes co-regulated by both proteins are mainly involved in the regulation of cell cycle and DNA repair. In particular, a protein-protein interaction prediction showed an involvement of p63 and PARP1 in the regulation of two different complexes: one involved in the homologous recombination and the other one involved in mitotic prometaphase. In agreement with these findings, the depletion of PARP1 in cSCC cells cause a decrease of cell proliferation and clonal expansion and an increase of the CDKN1A expression in a p53-independent-manner. Furthermore, 3D organotypic culture performed with cSCC cells depleted for PARP1 have shown a rescue of the tumorigenic phenotype with decreased invasiveness of the underlying substrate. These data suggest that PARP1 may sustain the transcriptional regulation of p63 promoting the transcription of genes mainly involved in DNA repair and cutaneous cancer proliferation.

During my PhD, I have also studied molecular mechanisms underlying the phenotype of genetic diseases caused by p63. Heterozygous mutations in the gene structure of p63 can cause different rare genetic disease including AEC, EEC and ADULT syndromes (Rinne et al., 2007) . All these pathologies have characteristic feature that are related to defects found in p63 null mice, such as severe or mild defects of the skin, limb malformation and orofacial defects. However, the different disorders related to p63, show some

phenotypic differences between them, most likely due to the different molecular behavior that p63 mutants have in the regulation of gene expression (Rinne et al., 2006a). Therefore, while skin fragility and severe, long-lasting skin erosions and orofacial defects characterize the AEC syndrome, the EEC syndrome present all the three features of p63 phenotype: severe ectodermal dysplasia, limb malformation and cleft lip/ palate defects. Ectrodactyly and syndactyly, excessive freckling, lacrimal duct anomalies, and mild ectodermal dysplasia, instead, characterize the ADULT syndrome (Rinne et al., 2007). Missense mutations or frameshift mutations, causing aberrant elongation or truncation of the protein, can occur in different p63 protein domains. Missense mutations or frameshift mutations generating elongated protein that cluster in C-terminal domain of p63, are causative of the AEC-syndrome (McGrath et al., 2001). We demonstrate that the inability to activate transcription is due to a propensity of aggregation of those mutants. Aggregation is caused by either aberrant protein elongation introducing aggregation-prone peptides, enhancing the intrinsic low aggregation propensity of the TI domain, or by conformational changes that expose peptides with a natural high aggregation propensity. Using a genetic strategy, which consists in the deletion of aggregating peptides from frameshift mutations or adding specific missense mutations to the aggregation-prone amino acids, we reversed the aggregation of the p63 mutants. The abolition of the aggregation rescued the p63 transcriptional activity as confirmed by luciferase-assay. This rescue is also visible with the conversion assay of fibroblast in iKC, restoring the ability of p63 to induce the conversion of the cells lost by the AEC-mutants.

Differently from the C-terminal domain mutants, the DNA binding domain mutants lose the ability to bind the DNA, impairing the transcriptional activity of p63. This feature is characteristic of EEC syndrome (Celli et al., 1999). Nevertheless, there are some pathological mutation, associated to EEC and ADULT syndrome, which occurs in the DNA binding domain still preserving the ability to bind the DNA (Duijf et al., 2002). Using the HDF conversion to iKC approach coupled to transcriptomic analysis, we discovered that the mutation R227Q (EEC) and R298Q (ADULT) behave as “partial

mutants" keeping the ability to bind the DNA and transactivate the gene expression. Coupling ChIP-seq data from Kowenhowen et al. (Kouwenhoven et al.) with RNA-seq analysis performed on iKC cells infected with the different p63 mutants, we have shown that the R298Q mutant is able to bind mainly the hemi-site of the p63 DNA motif with a distance between the two hemi-site > 0. This analysis suggest that the R298Q mutant do not recognized the typical full-response element (two hemi sites with 0 spacing). An explanation is that this effect may be due to the position of the mutation in the tetramer-interface of two p63 dimers, with each dimer binding to one hemi site. The wild-type p63 needs to form a tetramer, through the oligomerization domain, to bind the DNA and transactivate the gene expression (Deutsch et al., 2011). This would imply that the contact in the tetramer mediated by the WT and destroyed by the mutant occurs only in p63 binding site that have no space between the two hemi-sites zero spacing. If this hypothesis is correct, we would have discovered a completely new class of p63 DBD mutants, which only affect p63 binding sites with no space between the two hemi-site, but would still bind to hemi-sites or full-sites with a spacing > zero.

A separate discussion must be made for those frameshift mutations that fall in the C-terminal domain associated to EEC syndrome. These mutations cause the formation of a truncated protein structurally similar to the p63β isoform. Unlike the AEC mutants, which aggregate, these mutants do not have a propensity for aggregation and are capable of trans-activating, the genes they regulate, often with a hyper-activation of gene expression. This behavior, also found in the p63β isoform, may be due to the absence of the TI domain, which may act as a regulator of the trans-activator activity of p63.

Materials and Methods

Cell lines

Neonatal Human Dermal Fibroblast (HDFn) (Thermo Fisher Scientific), HEK293 and NIH3T3 were grown in Dulbecco's Modified Eagle Medium (DMEM) and 10% FBS (Euroclone).

BJ human Fibroblast were kindly provided by Dr. Davide Cacchiarelli and were cultured in DMEM/ F12 supplied with 10% FBS.

Human primary keratinocytes and the cSCC cell lines (SCC12, SCC13, IC1, T8, EB2, MET2) were kindly provided by Dr GP Dotto and were grown in Keratinocyte-SFM (Thermo Fisher Scientific) with L-glutamine supplemented with 30 µg/mL of Bovine Pituitary Extract (BPE), 0,24 ng/ml Epidermal Growth Factor (EGF) and Penicilline/ Streptomicyne (P/S) 1X.

For the 3D-organotypic culture, cells were growth in E-media [DMEM/HAM's F12 1:1, Gentamicin 10 µg/ml, Amphotericin B 25µg/ml, L-Glutamin 4mM, Hydrocortisone 0,4 µg/ml, Choleratoxin 10 ng/ml, 5% FBS + E-cocktail (Adenine 180 µM, Insulin 5 µg/ml, human Apotransferrin 5 µg/ml, Triiodothyronine T3 5 µg/ml)]

All cell lines were growth at 37°C in a humidified atmosphere of 5% (vol/vol) of CO2 in air.

3D- organotypic culture

To make the collagen plug, NIH3T3-J2 were trypsinized and re-suspended in reconstitution buffer composed of NaHCO3, HEPES and 0,05N NaOH supplied with 1/10 DMEM 10x (Sigma) and with 4mg/mL rat tail collagen (Corning). Upon the cell resuspension the cell solution is neutralized with NaOH 0.5N. Then, NIH3T3-J2 were plated in 12-well and incubate for 30 min at 37°C to allow the polymerization of the collagen. Each plug is submerged in DMEM + 10% of FBS.

Two days after the preparation of the collagen plug, SCC13 CTR and SCC13-shPARP1 were plated onto the plugs using the E-media supplied with 5ng/mL EGF.

After two days, the plugs with the cells were positioned on sterile grids in a 60mm dish to allow the stratification of cells in air lift. Every two days medium is changed with E-Media w/o EGF.

Upon 9 days, plugs with cells were fixed in formalin ON and embedded in paraffin.

Histology and Immunostaining

Human cSCC samples were obtained from Vecchio pellegrini, 5 mm serial paraffin sections were cut and immunostained with specific anitbodies. Formalin-fixed, paraffin-embedded human skin sections were stained with specific antibodies for p63 (4A4 santa-cruz 1:100), PARP1 (46D11 9532 CST 1:400) and CDH1 (biolegend 1:200). Quantitative fluorescence images were taken of the epidermal tissue or cancerous tissues for each sample. Total fluorescence was calculated using ImageJ software.

3D- organotypic culture sections were stained with Hematoxilyn-eosin.

HDFn cells were fixed with 4% of PFA and permiabilized with 0.5% NP40 in PBS. Cells were blocked using 0.5% NP40 in PBS supplied with 5% goat serum and incubated with specific antibody for KRT14 (Biolegend 1:1000).

Plasmid, transient transfection and luciferase assay

All p63 mutant constructs were obtained using the QuikChange site-directed mutagenesis kit (Agilent) starting from either pcDNA3.1-Myc-hΔNp63α using mutagenesis primers. For HDF to iKC conversion, wild type p63 and its mutants were cloned in pBABE in the BamHI site. All Cells were transfected using Lipofectamine 2000 (Thermo Fisher Scientific). Luciferase activity was determined 48 hr after transfection using the dual-luciferase reporter assay kit (Promega). pKRT14 promoter-luc were used as reporters. Renilla activity was used to normalize transfection efficiency.

Retroviral infection and conversion assay

High titer retroviral production was obtained in HEK293T cells by transient transfection of the pBABE constructs and of amphotropic viral envelope plasmid (pAmpho) using PEI (Thermo Fisher Scientific) in 1:4 DNA/ PEI ratio. Cell supernatants containing the retroviruses were collected 48 and 72 hr after transfection. Neonatal HDF and BJ-HDF were infected twice at 20-30% confluence with retroviruses carrying p63 and KLF4 (Chen et al., 2014) in the presence of 8 μg/ml Polybrene. Cells were passage, selected with 2 μg/ml puromycin 48 hr after the second infections, and grown after 48 hr of selection for 15-18 days in the absence of puromycin

Lentiviral preparation and cell infection.

For lentiviral preparation, HEK293T cells were co-transfected with viral packaging plasmids and our plasmid of interest using Lipofectamine2000 (Invitrogen), followed by virus collection after 48 hours. SCC cells were infected for 2 hours with high-titer lenti- and lentiviruses sufficient to infect the majority of cells. Two days after infection, cells were selected with 0.75 μg/ml of puromycin for 3 days.

siRNA transfection

SCC13 cells were seeded and transfected with specific siRNA targeting p63 and PARP1 using LIPO 2000 (Invitrogen) and incubated 6h at 37°C . To perform clonogenic and sphere assay, cells were re-plated 24h upon transfection.

	siRNA sequences	
gene	**Sequence (Sense) 5' to 3'**	**Sequence (Antisense) 5' to 3'**
siTP63	UCAUCUGGAUACCAUGUGUGUUCUG	CAGAACACACAUGGUAUCCAGAUGA
siPARP1	AAGCCUCCGCUCCUGAACAAU	AUUGUUCAGGAGCGGAGGCUU

Table 2: siRNA sequences used for transient transfection in cSCC cells.

Immunoprecipitation

cSCC and HEK293T cells were prepared using lysis buffer (Tris HCl 20 mM pH 7.9, KCl 120 mM, MgCl2 5 mM, EDTA 0.2 mM, NP-40 0.2%, Glycerol 10%, and DTT 1mM), adding Protease inhibitor (Roche) and phosphatase inhibitors and incubated for 10 min on ice. Upon max speed centrifugation, protein extracts were incubated with primary antibody conjugated with Dynabeads® Protein A and G (Life technologies). After incubation for 2 hours with gently rotation, samples were washed 4 times and then eluted boiling samples 5' at 95°C. The immunoprecipitates were processed by immunoblotting.

For the immunoprecipitation with macrodomain, cells were prepared using RIPA lysis buffer (Tris-HCl pH 7.9 100 mM, SDS 0.01%, Sodium De-oxycolate 0.5%, NP-40 1%, NaCl 150 mM) adding Protease inhibitor (Roche), Upon max speed centrifugation, protein extracts were incubated ON with the macrodomain Af_1521 and a mutated macrodomain. After incubation, samples were washed 3 times with RIPA buffer and 2 times with RIPA buffer w/o detergents and then eluted boiling samples 5' at 95°C. The immunoprecipitates were processed by immunoblotting.

Western blotting

Proteins were separated by SDS/PAGE and blotted onto Immobilon-P transfer membranes (Millipore). Membranes were blocked with PBS 0.2% Tween 20 with 5% nonfat dry milk and incubated with primary antibodies for 2 hours at room temperature (RT) or ON at 4°C. After washing three times with PBS 0.2% Tween 20, membranes were incubated for 1h at RT by using the appropriate horseradish peroxidase-conjugated secondary antibody (BioRad). Detection was performed by chemiluminescence (Clarity-Biorad). The following primary antibodies were used for immunoblotting analysis: p63 (124762 1:500 Abcam), KRT14 (Biolegend 1:5000), FLAG (anti- FLAG epitope M2, 1:500), MYC sc-40 (Santa cruz 1:500), PARP1 (46D11 9532 CST 1:500), p21 (sc-19 Santa cruz 1:1000), p53 DO-1 (Calbiochem 1:1000), β-actin (Santa cruz 1:5000).

RNA Isolation and RT-qPCR

total RNA was extracted using TRIzol reagent (Thermo Fisher Scientific) and cDNA was synthesized using SuperScript Vilo (Thermo Fisher Scientific) and Luna Superscript (NEB), Real time RT-PCR was performed using the SYBR Green PCR master mix (Thermo Fisher Scientific) and Luna Sybr (NEB) in an ABI PRISM 7500 (Thermo Fisher Scientific). Target genes were quantified using specific oligonucleotide primers and normalized for human RPLP0 expression. For the RNA-sequencing, RNA was isolated using the QiaGen Kit (RNAeasy Mini Kit)

	oligos sequences for RT-qPCR	
gene	**forward sequence**	**reverse sequence**
RPLP0	GACGGATTACACCTTCCCACTT	GGCAGATGGATCAGCCAAGA
TP63	GGCTGTTCCCCTCTACTCGAA	CATGAGCTGAGCCGTGAATTC
PARP1	GTGCAGTCGCCCATGTTTG	CACCTTCCAGAAGCAGGAGAA
CDKN1A	GAGACTCTCAGGGTCGAAAACG	TTAGGGCTTCCTCTTGGAGAAGA
KRT14	GGATGACTTCCGCACCAAGT	TCCACACTCATGCGCAGGT
DSP	TGCGAGCAGAGCTCATCGT	CGAGTCAGTTGTATTCCATCTCCAT
DSC3	TGAAAATGACAACCACCCTGTTT	CCCCCACTGTAGTACCAGGTCTA
IRF6	TGAAGGCAGGAAGAAGACAGC	ACCAAGTCCCCAGGAGCTCT

Table 3: oligo sequences of genes analyzed by RT-qPCR.

RNA-seq

RNA-seq libraries were prepared with the Quant-Seq FWD 30 mRNA-Seq Kit (Lexogen, Austria), sequenced on an Illumina Hi-Seq 4000, and quantified after alignment to the human genome reference hg19. Total RNA was isolated and sequenced starting from 3' UTR to identify all open reading frame transcripts. The reads were counted for each experiment and each cell population was compered individually with the equivalent control. Data were log2 transformed and filtrated.

Chromatin immunoprecipitation (ChIP)

For ChIP analysis, about 2 million cells per cell line were cross-linked with 1% formaldehyde for 10 min at 37°C, washed in PBS and resuspended in SDS lysis buffer (50 mM Tris-HCl at pH 8.1, 10 mM EDTA, 1% SDS, 1), and sonicated in order to obtain

chromatin fragment lengths of 100–1000 bp. Chromatin was diluted in ChIP dilution buffer (16.7mM Tris-HCl at pH 8.1, 167 mM NaCl, 1.2 mM EDTA, 1.1% Triton X-100, 0.01% SDS) and incubated overnight at 4°C specific antibodies conjugated with Dynabeads® Protein A and G (ThermoFisher Scientific). Immunoprecipitates were washed with Low salt buffer, High salt buffer and LiCl Immune complex wash buffer (50 mM HEPES at pH 7.6, 0.5 M LiCl, 1 mM EDTA, 0.7% Na deoxycholate, 1% NP-40) and twice with TE buffer. DNA was eluted in 1% SDS plus 0.1 M NaHCO3 and purified QiaQuick columns (ThermoFisher Scientific), and quantified using Qubit assay (Invitrogen). DNA was used as the template for qPCR or for library construction of Illumina sequencing. All qPCRs were performed with SYBR Select Master mix (Applied Biosystems) on a 7500 Real-Time PCR system (Applied Biosystems). P63 antibody (124762 Abcam) was used for ChIP.

ChIP-seq data analysis

All 50-bp sequence reads were uniquely mapped to the human genome NCBI build 37 (hg19) using bwa 0.6.1 with standard parameters [67]. p63 ChIP-seq datasets were normalized to the same sequencing depth by randomly removing aligned reads. Duplicated reads were removed before normalization. Peak recognition for p63 ChIP-seq was performed using MACS2, an updated version of MACS [68] that is specifically designed to process mixed signal types (https://github.com/taoliu/MACS) with default settings and a P-value threshold of 1E-9 using a genomic DNA as background control. Peaks were mapped to RefSeq genes, downloaded from UCSC Genome Browser (hg19), to determine genomic location of the p63 binding sites.

Transcriptomic analysis

Published gene expression profiles from 30 cutaneous SCC, 10 AK and 32 normal skin samples analyzed with Affymetrix Human Genome U133 Plus 2.0 array were obtained from the Gene Expression Omnibus (GEO) database (GSE42677; GSE45216). Raw .CEL data were analyzed with RMA (Robust Multichip Average) and corrected for batch

effect with the remove Batch Effect function, available within the LIMMA package. For the RNA-seq, results were expressed as log2 intensity values and visualized using heat map generated with Morpheus. Genes were filtered using the FDR≤0.05 and the biological process were identified using DAVID GO (david-d.ncifcrf.gov/). Heat maps were performed using MORPHEUS (broadinstitute.org/Morpheus).

BrdU

To evaluate DNA synthesis, two days after transfections cells were labeled with 5-bromo-20-deoxy-uridine (ThermoFisher Scientific) BrdU labeling. SCC cell were transfected as previously described. Cells were labeled with BrdU (ThermoFisher Scientific; 1:100) for 2 h and subsequently fixed with 4% paraformaldehyde.

After fixation, cells were permeabilized with NP-40 0.1%, and the DNA was denatured with 50 mM NaOH. BrdU was detected with mouse monoclonal antibodies (G3G4; Developmental Studies Hybridoma Bank, The University of Iowa) and rabbit-anti mouse TRITC (Dako Cytomation). DNA was counterstained with DAPI (100 ng/mL).

Clonogenic assay

Cells were plated on 60mm dishes (500 cells/plate; duplicate plates/condition) and cultured for 10 days. Medium was exchanged every 2 days. After 10 days, the colonies were fixed with 4% formaldehyde and incubated 15 min at 37°C. Subsequently, colonies were stained with 1% crystal violet (Sigma). The number of colonies were counted and analyzed using ImageJ.

Sphere assay

cells were trypsinized, centrifuged, then resuspended in spheroid media: DMEM/F12 (DMT-10-090-CV, Corning); 2% B27 serum free supplement (17504-044, ThermoFisher Scientific); 0.4% BSA (B4287, Sigma); 20 ng/ml EGF (E4269, Sigma); 4 ug/ml insulin (19278, Sigma). 40,000 cells per well were plated in ultra-low attachment plates (3471, Corning Costar) and allowed to grow for 10 days.

Statistical analyses

Statistical significance between two groups in the figures was noted by asterisks ($P < 0.05$ [$*$], $P < 0.01$ [$**$], $P < 0.001$ [$***$], and $P < 0.0001$ [$****$]). The data are presented as mean ± SD, and statistical analysis was performed using unpaired two-tailed Student's t- test. Analyses of multiple groups were performed using one-way ANOVA.

Bibliography

Amiel, J., Bougeard, G., Francannet, C., Raclin, V., Munnich, A., Lyonnet, S., and Frebourg, T. (2001). TP63 gene mutation in ADULT syndrome. European Journal of Human Genetics *9*, 642-645.

Antonini, D., Rossi, B., Han, R., Minichiello, A., Di Palma, T., Corrado, M., Banfi, S., Zannini, M., Brissette, J. L., and Missero, C. (2006). An autoregulatory loop directs the tissue-specific expression of p63 through a long-range evolutionarily conserved enhancer. Mol Cell Biol *26*, 3308-3318.

Antonini, D., Sirico, A., Aberdam, E., Ambrosio, R., Campanile, C., Fagoonee, S., Altruda, F., Aberdam, D., Brissette, J. L., and Missero, C. A composite enhancer regulates p63 gene expression in epidermal morphogenesis and in keratinocyte differentiation by multiple mechanisms. Nucleic Acids Res *43*, 862-874.

Bai, P. Biology of Poly(ADP-Ribose) Polymerases: The Factotums of Cell Maintenance. Mol Cell *58*, 947-958.

Bailey, T. L., Williams, N., Misleh, C., and Li, W. W. (2006). MEME: discovering and analyzing DNA and protein sequence motifs. Nucleic Acids Res *34*, W369-373.

Bao, X., Rubin, A. J., Qu, K., Zhang, J., Giresi, P. G., Chang, H. Y., and Khavari, P. A. A novel ATAC-seq approach reveals lineage-specific reinforcement of the open chromatin landscape via cooperation between BAF and p63. Genome Biol *16*, 284.

Baroni, A., Buommino, E., De Gregorio, V., Ruocco, E., Ruocco, V., and Wolf, R. Structure and function of the epidermis related to barrier properties. Clin Dermatol *30*, 257-262.

Belyi, V. A., Ak, P., Markert, E., Wang, H., Hu, W., Puzio-Kuter, A., and Levine, A. J. The origins and evolution of the p53 family of genes. Cold Spring Harb Perspect Biol *2*, a001198.

Blanpain, C., and Fuchs, E. (2009). Epidermal homeostasis: a balancing act of stem cells in the skin. Nat Rev Mol Cell Biol *10*, 207-217.

Blanpain, C., Lowry, W. E., Pasolli, H. A., and Fuchs, E. (2006). Canonical notch signaling functions as a commitment switch in the epidermal lineage. Genes Dev *20*, 3022-3035.

Caiafa, P., Guastafierro, T., and Zampieri, M. (2009). Epigenetics: poly(ADP-ribosyl)ation of PARP-1 regulates genomic methylation patterns. FASEB J *23*, 672-678.

Caiafa, P., and Zampieri, M. (2005). DNA methylation and chromatin structure: the puzzling CpG islands. J Cell Biochem *94*, 257-265.

Celli, J., Duijf, P., Hamel, B. C., Bamshad, M., Kramer, B., Smits, A. P., Newbury-Ecob, R., Hennekam, R. C., Van Buggenhout, G., van Haeringen, A., *et al.* (1999). Heterozygous germline mutations in the p53 homolog p63 are the cause of EEC syndrome. Cell *99*, 143-153.

Chan, I., Harper, J. I., Mellerio, J. E., and McGrath, J. A. (2004). ADULT ectodermal dysplasia syndrome resulting from the missense mutation R298Q in the p63 gene. Clinical and Experimental Dermatology *29*, 669-672.

Chen, Y. F., Mistry, D. S., and Sen, G. L. (2014). Highly Rapid and Efficient Conversion of Human Fibroblasts to Keratinocyte-Like Cells. Journal of Investigative Dermatology *134*, 335-344.
Chikh, A., Matin, R. N., Senatore, V., Hufbauer, M., Lavery, D., Raimondi, C., Ostano, P., Mello-Grand, M., Ghimenti, C., Bahta, A., *et al.* iASPP/p63 autoregulatory feedback loop is required for the homeostasis of stratified epithelia. EMBO J *30*, 4261-4273.
Cotsarelis, G., Sun, T. T., and Lavker, R. M. (1990). Label-retaining cells reside in the bulge area of pilosebaceous unit: implications for follicular stem cells, hair cycle, and skin carcinogenesis. Cell *61*, 1329-1337.
Daniels, C. M., Ong, S. E., and Leung, A. K. The Promise of Proteomics for the Study of ADP-Ribosylation. Mol Cell *58*, 911-924.
De Rosa, L., Antonini, D., Ferone, G., Russo, M. T., Yu, P. B., Han, R., and Missero, C. (2009). p63 Suppresses non-epidermal lineage markers in a bone morphogenetic protein-dependent manner via repression of Smad7. J Biol Chem *284*, 30574-30582.
Deutsch, G. B., Zielonka, E. M., Coutandin, D., Weber, T. A., Schafer, B., Hannewald, J., Luh, L. M., Durst, F. G., Ibrahim, M., Hoffmann, J., *et al.* (2011). DNA Damage in Oocytes Induces a Switch of the Quality Control Factor TAp63 alpha from Dimer to Tetramer. Cell *144*, 566-576.
Devos, M., Gilbert, B., Denecker, G., Leurs, K., Mc Guire, C., Lemeire, K., Hochepied, T., Vuylsteke, M., Lambert, J., Van Den Broecke, C., *et al.* Elevated DeltaNp63alpha Levels Facilitate Epidermal and Biliary Oncogenic Transformation. J Invest Dermatol *137*, 494-505.
DeYoung, M. P., Johannessen, C. M., Leong, C. O., Faquin, W., Rocco, J. W., and Ellisen, L. W. (2006). Tumor-specific p73 up-regulation mediates p63 dependence in squamous cell carcinoma. Cancer Res *66*, 9362-9368.
Doege, C. A., Inoue, K., Yamashita, T., Rhee, D. B., Travis, S., Fujita, R., Guarnieri, P., Bhagat, G., Vanti, W. B., Shih, A., *et al.* Early-stage epigenetic modification during somatic cell reprogramming by Parp1 and Tet2. Nature *488*, 652-655.
Duijf, P. H. G., Vanmolkot, K. R. J., Propping, P., Friedl, W., Krieger, E., McKeon, F., Dotsch, V., Brunner, H. G., and van Bokhoven, H. (2002). Gain-of-function mutation in ADULT syndrome reveals the presence of a second transactivation domain in p63. Human Molecular Genetics *11*, 799-804.
El-Khamisy, S. F., Masutani, M., Suzuki, H., and Caldecott, K. W. (2003). A requirement for PARP-1 for the assembly or stability of XRCC1 nuclear foci at sites of oxidative DNA damage. Nucleic Acids Res *31*, 5526-5533.
Feng, F. Y., de Bono, J. S., Rubin, M. A., and Knudsen, K. E. Chromatin to Clinic: The Molecular Rationale for PARP1 Inhibitor Function. Mol Cell *58*, 925-934.
Fernandez-Escamilla, A. M., Rousseau, F., Schymkowitz, J., and Serrano, L. (2004). Prediction of sequence-dependent and mutational effects on the aggregation of peptides and proteins. Nat Biotechnol *22*, 1302-1306.
Ferone, G., Mollo, M. R., Thomason, H. A., Antonini, D., Zhou, H. Q., Ambrosio, R., De Rosa, L., Salvatore, D., Getsios, S., van Bokhoven, H., *et al.* (2013). p63 control of

desmosome gene expression and adhesion is compromised in AEC syndrome. Human Molecular Genetics *22*, 531-543.
Ferone, G., Thomason, H. A., Antonini, D., De Rosa, L., Hu, B., Gemei, M., Zhou, H. Q., Ambrosio, R., Rice, D. P., Acampora, D., *et al.* (2012). Mutant p63 causes defective expansion of ectodermal progenitor cells and impaired FGF signalling in AEC syndrome. Embo Molecular Medicine *4*, 192-205.
Gagne, J. P., Isabelle, M., Lo, K. S., Bourassa, S., Hendzel, M. J., Dawson, V. L., Dawson, T. M., and Poirier, G. G. (2008). Proteome-wide identification of poly(ADP-ribose) binding proteins and poly(ADP-ribose)-associated protein complexes. Nucleic Acids Res *36*, 6959-6976.
Gao, F., Kwon, S. W., Zhao, Y., and Jin, Y. (2009). PARP1 poly(ADP-ribosyl)ates Sox2 to control Sox2 protein levels and FGF4 expression during embryonic stem cell differentiation. J Biol Chem *284*, 22263-22273.
Hassa, P. O., Buerki, C., Lombardi, C., Imhof, R., and Hottiger, M. O. (2003). Transcriptional coactivation of nuclear factor-kappaB-dependent gene expression by p300 is regulated by poly(ADP)-ribose polymerase-1. J Biol Chem *278*, 45145-45153.
Hassa, P. O., Haenni, S. S., Buerki, C., Meier, N. I., Lane, W. S., Owen, H., Gersbach, M., Imhof, R., and Hottiger, M. O. (2005). Acetylation of poly(ADP-ribose) polymerase-1 by p300/CREB-binding protein regulates coactivation of NF-kappaB-dependent transcription. J Biol Chem *280*, 40450-40464.
Hibi, K., Trink, B., Patturajan, M., Westra, W. H., Caballero, O. L., Hill, D. E., Ratovitski, E. A., Jen, J., and Sidransky, D. (2000). AIS is an oncogene amplified in squamous cell carcinoma. Proc Natl Acad Sci U S A *97*, 5462-5467.
Huambachano, O., Herrera, F., Rancourt, A., and Satoh, M. S. Double-stranded DNA binding domain of poly(ADP-ribose) polymerase-1 and molecular insight into the regulation of its activity. J Biol Chem *286*, 7149-7160.
Ianakiev, P., Kilpatrick, M. W., Toudjarska, I., Basel, D., Beighton, P., and Tsipouras, P. (2000). Split-hand/split-foot malformation is caused by mutations in the p63 gene on 3q27. Am J Hum Genet *67*, 59-66.
Inman, G. J., Wang, J., Nagano, A., Alexandrov, L. B., Purdie, K. J., Taylor, R. G., Sherwood, V., Thomson, J., Hogan, S., Spender, L. C., *et al.* The genomic landscape of cutaneous SCC reveals drivers and a novel azathioprine associated mutational signature. Nat Commun *9*, 3667.
Jungmichel, S., Rosenthal, F., Altmeyer, M., Lukas, J., Hottiger, M. O., and Nielsen, M. L. Proteome-wide identification of poly(ADP-Ribosyl)ation targets in different genotoxic stress responses. Mol Cell *52*, 272-285.
Keyes, W. M., Pecoraro, M., Aranda, V., Vernersson-Lindahl, E., Li, W., Vogel, H., Guo, X., Garcia, E. L., Michurina, T. V., Enikolopov, G., *et al.* DeltaNp63alpha is an oncogene that targets chromatin remodeler Lsh to drive skin stem cell proliferation and tumorigenesis. Cell Stem Cell *8*, 164-176.
Kim, M. Y., Mauro, S., Gevry, N., Lis, J. T., and Kraus, W. L. (2004). NAD+-dependent modulation of chromatin structure and transcription by nucleosome binding properties of PARP-1. Cell *119*, 803-814.

King, K. E., Ponnamperuma, R. M., Yamashita, T., Tokino, T., Lee, L. A., Young, M. F., and Weinberg, W. C. (2003). deltaNp63alpha functions as both a positive and a negative transcriptional regulator and blocks in vitro differentiation of murine keratinocytes. Oncogene *22*, 3635-3644.
Kohler, S., Carmody, L., Vasilevsky, N., Jacobsen, J. O. B., Danis, D., Gourdine, J. P., Gargano, M., Harris, N. L., Matentzoglu, N., McMurry, J. A., *et al.* Expansion of the Human Phenotype Ontology (HPO) knowledge base and resources. Nucleic Acids Res *47*, D1018-D1027.
Koster, M. I., Kim, S., Mills, A. A., DeMayo, F. J., and Roop, D. R. (2004). p63 is the molecular switch for initiation of an epithelial stratification program. Genes Dev *18*, 126-131.
Koster, M. I., and Roop, D. R. (2004). The role of p63 in development and differentiation of the epidermis. J Dermatol Sci *34*, 3-9.
Kouwenhoven, E. N., Oti, M., Niehues, H., van Heeringen, S. J., Schalkwijk, J., Stunnenberg, H. G., van Bokhoven, H., and Zhou, H. Transcription factor p63 bookmarks and regulates dynamic enhancers during epidermal differentiation. EMBO Rep *16*, 863-878.
Kraus, W. L. (2008). Transcriptional control by PARP-1: chromatin modulation, enhancer-binding, coregulation, and insulation. Curr Opin Cell Biol *20*, 294-302.
Kraus, W. L., and Hottiger, M. O. PARP-1 and gene regulation: progress and puzzles. Mol Aspects Med *34*, 1109-1123.
Kraus, W. L., and Lis, J. T. (2003). PARP goes transcription. Cell *113*, 677-683.
Krishnakumar, R., Gamble, M. J., Frizzell, K. M., Berrocal, J. G., Kininis, M., and Kraus, W. L. (2008). Reciprocal binding of PARP-1 and histone H1 at promoters specifies transcriptional outcomes. Science *319*, 819-821.
Krishnakumar, R., and Kraus, W. L. PARP-1 regulates chromatin structure and transcription through a KDM5B-dependent pathway. Mol Cell *39*, 736-749.
Langelier, M. F., Planck, J. L., Roy, S., and Pascal, J. M. Crystal structures of poly(ADP-ribose) polymerase-1 (PARP-1) zinc fingers bound to DNA: structural and functional insights into DNA-dependent PARP-1 activity. J Biol Chem *286*, 10690-10701.
LeBoeuf, M., Terrell, A., Trivedi, S., Sinha, S., Epstein, J. A., Olson, E. N., Morrisey, E. E., and Millar, S. E. Hdac1 and Hdac2 act redundantly to control p63 and p53 functions in epidermal progenitor cells. Dev Cell *19*, 807-818.
Leoyklang, P., Siriwan, P., and Shotelersuk, V. (2006). A mutation of the p63 gene in non-syndromic cleft lip. J Med Genet *43*, e28.
Li, L., Wang, Y., Torkelson, J. L., Shankar, G., Pattison, J. M., Zhen, H. H., Fang, F., Duren, Z., Xin, J., Gaddam, S., *et al.* TFAP2C- and p63-Dependent Networks Sequentially Rearrange Chromatin Landscapes to Drive Human Epidermal Lineage Commitment. Cell Stem Cell *24*, 271-284 e278.
Li, M., and Yu, X. Function of BRCA1 in the DNA damage response is mediated by ADP-ribosylation. Cancer Cell *23*, 693-704.

Li, Y. Y., Hanna, G. J., Laga, A. C., Haddad, R. I., Lorch, J. H., and Hammerman, P. S. Genomic analysis of metastatic cutaneous squamous cell carcinoma. Clin Cancer Res *21*, 1447-1456.
Lin-Shiao, E., Lan, Y., Coradin, M., Anderson, A., Donahue, G., Simpson, C. L., Sen, P., Saffie, R., Busino, L., Garcia, B. A., *et al.* KMT2D regulates p63 target enhancers to coordinate epithelial homeostasis. Genes Dev *32*, 181-193.
Liu, Z., and Kraus, W. L. Catalytic-Independent Functions of PARP-1 Determine Sox2 Pioneer Activity at Intractable Genomic Loci. Mol Cell *65*, 589-603 e589.
Luijsterburg, M. S., de Krijger, I., Wiegant, W. W., Shah, R. G., Smeenk, G., de Groot, A. J. L., Pines, A., Vertegaal, A. C. O., Jacobs, J. J. L., Shah, G. M., and van Attikum, H. PARP1 Links CHD2-Mediated Chromatin Expansion and H3.3 Deposition to DNA Repair by Non-homologous End-Joining. Mol Cell *61*, 547-562.
Marteijn, J. A., Lans, H., Vermeulen, W., and Hoeijmakers, J. H. Understanding nucleotide excision repair and its roles in cancer and ageing. Nat Rev Mol Cell Biol *15*, 465-481.
Martincorena, I., Roshan, A., Gerstung, M., Ellis, P., Van Loo, P., McLaren, S., Wedge, D. C., Fullam, A., Alexandrov, L. B., Tubio, J. M., *et al.* Tumor evolution. High burden and pervasive positive selection of somatic mutations in normal human skin. Science *348*, 880-886.
Masse, I., Barbollat-Boutrand, L., Molina, M., Berthier-Vergnes, O., Joly-Tonetti, N., Martin, M. T., Caron de Fromentel, C., Kanitakis, J., and Lamartine, J. Functional interplay between p63 and p53 controls RUNX1 function in the transition from proliferation to differentiation in human keratinocytes. Cell Death Dis *3*, e318.
Massion, P. P., Taflan, P. M., Jamshedur Rahman, S. M., Yildiz, P., Shyr, Y., Edgerton, M. E., Westfall, M. D., Roberts, J. R., Pietenpol, J. A., Carbone, D. P., and Gonzalez, A. L. (2003). Significance of p63 amplification and overexpression in lung cancer development and prognosis. Cancer Res *63*, 7113-7121.
McDade, S. S., Henry, A. E., Pivato, G. P., Kozarewa, I., Mitsopoulos, C., Fenwick, K., Assiotis, I., Hakas, J., Zvelebil, M., Orr, N., *et al.* Genome-wide analysis of p63 binding sites identifies AP-2 factors as co-regulators of epidermal differentiation. Nucleic Acids Res *40*, 7190-7206.
McGrath, J. A., Duijf, P. H., Doetsch, V., Irvine, A. D., de Waal, R., Vanmolkot, K. R., Wessagowit, V., Kelly, A., Atherton, D. J., Griffiths, W. A., *et al.* (2001). Hay-Wells syndrome is caused by heterozygous missense mutations in the SAM domain of p63. Hum Mol Genet *10*, 221-229.
Messner, S., and Hottiger, M. O. Histone ADP-ribosylation in DNA repair, replication and transcription. Trends Cell Biol *21*, 534-542.
Mills, A. A., Zheng, B., Wang, X. J., Vogel, H., Roop, D. R., and Bradley, A. (1999). p63 is a p53 homologue required for limb and epidermal morphogenesis. Nature *398*, 708-713.
Missero, C. The genetic evolution of skin squamous cell carcinoma: tumor suppressor identity matters. Exp Dermatol *25*, 863-864.

Missero, C., and Antonini, D. Crosstalk among p53 family members in cutaneous carcinoma. Exp Dermatol *23*, 143-146.
Nguyen, B. C., Lefort, K., Mandinova, A., Antonini, D., Devgan, V., Della Gatta, G., Koster, M. I., Zhang, Z., Wang, J., Tommasi di Vignano, A., *et al.* (2006). Cross-regulation between Notch and p63 in keratinocyte commitment to differentiation. Genes Dev *20*, 1028-1042.
Pattison, J. M., Melo, S. P., Piekos, S. N., Torkelson, J. L., Bashkirova, E., Mumbach, M. R., Rajasingh, C., Zhen, H. H., Li, L., Liaw, E., *et al.* Retinoic acid and BMP4 cooperate with p63 to alter chromatin dynamics during surface epithelial commitment. Nat Genet *50*, 1658-1665.
Petesch, S. J., and Lis, J. T. Activator-induced spread of poly(ADP-ribose) polymerase promotes nucleosome loss at Hsp70. Mol Cell *45*, 64-74.
Pickering, C. R., Zhou, J. H., Lee, J. J., Drummond, J. A., Peng, S. A., Saade, R. E., Tsai, K. Y., Curry, J. L., Tetzlaff, M. T., Lai, S. Y., *et al.* Mutational landscape of aggressive cutaneous squamous cell carcinoma. Clin Cancer Res *20*, 6582-6592.
Pines, A., Vrouwe, M. G., Marteijn, J. A., Typas, D., Luijsterburg, M. S., Cansoy, M., Hensbergen, P., Deelder, A., de Groot, A., Matsumoto, S., *et al.* PARP1 promotes nucleotide excision repair through DDB2 stabilization and recruitment of ALC1. J Cell Biol *199*, 235-249.
Propping, P., Friedl, W., Wienker, T. F., Uhlhaas, S., and Zerres, K. (2000). ADULT syndrome allelic to limb mammary syndrome (LMS)? American Journal of Medical Genetics *90*, 179-182.
Propping, P., and Zerres, K. (1993). Adult-Syndrome - an Autosomal-Dominant Disorder with Pigment Anomalies, Ectrodactyly, Nail Dysplasia, and Hypodontia. American Journal of Medical Genetics *45*, 642-648.
Qu, J., Tanis, S. E. J., Smits, J. P. H., Kouwenhoven, E. N., Oti, M., van den Bogaard, E. H., Logie, C., Stunnenberg, H. G., van Bokhoven, H., Mulder, K. W., and Zhou, H. Mutant p63 Affects Epidermal Cell Identity through Rewiring the Enhancer Landscape. Cell Rep *25*, 3490-3503 e3494.
Ramsey, M. R., He, L., Forster, N., Ory, B., and Ellisen, L. W. Physical association of HDAC1 and HDAC2 with p63 mediates transcriptional repression and tumor maintenance in squamous cell carcinoma. Cancer Res *71*, 4373-4379.
Ramsey, M. R., Wilson, C., Ory, B., Rothenberg, S. M., Faquin, W., Mills, A. A., and Ellisen, L. W. FGFR2 signaling underlies p63 oncogenic function in squamous cell carcinoma. J Clin Invest *123*, 3525-3538.
Rangarajan, A., Talora, C., Okuyama, R., Nicolas, M., Mammucari, C., Oh, H., Aster, J. C., Krishna, S., Metzger, D., Chambon, P., *et al.* (2001). Notch signaling is a direct determinant of keratinocyte growth arrest and entry into differentiation. EMBO J *20*, 3427-3436.
Reale, A., Matteis, G. D., Galleazzi, G., Zampieri, M., and Caiafa, P. (2005). Modulation of DNMT1 activity by ADP-ribose polymers. Oncogene *24*, 13-19.
Restivo, G., Nguyen, B. C., Dziunycz, P., Ristorcelli, E., Ryan, R. J., Ozuysal, O. Y., Di Piazza, M., Radtke, F., Dixon, M. J., Hofbauer, G. F., *et al.* IRF6 is a mediator of Notch

pro-differentiation and tumour suppressive function in keratinocytes. EMBO J *30*, 4571-4585.
Rice, R. H., and Green, H. (1977). The cornified envelope of terminally differentiated human epidermal keratinocytes consists of cross-linked protein. Cell *11*, 417-422.
Rinne, T., Brunner, H. G., and van Bokhoven, H. (2007). p63-associated disorders. Cell Cycle *6*, 262-268.
Rinne, T., Hamel, B., van Bokhoven, H., and Brunner, H. G. (2006a). Pattern of p63 mutations and their phenotypes--update. Am J Med Genet A *140*, 1396-1406.
Rinne, T., Spadoni, E., Kjaer, K. W., Danesino, C., Larizza, D., Kock, M., Huoponen, K., Savontaus, M. L., Aaltonen, M., Duijf, P., *et al.* (2006b). Delineation of the ADULT syndrome phenotype due to arginine 298 mutations of the p63 gene. European Journal of Human Genetics *14*, 904-910.
Robu, M., Shah, R. G., Petitclerc, N., Brind'Amour, J., Kandan-Kulangara, F., and Shah, G. M. Role of poly(ADP-ribose) polymerase-1 in the removal of UV-induced DNA lesions by nucleotide excision repair. Proc Natl Acad Sci U S A *110*, 1658-1663.
Rocco, J. W., Leong, C. O., Kuperwasser, N., DeYoung, M. P., and Ellisen, L. W. (2006). p63 mediates survival in squamous cell carcinoma by suppression of p73-dependent apoptosis. Cancer Cell *9*, 45-56.
Romano, R. A., Smalley, K., Liu, S., and Sinha, S. Abnormal hair follicle development and altered cell fate of follicular keratinocytes in transgenic mice expressing DeltaNp63alpha. Development *137*, 1431-1439.
Romano, R. A., Smalley, K., Magraw, C., Serna, V. A., Kurita, T., Raghavan, S., and Sinha, S. DeltaNp63 knockout mice reveal its indispensable role as a master regulator of epithelial development and differentiation. Development *139*, 772-782.
Rybanska, I., Ishaq, O., Chou, J., Prakash, M., Bakhsheshian, J., Huso, D. L., and Franco, S. PARP1 and DNA-PKcs synergize to suppress p53 mutation and telomere fusions during T-lineage lymphomagenesis. Oncogene *32*, 1761-1771.
Saladi, S. V., Ross, K., Karaayvaz, M., Tata, P. R., Mou, H., Rajagopal, J., Ramaswamy, S., and Ellisen, L. W. ACTL6A Is Co-Amplified with p63 in Squamous Cell Carcinoma to Drive YAP Activation, Regenerative Proliferation, and Poor Prognosis. Cancer Cell *31*, 35-49.
Schultz, J., Ponting, C. P., Hofmann, K., and Bork, P. (1997). SAM as a protein interaction domain involved in developmental regulation. Protein Sci *6*, 249-253.
Sen, G. L., Boxer, L. D., Webster, D. E., Bussat, R. T., Qu, K., Zarnegar, B. J., Johnston, D., Siprashvili, Z., and Khavari, P. A. ZNF750 is a p63 target gene that induces KLF4 to drive terminal epidermal differentiation. Dev Cell *22*, 669-677.
Senoo, M., Pinto, F., Crum, C. P., and McKeon, F. (2007). p63 Is essential for the proliferative potential of stem cells in stratified epithelia. Cell *129*, 523-536.
Sethi, I., Sinha, S., and Buck, M. J. Role of chromatin and transcriptional co-regulators in mediating p63-genome interactions in keratinocytes. BMC Genomics *15*, 1042.
Slavotinek, A. M., Tanaka, J., Winder, A., Vargervik, K., Haggstrom, A., and Bamshad, M. (2005). Acro-dermato-ungual-lacrimal-tooth (ADULT) syndrome: Report of a child

with phenotypic overlap with ulnar-mammary syndrome and a new mutation in TP63. American Journal of Medical Genetics Part A *138A*, 146-149.
Soares, E., Xu, Q., Li, Q., Qu, J., Zheng, Y., Raeven, H. H. M., Brandao, K. O., Petit, I., van den Akker, W. M. R., van Heeringen, S. J., *et al.* Single-cell RNA-seq identifies a reversible mesodermal activation in abnormally specified epithelia of p63 EEC syndrome. Proc Natl Acad Sci U S A *116*, 17361-17370.
South, A. P., Purdie, K. J., Watt, S. A., Haldenby, S., den Breems, N., Dimon, M., Arron, S. T., Kluk, M. J., Aster, J. C., McHugh, A., *et al.* NOTCH1 mutations occur early during cutaneous squamous cell carcinogenesis. J Invest Dermatol *134*, 2630-2638.
Spagnolo, L., Barbeau, J., Curtin, N. J., Morris, E. P., and Pearl, L. H. Visualization of a DNA-PK/PARP1 complex. Nucleic Acids Res *40*, 4168-4177.
Takahashi, K., and Yamanaka, S. (2006). Induction of pluripotent stem cells from mouse embryonic and adult fibroblast cultures by defined factors. Cell *126*, 663-676.
Tonon, G., Wong, K. K., Maulik, G., Brennan, C., Feng, B., Zhang, Y., Khatry, D. B., Protopopov, A., You, M. J., Aguirre, A. J., *et al.* (2005). High-resolution genomic profiles of human lung cancer. Proc Natl Acad Sci U S A *102*, 9625-9630.
Tulin, A., and Spradling, A. (2003). Chromatin loosening by poly(ADP)-ribose polymerase (PARP) at Drosophila puff loci. Science *299*, 560-562.
van Bokhoven, H., and Brunner, H. G. (2002). Splitting p63. Am J Hum Genet *71*, 1-13.
van Bokhoven, H., Hamel, B. C., Bamshad, M., Sangiorgi, E., Gurrieri, F., Duijf, P. H., Vanmolkot, K. R., van Beusekom, E., van Beersum, S. E., Celli, J., *et al.* (2001). p63 Gene mutations in eec syndrome, limb-mammary syndrome, and isolated split hand-split foot malformation suggest a genotype-phenotype correlation. Am J Hum Genet *69*, 481-492.
van Bokhoven, H., Jung, M., Smits, A. P., van Beersum, S., Ruschendorf, F., van Steensel, M., Veenstra, M., Tuerlings, J. H., Mariman, E. C., Brunner, H. G., *et al.* (1999). Limb mammary syndrome: a new genetic disorder with mammary hypoplasia, ectrodactyly, and other Hand/Foot anomalies maps to human chromosome 3q27. Am J Hum Genet *64*, 538-546.
Vanbokhoven, H., Melino, G., Candi, E., and Declercq, W. p63, a story of mice and men. J Invest Dermatol *131*, 1196-1207.
Wang, X., Pasolli, H. A., Williams, T., and Fuchs, E. (2008). AP-2 factors act in concert with Notch to orchestrate terminal differentiation in skin epidermis. J Cell Biol *183*, 37-48.
Watanabe, H., Ma, Q., Peng, S., Adelmant, G., Swain, D., Song, W., Fox, C., Francis, J. M., Pedamallu, C. S., DeLuca, D. S., *et al.* SOX2 and p63 colocalize at genetic loci in squamous cell carcinomas. J Clin Invest *124*, 1636-1645.
Watt, F. M. (2002). The stem cell compartment in human interfollicular epidermis. J Dermatol Sci *28*, 173-180.
Yang, A., Kaghad, M., Caput, D., and McKeon, F. (2002). On the shoulders of giants: p63, p73 and the rise of p53. Trends Genet *18*, 90-95.
Yang, A., Kaghad, M., Wang, Y., Gillett, E., Fleming, M. D., Dotsch, V., Andrews, N. C., Caput, D., and McKeon, F. (1998). p63, a p53 homolog at 3q27-29, encodes multiple

products with transactivating, death-inducing, and dominant-negative activities. Mol Cell *2*, 305-316.
Yang, A., Schweitzer, R., Sun, D., Kaghad, M., Walker, N., Bronson, R. T., Tabin, C., Sharpe, A., Caput, D., Crum, C., and McKeon, F. (1999a). p63 is essential for regenerative proliferation in limb, craniofacial and epithelial development. Nature *398*, 714-718.
Yang, A., Schweitzer, R., Sun, D. Q., Kaghad, M., Walker, N., Bronson, R. T., Tabin, C., Sharpe, A., Caput, D., Crum, C., and McKeon, F. (1999b). p63 is essential for regenerative proliferation in limb, craniofacial and epithelial development. Nature *398*, 714-718.
Zhang, W., Remenyik, E., Zelterman, D., Brash, D. E., and Wikonkal, N. M. (2001). Escaping the stem cell compartment: sustained UVB exposure allows p53-mutant keratinocytes to colonize adjacent epidermal proliferating units without incurring additional mutations. Proc Natl Acad Sci U S A *98*, 13948-13953.